



UNIVERSITA' DEGLI STUDI DI PADOVA

DIPARTIMENTO DI SCIENZE CHIMICHE

LAUREA MAGISTRALE IN CHIMICA

**Design, Synthesis and XRD Structural Characterization of New
Coordination Polymers Based on Trinuclear Unit $[\text{Cu}_3(\mu_3\text{-OH})(\text{pz})_3]^{2+}$
(pz=pyrazolate ion) and Mono- or Bicarboxylates**

RELATORE: Prof. Luciano Pandolfo

CORRELATORE: Prof. Fabrizio Nestola

CONTRORELATORE: Prof. Mauro Carraro

LAUREANDA: Rebecca Scatena

Anno Accademico 2014/2015

A Davide

INDEX

| | |
|------------------------------------------------------|-----------|
| 1. INTRODUCTION | 1 |
| 1.1 Coordination Polymers | 1 |
| 1.2 Porosity | 7 |
| 1.3 Application of Coordination Polymers | 12 |
| 1.3.1 Catalysis | 12 |
| 1.3.2 Selective gas adsorption | 18 |
| 1.4 Structural determination | 23 |
| 2. OBJECT OF THE THESIS WORK | 31 |
| 3. EXPERIMENTAL SECTION | 33 |
| 3.1 Materials and Methods | 33 |
| 3.2 Synthetic Procedures | 34 |
| 4. SC-XRD STRUCTURE DETERMINATION | 41 |
| 4.1 Data Collection | 41 |
| 4.2 Data Processing | 41 |
| 4.3 Data Elaboration | 44 |
| 4.4 Structure Solution by Direct Methods with SIR-92 | 45 |
| 4.5 Structure Refinement with SHELXL-2004 | 47 |
| 5. STRUCTURES DESCRIPTION | 51 |
| 6. CONCLUSIONS AND FUTURE PERSPECTIVES | 81 |
| REFERENCES | 84 |
| APPENDIX A Crystal data and structure refinement | 89 |
| APPENDIX B Bond lengths and angles | 99 |
| APPENDIX C XRPD Diffractograms | 113 |



Notes

Legend of the Abbreviations

| | | |
|----------------------------|-----------------------------------|-----------------------|
| Hpz | Pyrazole | $C_3H_4N_2$ |
| pz | Pyrazolate ion | $[C_3H_3N_2]^-$ |
| H ₂ Clac | Chloroacetic acid | $C_2H_3ClO_2$ |
| Clac | Chloroacetate ion | $[C_2H_2ClO_2]^-$ |
| H ₂ PheDiAcr | 1,4-Phenylenediacrylic acid | $C_{12}H_{10}O_4$ |
| PheDiAcr | 1,4-Phenylenediacrylate ion | $[C_{12}H_8O_4]^{2-}$ |
| H ₂ BipheDiCarb | Biphenyl-4,4'-dicarboxylic acid | $C_{14}H_{10}O_4$ |
| BipheDiCarb | Biphenyl-4,4'-dicarboxylate ion | $[C_{14}H_8O_4]^{2-}$ |
| H ₂ Muc | <i>trans,trans</i> -Muconic acid | $C_6H_6O_4$ |
| Muc | <i>trans,trans</i> -Muconate ion | $[C_6H_4O_4]^{2-}$ |
| H ₂ HyMuc | <i>trans</i> -β-Hydromuconic acid | $C_6H_8O_4$ |
| HyMuc | <i>trans</i> -β-Hydromuconate ion | $[C_6H_6O_4]^{2-}$ |
| H ₂ MeSuc | Methylsuccinic acid | $C_5H_8O_4$ |
| MeSuc | Methylsuccinate ion | $[C_5H_6O_4]^{2-}$ |
| (S)-H ₂ MeSuc | (S)-Methylsuccinic acid | $C_5H_8O_4$ |
| (S)-MeSuc | (S)-Methylsuccinate ion | $[C_5H_6O_4]^{2-}$ |
| H ₂ DimeSuc | 2,2-Dimethylsuccinic acid | $C_6H_{10}O_4$ |
| DimeSuc | 2,2-Dimethylsuccinate ion | $[C_6H_8O_4]^{2-}$ |
| MeOH | Methanol | CH_4O |
| DMF | N,N-Dimethylformamide | C_3H_7NO |

The thesis reports images of molecular structures obtained using Mercury 3.5.1 software (C. F. Macrae, I. J. Bruno, J. A. Chisholm, P. R. Edgington, P. McCabe, E. Pidcock, L. Rodriguez-Monge, R. Taylor, J. van der Streek, P. A. Wood, *J. Appl. Cryst.*, **2008**, 41, 466-470).

Legend of colors used for atoms labelling:

| | | | |
|----------|-----------------------------------------------------------------------------------|----------|-------------------------------------------------------------------------------------|
| Copper |  | Oxygen |  |
| Carbon |  | Nitrogen |  |
| Chlorine |  | Hydrogen |  |

1. INTRODUCTION

1.1 Coordination Polymers

Coordination Polymers, *CPs*, are an emerging class of porous materials composed by metal-containing nodes and organic linkers.^{1,2} These materials were firstly presented by Robson,³ in 1989, as “*a new and potentially extensive class of solid polymeric materials with unprecedented and possibly useful properties*” obtained by connection of geometrically-different coordinated metal centers with “*rod-like*” units.

Due to their functional and structural tunability,⁴ the *CPs* area has become one of the fastest growing fields in chemistry. This is demonstrated through the ever-scaling number of structures reported in the *Cambridge Structural Database CSD*⁵ [Figure 1].

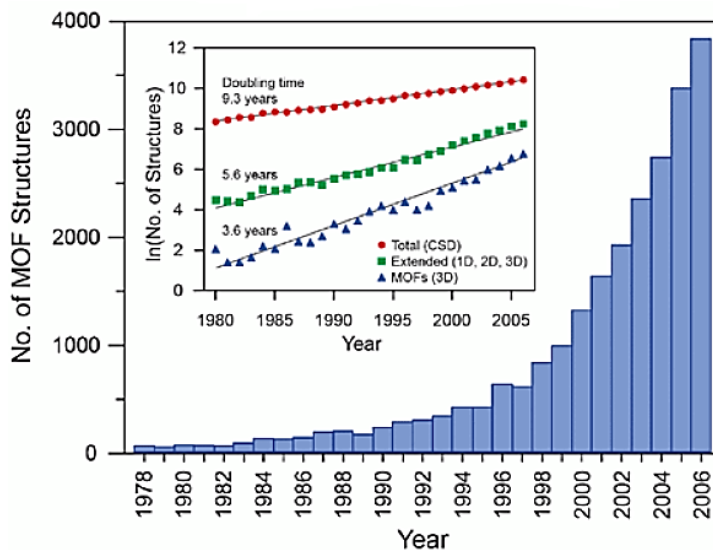


Figure 1. Number of Metal Organic Framework structure reported in the Cambridge Structural Database (CSD) from 1978 through 2006.⁵

The bar graph illustrates the growing of the number of reports, in the inset is evidenced the natural log of the number of the structures as a function of time,

showing the very short doubling time for MOF structures compared to the total number of structures archived in the database.

CPs have been a topical research field in crystal engineering, solid-state chemistry and material science for more than two decades, because these compounds can exhibit not only versatile structures, but also unique chemical and physical properties for potential applications.⁶

Coordination Polymers are also known as *Metal Organic Frameworks*, MOF, although these terms are not strictly identical.⁷ IUPAC defined Coordination Polymer a compound obtained by the repetition of coordination entities in 1, 2, or 3 dimensions, while the term *MOF* indicates a coordination network with organic ligands containing potential voids.⁸ Then Coordination Polymers is the general term to speaking and to consider all this structural class, while to indicate Porous Coordination Polymers the acronym PCPs is often use.

CPs are classified as hybrid organic-inorganic materials, on which the metal fragment and the organic one are respectively called *node* and *linker*, where the latter is an organic ligand that must have a polytopic group to coordinate two or more metallic moieties⁹. The *node* is suitably constituted by metal ions mainly of transition series, due to their wide range of oxidation states and that may exhibit different coordination geometries, influencing the CPs characteristics.

The coordination geometry is also influenced by the linker choice, according to its steric hindrance and its position in the spectrochemical series: halides < oxygen-donors < nitrogen-donors < carbon-donors.

Generally, the ligands used in the CPs synthesis can be neutral or anionic: the latter are typically polycarboxylates systems [Figure 2], while the most classic representative of the first category are heteroatomic systems based on nitrogen donors [Figure 3].

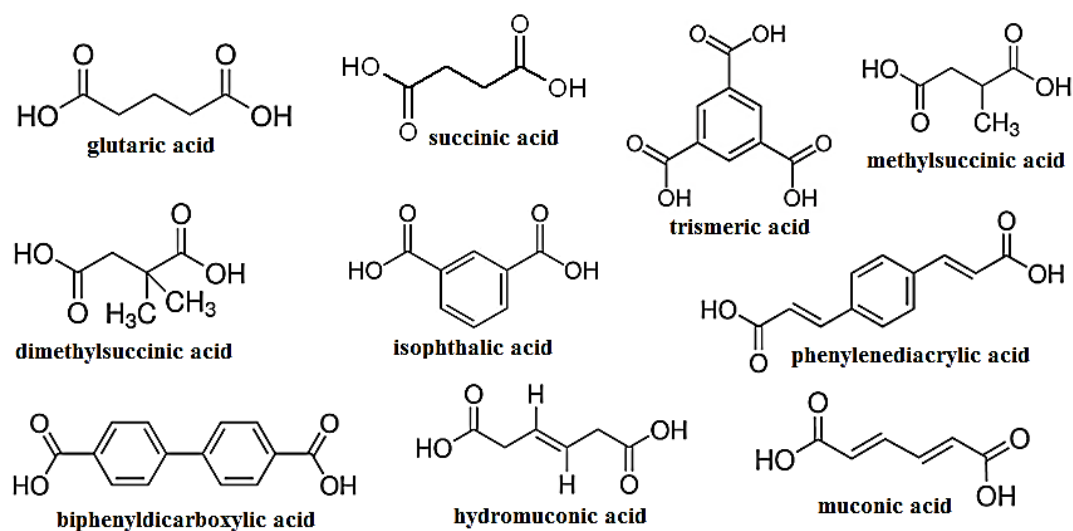


Figure 2. Examples of polycarboxylic acids which generate O-donor ligands by deprotonation.

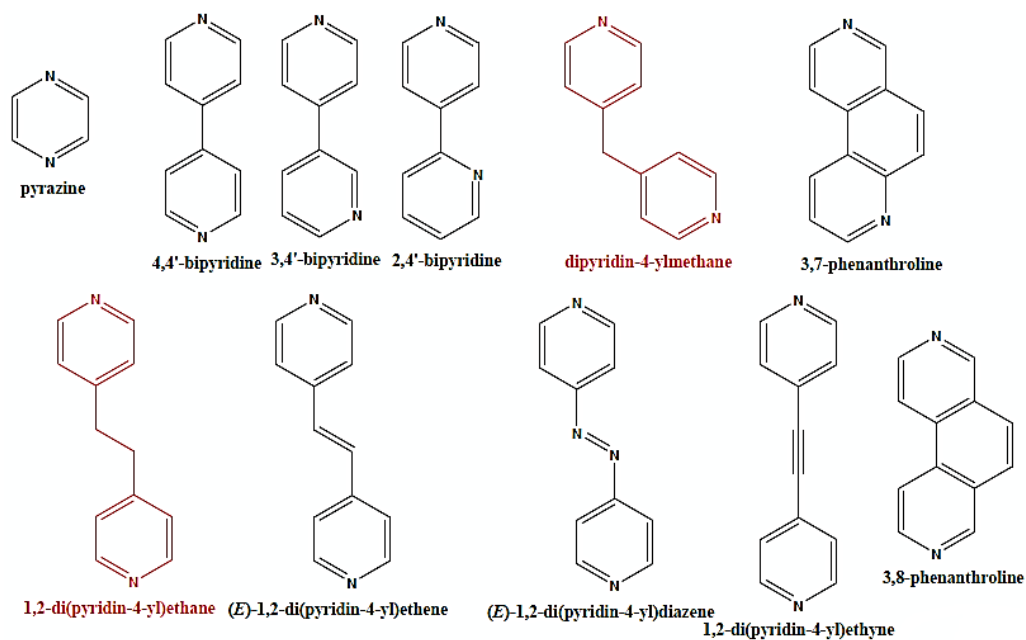


Figure 3. Typical N-donor ligands. In black are represented the rigid linkers and in red the flexible ones.

On the other hand, the ligand polyhapticity may be due to the presence of two or more functional groups or to the presence of a group which is itself polytopic. A

typical example is provided by the carboxylate group which presents different coordination modality, schematically represented in Figure 4.

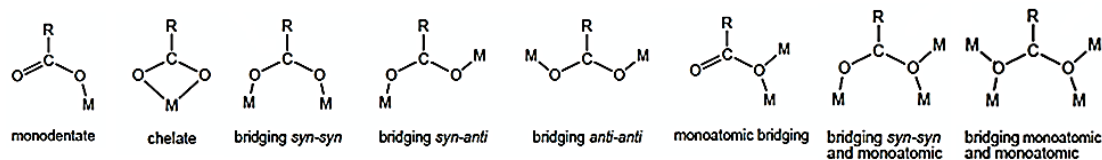


Figure 4. Coordination modes of the carboxylate group.

The *monodentate* and *chelate* coordination modes are monotopic, while the other ones are polytopic so they can generate CPs.

The *linker* comprehends the functional, donor, groups and a central fragment defined *spacer*. The *spacer* connects the donor fragments and often plays a relevant role in the definition of the CP geometry, representing the more easily tunable part of the entire structure. The choice of ligands structural features is at the base to obtain compounds having different structural peculiarities. It is possible to employ rigid linkers with various sizes, flexible linkers characterized by different steric hindrance and conformational freedom and so on. The rigid linkers are preferred in the structure design because during the assembly they may retain a greater structural control. They present a unique directionality unlike flexible spacers containing aliphatic chains that, through the free rotation around bonds, may take the more stable conformation, causing variations in the assembly directionality.

The *node-linker* moiety forms the repetitive unit which is often defined as *Secondary Building Unit*, SBU. The periodical repetition of SBUs through coordination bonds form one-, two-, or three-dimensional structures that can be porous [Figure 5]. The recurrent structural motif is normally characterized by considerable stability and it is constituted by a well-defined number of metal centers (one or more), joined by polytopic linkers, to favor the polymeric development.

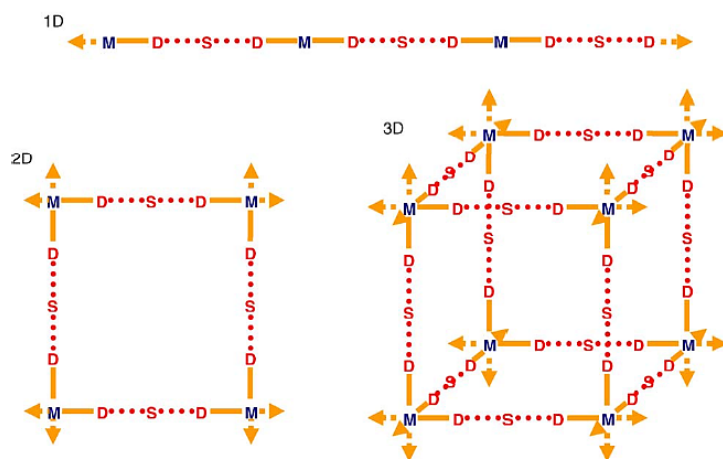


Figure 5. Schematic examples of polymeric structures with 1D, 2D and 3D extensions constituted by metal *node* (M), donor *linker* (D) and *spacer* (S).¹⁰

For instance, it is possible to use rigid ligands with the same functional group and different spacers; changing the length of the rigid spacer only the distance among nodes is modified while the system morphology is maintained. These cases can give iso-reticular series among which, the most explanatory is the *IsoReticular Metal Organic Framework* (IRMOF) series, synthesized by O. Yaghi research group¹¹ [Figure 6].

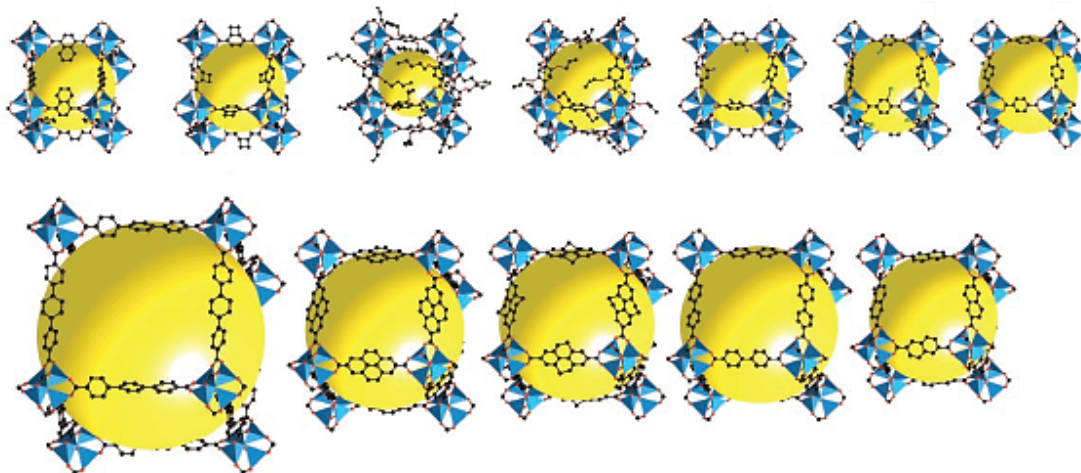


Figure 6. Single Crystal X-ray structures of IRMOF's series. Blue polyhedral represents Zn_4O moiety. The yellow spheres represent the largest Van der Waals spheres that would fit in the cavities without touching the frame-works (hydrogen atoms are omitted).¹¹

Besides the coordination bonds, various typologies of non-covalent interactions may contribute to the final geometry and stability of CPs.

An important role in the structure packing is given by the attractive or repulsive forces between molecules, or parts of the same molecule, other than those due to covalent bonds or electrostatic interactions among ions. These are classified as Van der Waals forces as: i) permanent dipole-permanent dipole; ii) permanent dipole-induced dipole; and iii) instantaneous dipole-induced dipole (London dispersion forces). These interactions are relatively weak compared to normal chemical bonds, nevertheless they may play a role in the self-assembly of CPs.

Among the non-covalent interaction the most relevant is the H-bond (D-H \cdots A) which is determined by a distance lower than 3.5 Å between the heteroatoms and a D-H \cdots A angle larger than 90°. Within this range, the ideal length for a strong H-bond is about 2.7 Å and an angle of 170-180° [Figure 7].

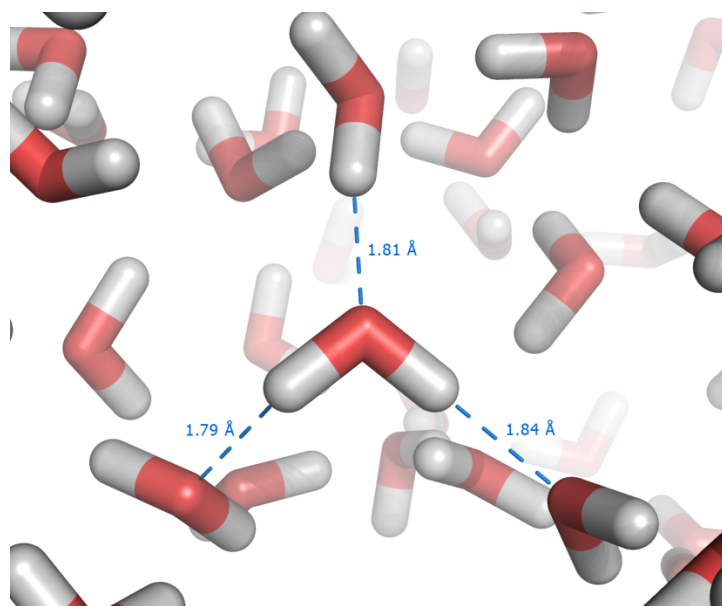


Figure 7. Representation of H-bonds between water molecules. The figure shows the distance between hydrogen and acceptor atom.

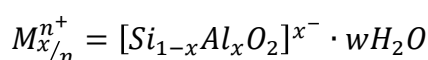
Finally, in the supramolecular structures are often found π - π stacking interactions that involve the electron density of faced aromatic rings presenting energy of about 10 KJ/mol.

1.2 Porosity

The potential applications of Coordination Polymers are mainly based on their possible porosity. Nevertheless, the presence of empty spaces (pores) in materials is an uncommon feature. This is due to the tendency to maximize the attractive intermolecular forces, in order to obtain the highest energy stabilization. Anyway, porosity is a desired characteristic because allows the diffusions into the materials bulk of molecular guests with shape- and size-selectivity according to the shape and size of the pores themselves. Additionally, the possible presence of functional groups in the structures cavities may develop specific host-guest interaction, thus obtaining chemoselectivity. By these specific interactions the guest could be activated undergoing chemical transformations. Moreover, guest molecules may be exchanged with other species previously embedded in the pores or trapped in the material.

Thanks to these properties porous materials are widely used in chemical industry. The traditional, most known porous materials are zeolites and activated carbons.

Zeolites are based on a completely inorganic structure of alkaline or alkaline earth alumina-silicates with generic formula:



where M stands for metal. Zeolites are crystalline solids obtained by the packing of corner-sharing tetrahedral TO_4 (T=Si, Al) which defines interconnected tunnels or cages in which water molecules and M^{n+} ions are inserted.¹² The porosity is provided through the elimination of the water molecules, the framework usually remaining unaffected by this. The resulted system is a three-dimensional arrangement of regular pores [Figure 8].

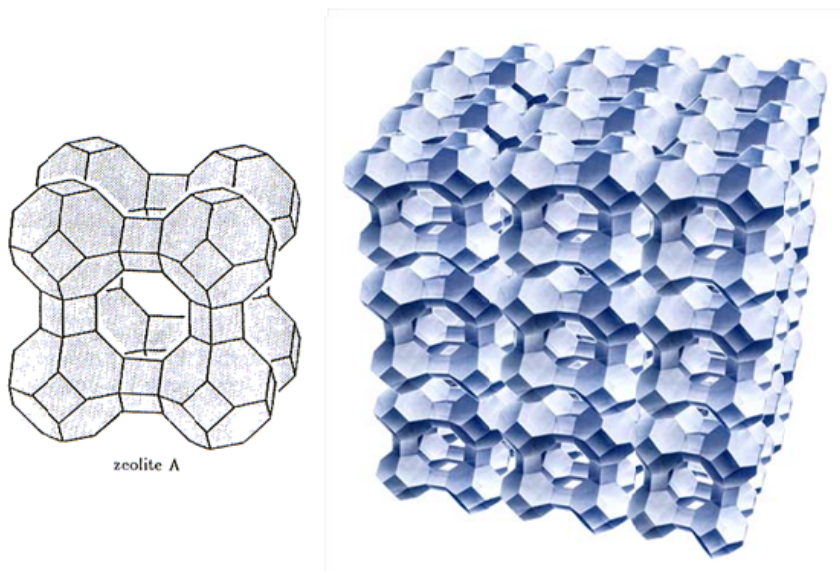


Figure 8. Schematic representation of Zeolite A pores and its 3D development.

The cavities, whose structure is usually determined by the number of polyhedra surrounding the pore, were initially exploited for molecular-sieve requirements in gas separation and catalytic processes. The channels characterized by a dimensional range of few nanometers, place the zeolites in the class of microporous materials. A peculiarity of zeolite structure is the high stability which allows their employing in hard temperature and pressure conditions.

The activated carbons are a class of completely carbon based materials, they present both high porosity and specific surface area. Their structures involve a twisted network of defective hexagonal carbon layers, cross linked by aliphatic bridging groups [Figure 9].

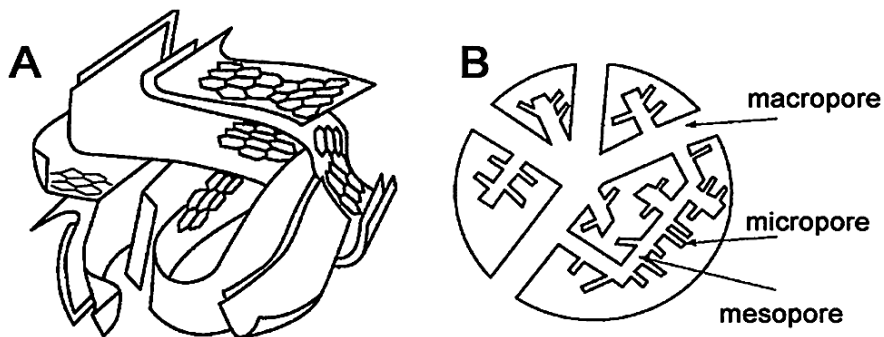


Figure 9. Schematic representations of activated carbons porous structure.

The limit of this typology of materials is the broad pore size distribution which ranges from about 2 nm to 50 nm.¹³ Because of this, pores may be oversized or inaccessible, causing an intrinsic loss of selectivity to the required applications.

The control and fine-tuning of the frameworks for both zeolites and activated carbons are not easy by current synthetic methods.

Compared with other type of molecular materials, CPs have a much higher tendency to form open framework structures robust enough to serve as porous materials. As already mentioned Coordination Polymers are mainly constructed from coordination bonds with the addition of other interactions, such as hydrogen and metal–metal bonds, π – π , CH– π , electrostatic, and van der Waals interactions, and, therefore, networks that are both robust and flexible can be made. In addition, thanks to these interactions, the transition-metal ions required for catalytic sites may be introduced into the pore walls.¹⁴

Although PCPs are normally less stable than activated carbons and zeolites, their crystalline, diversified, designable and tailorable structures where the pore and size surface can be tuned by molecules and framework designs, are highly desirable. However, since nature dislikes vacuum it is practically impossible to synthesize compounds containing vacant space, and the pores will always be filled with some sort of guest molecules which have to be suitably chosen to be volatile and/or easily exchangeable. In crystal engineering, defined as the design and synthesis of pre-determined solid structures having desired properties, the bridging organic ligands used as building blocks can be modified, easily enabling the preparation of tailored structures to obtain pores. However, with large linkers interpenetration and/or catenation frequently occur.

Structurally, there are four types of porous structures: 0D cavities are completely surrounded by wall molecules, in these cavities; channels (1D); layers (2D); and intersecting channels (3D) [Figure 10].

a) Dots (0D cavity) b) Channels (1D space) c) Layers (2D space) d) Intersecting channels (3D space)

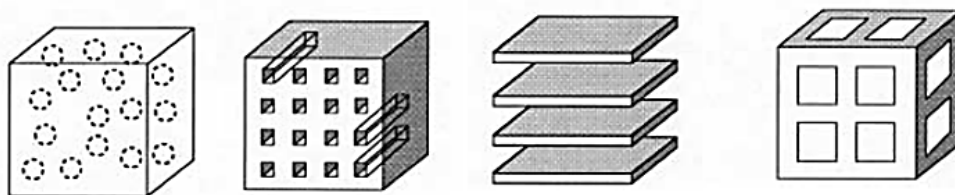


Figure 10. Classes of porous materials based on spatial dimensions.¹⁵

In addition, porous coordination compounds have been classified by Kitagawa¹⁵ in the three categories named *generations*. The 1st generation compounds have microporous frameworks which are sustained only by the presence of guest molecules and show irreversible framework collapse on their removal. The 2nd generation compounds have stable and robust porous frameworks, which show permanent porosity even when guest molecules are removed. The 3rd generation compounds have flexible and dynamic frameworks, which respond to external stimuli, such as light, electric field, guest molecules, and may modify form and dimensions of their channels or pores reversibly [Figure 11].

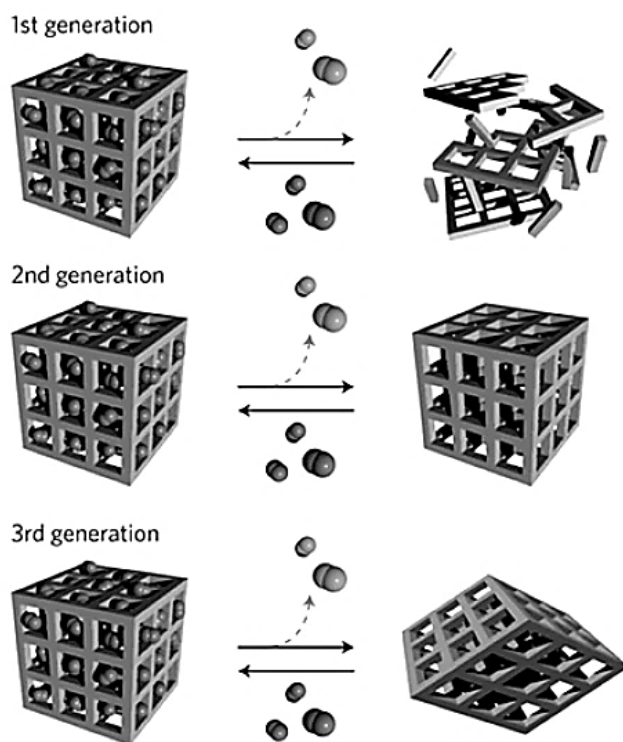


Figure 11. Schematic representation of the classification of Porous Coordination Polymers with respect to their sorption-desorption behavior.¹⁶

In the latter category take a relevant part the so-called *breathing MOFs* which origin from PCPs accommodating guest molecules with “elastic” hydrogen bonds, achieving optimal packing with guest molecules and revealing conformational flexibility unlike rigid systems. The state of the host component without guest molecules forms a new crystalline phase. Therefore, a change in pores size according to adsorption or release of guest molecules occurs. Dynamic pores could come from a bi-stable framework, on which structural rearrangement of molecules proceeds from a “close” phase to the “open” phase responding to guest molecules presence.¹⁷ The flexibility of the structures can be due to changes in flexible linkers or, more often, in the variation of the coordination bond angles around the metal centers.

For instance, the Metal Organic Frameworks MIL-53LT¹⁸ built up from chromium(III) octahedral node and terephthalate linkers forms a three-dimensional framework with a one-dimensional rhombic section channels whose dimensions decrease when water is trapped [Figure 12]. This is due to the formation of strong H-bonds between absorbed water and carboxylate oxygen atoms, thereby causing the constriction of the structure by variation of coordination angles around the metal.

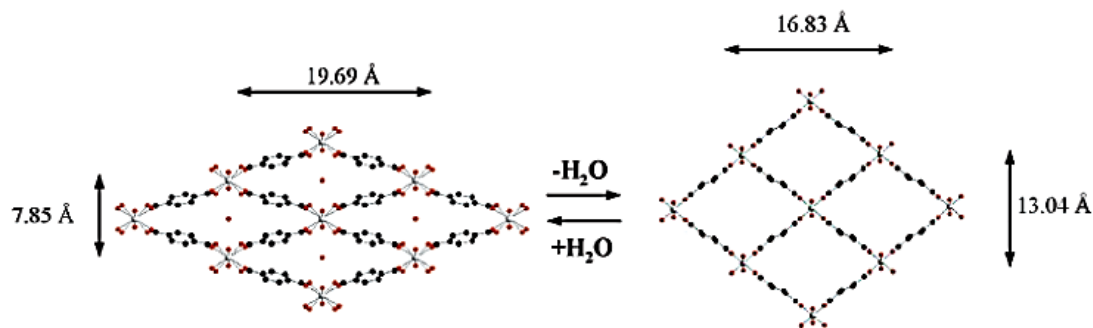


Figure 12. Schematic representation of reversible hydration-dehydration of MIL-53.¹⁸

1.3 Applications of Coordination Polymers

Coordination Polymers are becoming one of the most rapidly developing fields in chemical and material sciences as an important family of porous materials not only because of their intriguing network topologies but also due to their exploitable properties for potential applications in catalysis, gas adsorption and separation.^{19,20}

The use of appropriate metals and linkers for the field of application into account, constitutes a significant advantage over the already mentioned industrial porous materials, because they allows to develop a greater specificity.

1.3.1 Catalysis

On the basis of the known principle of *Green Chemistry*²¹ according to which the catalytic systems are preferable to the use of stoichiometric reagents and, therefore, should be used whenever possible, the development of new catalysts and the study of their mechanism of action are of great interest to reduce waste.

The homogeneous catalysts are usually constituted by coordination complexes and are normally single site catalysts.²² They are characterized by a single type of catalytic sites, all equal to each other, and defined at the molecular level. The homogeneous catalysts allow a better contact with the reactants, since the active site is more accessible, thus entailing a high catalytic activity and higher reaction selectivity.²³ For this reason main enantioselective processes take place in the homogeneous phase. However, the homogeneous catalysts cannot be easily removed from the reaction medium due to their small size and affinity to the solvent. The activity of this class of catalysts is also limited to relatively low temperatures, since their stability decreases markedly with the increase of the temperature. These drawbacks can be overcome through the use of heterogeneous catalysts (for example: oxides or sulfides of transition metals, noble metal particles). However, this alternative is limited by the low selectivity and deactivation of catalysts caused by

processes such as metal leaching and poisoning. In addition, heterogeneous catalysts require complex preparation procedures which are often difficult to reproduce. The heterogeneous catalysts are often not well defined at the molecular level, the active sites are not all the same and they may have different activity and selectivity. The structure of the heterogeneous catalysts allows intrinsically reduced accessibility to the active sites, and makes the catalytic activity significantly limited by mass transfer processes. Support matrices can be used to immobilize soluble catalysts, combining some advantages of homogeneous and heterogeneous catalysts, such as: a simple preparation, a greater ease of study of the mechanism and an easy recovery/removal from the reaction medium. However it is important to evaluate the possible involvement of the substrate in the reaction, which may lead to some inhibition of the activity but also to synergic effects that lead to increase of the activity or selectivity.

In this context, the CPs structures carry peculiarities required to an ideal catalyst and, therefore, represent a promising solution to the above presented catalysts limits.²⁴

The pores of CPs can be tailored in a systematic way allowing the optimization for specific catalytic applications. Besides the high metal content of CPs, one of their greatest advantages is that the active sites are all identical due to the highly crystalline nature of the material.

Although catalysis is one of the most promising application of such materials, only a few examples have been reported to date. Size- and shape-selectivity is based on porosity so the presence of permanent pores is required. The “node and spacer” approach is very attractive for shape-selective catalysis because it provides a route to networks with tunable pore size.²⁵

The synthesis of catalytically active systems can occur in two ways:²⁶ the first modality provides the presence of coordinatively unsaturated metal centers within the structure, obtained also with the presence of coordinated molecules easily removable without distortion of the structure [Figure 13]; the second one requires instead that the catalytic sites are included in the organic linkers structure [Figure 14].

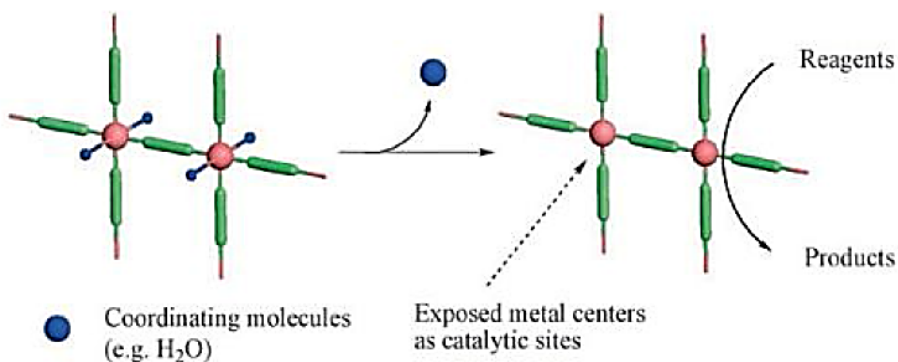


Figure 13. Coordinatively unsaturated metal centers.²⁶

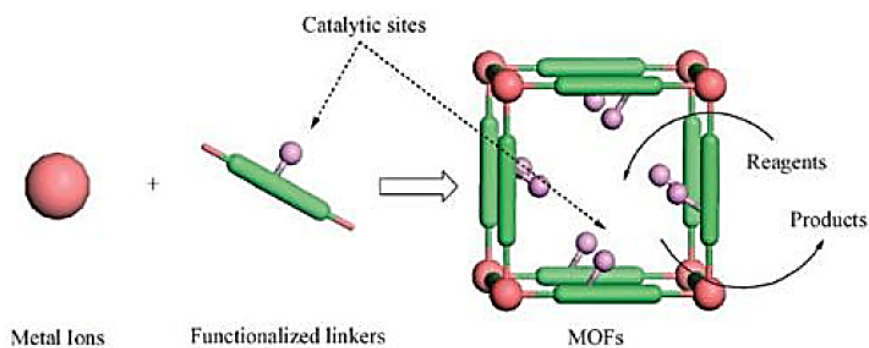


Figure 14. Insertion of catalytic sites in the linkers structure.²⁶

For instance, a porous coordination polymer based on the $[\text{Cu}_3(\text{btc})_2(\text{H}_2\text{O})_3]$ (btc = benzene tricarboxylate ion) SBU presents a *paddlewheel* structure with H₂O molecules facing to cavities.²⁷ These water molecules are easily removed by vacuum, therefore, the Lewis acid Cu(II) results accessible and is active in cyanosilylation of benzaldehyde²⁸ [Figure 15].

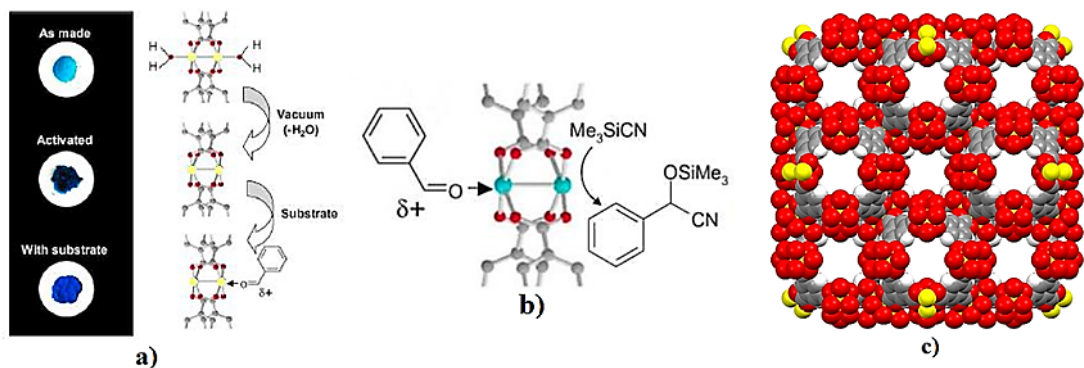


Figure 15. a) color change of $[\text{Cu}_3(\text{btc})_2(\text{H}_2\text{O})_3]$ due to activation under vacuum and substrate adsorption; b) reaction mechanism;²⁸ c) porous packing of the $[\text{Cu}_3(\text{btc})_2(\text{H}_2\text{O})_3]$.²⁷

Kitagawa and co-workers synthesized a 3D porous coordination polymer functionalized with amide groups, $[\text{Cd}(4\text{-btapa})_2(\text{NO}_3)_2] \cdot 6\text{H}_2\text{O} \cdot 2\text{DMF}$ (4-btapa = 1,3,5-benzene tricarboxylic acid tris[N-(4-pyridyl)amide]).²⁹ The amide groups are ordered uniformly on the channel surfaces [Figure 16a] and facilitate the selective accommodation and activation of guests within the channels. Knoevenagel condensation reactions of benzaldehyde with active methylene compounds (*e.g.* malononitrile, ethyl cyanoacetate, and cyano-acetic acid *tert*-butyl ester) were attempted [Figure 16b]. While malononitrile proved to be a good substrate (98% conversion), the other substrates produced negligible results, thus implicating a relationship between the size of the reactants and the pore window of the host.

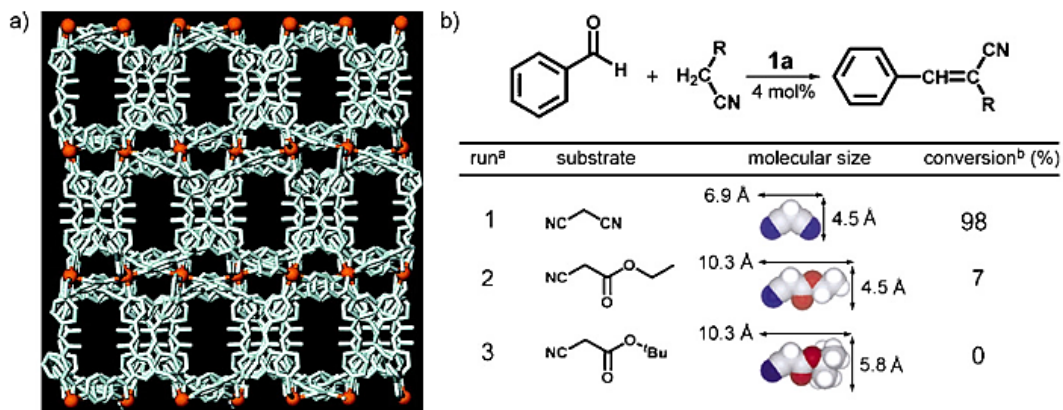


Figure 16. a) Crystal structure to form another type of zigzag channels with dimensions of $3.3\text{Å} \times 3.6\text{Å}$. b) Knoevenagel condensation reaction of benzaldehyde with substrates.²⁹

Seo et al. reported the synthesis of a homochiral metal-organic porous material, $[Zn_3(\mu_3-O)(L)_6] \cdot 2H_2O \cdot 12H_2O$ (referred to as D-POST-1, L = 4-pyridylamide of D-tartaric acid), which uses enantiopure metal-organic clusters as secondary building blocks³⁰ [Figure 17a].

The presence of the pyridyl groups exposed in the channels also provides POST-1 with unique opportunities in catalysis. The catalytic transesterification of ethanol occurred in 77% yield with POST-1 [Figure 17b]. The transesterification with bulkier alcohols such as isobutanol, neopentanol and 3,3,3-triphenyl-1-propanol occurred at a much slower or even negligible rate under otherwise identical reaction conditions [Figure 17c]. Such size selectivity suggests that the catalysis occurs in the channels. The reaction of racemic alcohols produces the corresponding esters with enantiomeric excess in favor of S or R enantiomer depending on the use of D-POST-1 or L-POST-1, respectively.

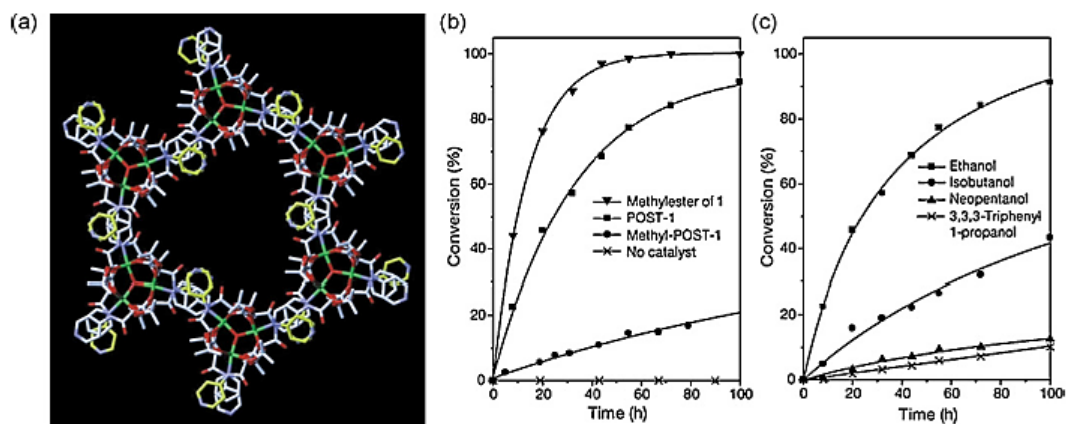


Figure 17. a) The hexagonal framework with large pores that is formed with the trinuclear secondary building units. b) Catalytic activity of POST-1 in transesterification reactions with ethanol, and c) with different alcohols.³⁰

The use of the nanochannels of some PCPs as polymerization sites can allow greater control of the reactions and the formation of single, well-ordered, chains of polymer within the channels of the CP itself.

In this regard, polymerization studies were carried out with the CP $[\text{Cu}_2(\text{pzdc})_2(\text{pyz})]$ (pzdc =pyrazine-2,3-dicarboxylate, pyz =pyrazine) which possess channels having a cross section of $4.0 \times 6.0 \text{ \AA}$, in which the substituted acetylenes entrance is possible.³¹ These channels present on their walls oxygen atoms of the carboxylate groups which allow to adsorb acetylene in a specific way, thanks to the formation of H-bonds between oxygen and -CH groups [Figure 18]. Using more acidic mono-substituted acetylenes, thanks to the presence of electron-withdrawing groups, the extraction of the proton and the consequent generation of a reactive acetylide are obtained. The latter begins an anionic polymerization and form linear polymers with trans configuration, selectively due to steric directionality imposed by the channels.

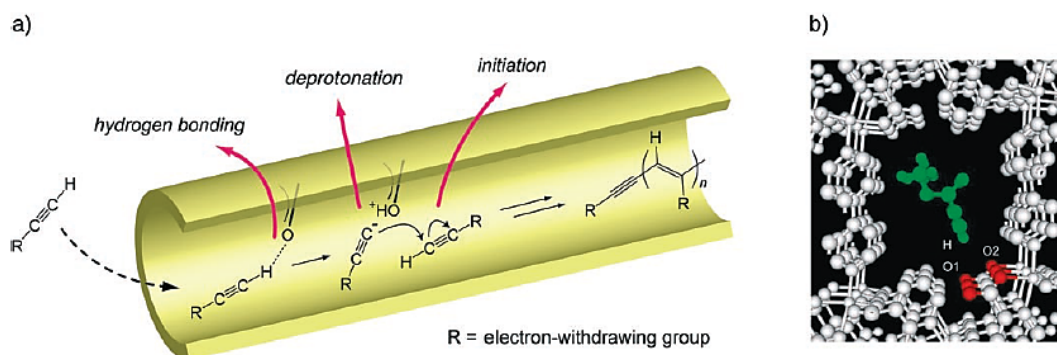


Figure 18. a) Polymerization mechanism by $[\text{Cu}_2(\text{pzdc})_2(\text{pyz})]$ coordination polymer. b) the green-acetylene molecule directionally interacted through H-bonds with red-oxygen of the carboxylate groups of the CP.³¹

A three-dimensional porous CP based on the trinuclear triangular $[\text{Cu}_3(\mu_3\text{-OH})(\text{C}_4\text{H}_2\text{N}_2\text{O}_2)_3(\text{H}_3\text{O})] \cdot 2\text{C}_2\text{H}_5\text{OH} \cdot 4\text{H}_2\text{O}$ SBU exhibits high catalytic activity for the oxidation of CO to CO_2 ³² [Figure 19].

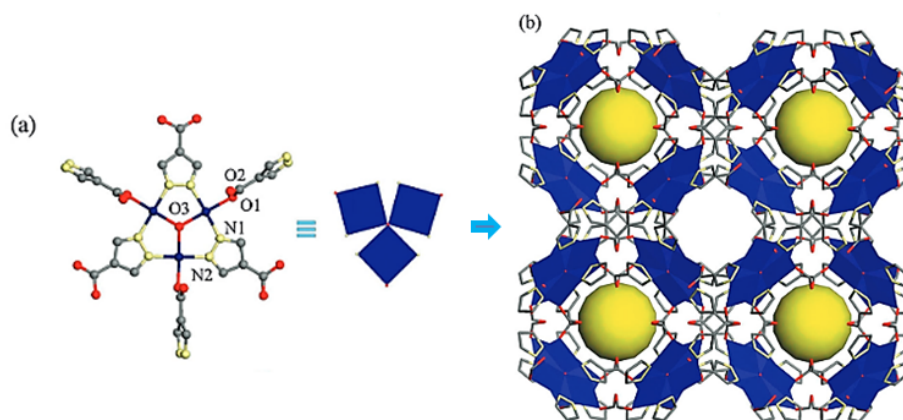


Figure 19. (a) The trinuclear triangular building unit of $[\text{Cu}_3(\mu_3\text{-OH})(\text{C}_4\text{H}_2\text{N}_2\text{O}_2)_3(\text{H}_3\text{O})] \cdot 2\text{C}_2\text{H}_5\text{OH} \cdot 4\text{H}_2\text{O}$ with coordination-unsaturated Cu (II) sites. (b) The 3D PCP with open channels.³²

This compound, obtained by self-assembly of the trinuclear triangular Cu(II) building units presents high porosity (47% empty volumes from the PLATON calculations), dense active metal sites and gives a conversion rate of 100% for the oxidation of CO to CO₂.

1.3.2 Selective gas adsorption

The release of anthropogenic toxic pollutants into the atmosphere is a worldwide risk of growing concern. Common hazardous compounds such as NO_x, SO_x, CO, CO₂, H₂S, NH₃, other nitrogen (e.g. hydrogen cyanide) or sulfur-containing compounds (e.g. organothiols), hydrocarbons, volatile organic compounds (benzene, toluene, methanol, etc.) are of major concern for environmental air pollution.

In view of all the above, the effective sensing, capture and eventually the degradation of these harmful chemicals is of great importance both for the protection of the environment and for health issues. Noteworthy, porous materials are at the forefront of minimizing the undesired effects of toxic gases.

In this regard, PCPs emerged as a consequence of their fascinating potential applications in adsorption and sensing.^{33,34}

The use of porous materials with adequate pore size/shape is not enough for an efficient capture of unsafe gases/vapors and other, more specific, interactions between the hazardous adsorbates and the host are desirable.

For example, the presence of open metal sites (coordinatively unsaturated metal centers) or certain functionalizations on the pore surface may enhance the adsorption selectivity/efficiency of MOFs towards certain toxic compounds via coordination bonds, acid-base/electrostatic interactions, π -complex/H-bonding formation.

In addition, the design of specific interaction in order to selectively adsorb guests molecules has an important industrial interest due to the potential applications in storage and separation.

An example of capture and degradation has been reported by Hill and co-workers.³⁵ The redox active polyoxometalate (POM) $[\text{CuPW}_{11}\text{O}_{39}]_5$ encapsulated in $[\text{Cu}_3(\text{btc})_2]$ operates for the catalytic air based oxidative degradation of H_2S and mercaptane molecules [Figure 19]. Indeed, the $[\text{Cu}_3(\text{btc})_2] \cdot [\text{CuPW}_{11}\text{O}_{39}]$ hybrid material catalyzes the rapid chemo- and shape-selective oxidation of thiols into disulfides and, more significantly, the rapid and sustained removal of toxic H_2S via $\text{H}_2\text{S} + 1/2\text{O}_2 \rightarrow 1/8\text{S}_8 + \text{H}_2\text{O}$ (4000 turnovers in 20 h) while the POM or the MOF alone are catalytically slow or inactive [Figure 20].

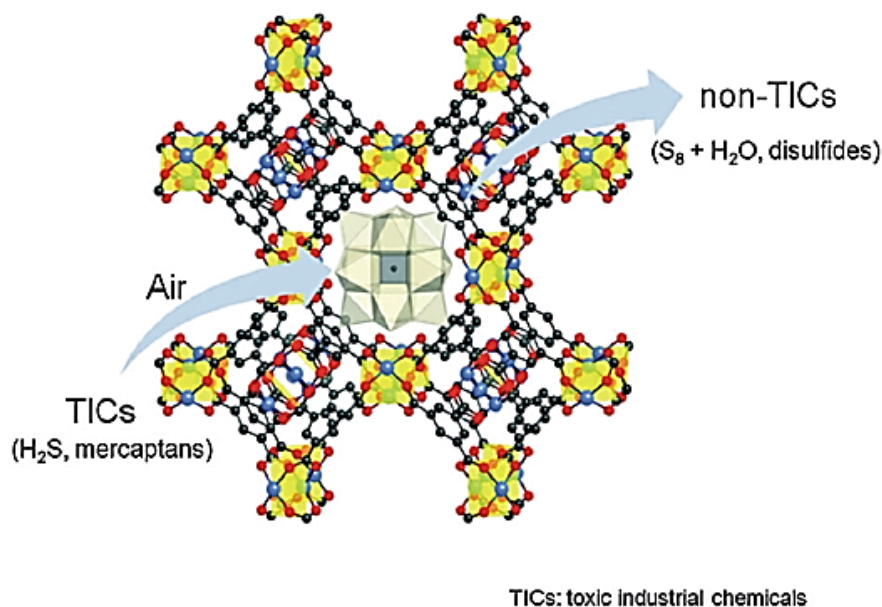


Figure 20. Schematic representation of the selective air oxidation of thiols to disulfides and the oxidation of toxic H_2S to S_8 by $[\text{Cu}_3(\text{btc})_2] \cdot [\text{CuPW}_{11}\text{O}_{39}]$.³⁵

A PCP based on the trinuclear triangular Cu_3 -Pyrazolate complex (UPR-2) presents a selective adsorption of CO_2 . UPR-2 contains $[\text{Cu}_3(\mu_3\text{-OH})(\mu\text{-pz})_3]$ node and 4,4'-bipy as linkers resulting in a three-fold interpenetrated 3D framework³⁶ [Figure 21].

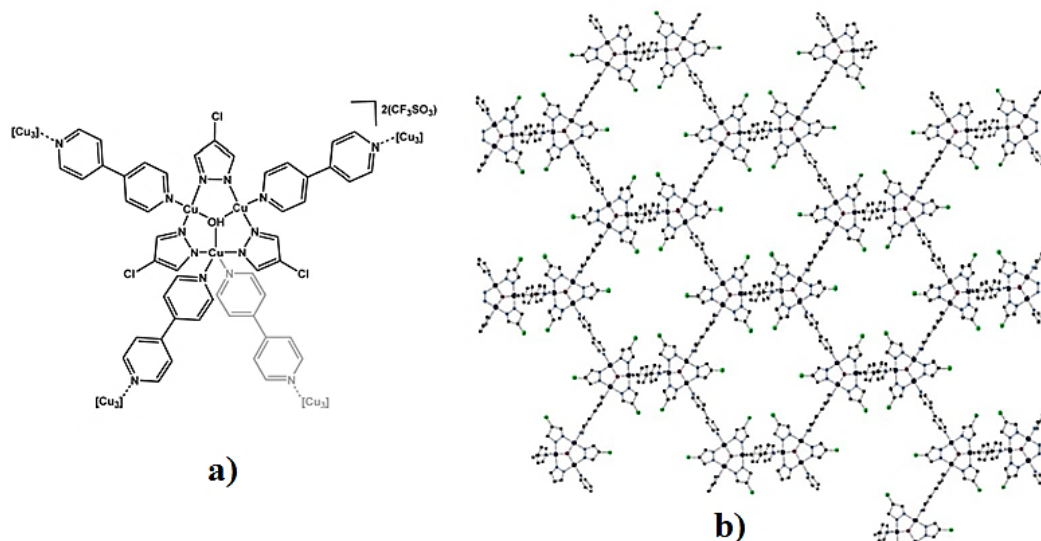


Figure 21. a) SBU showing a four-connecting node. b) One of the three interpenetrating nets of UPR-2.³⁶

UPR-2 in the 0-10 atm range shows low CO_2 sorption capacity but high selectivity over N_2 and H_2 . The different profiles of sorption and desorption are attributed to structural flexibility of the crystal lattice [Figure 22].

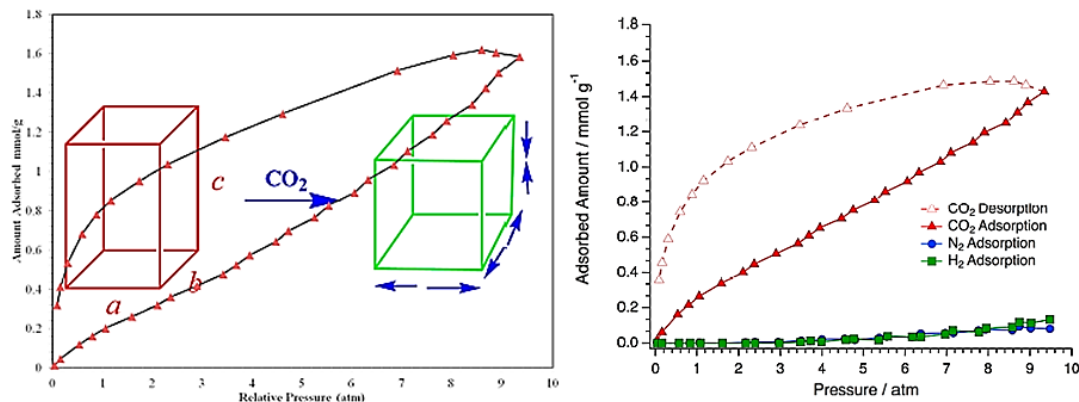


Figure 22. Adsorption isotherm of UPR-2 evidencing (on the left) the hysteretic sorption-desorption profile due to structural flexibility and (on the right) the selective adsorption on CO_2 over N_2 and H_2 .³⁶

The $[\text{Cu}_2(\text{pzdc})_2(\text{pyz})]$, previously reported as catalyst for polymerization reaction, presents high levels of selective sorption of acetylene molecules as compared to carbon dioxide.³⁷

The pores, with a cross-section of $4 \times 6 \text{ \AA}$ can accommodate both of C_2H_2 and CO_2 molecules. Both molecules can potentially be strongly confined in the pore without any chemical interaction, by means of the deep, van der Waals type, potential energy well. On the other hand, pores are also characterized by the presence of carboxylate oxygen atoms acting as basic adsorption sites for guest molecules. Accordingly, this CP exerts an effective sorption ability for small molecules having acidic parts owing to the deep, van der Waals type, potential-energy well and additional hydrogen-bonding interactions.

The C_2H_2 molecule has a linear form with acidic hydrogen atoms at both ends. The CO_2 molecule has a rod-shaped form with dimensions $3 \times 5 \text{ \AA}$, similar to that of C_2H_2 , but it has no acidic protons. Thus this material is a feasible adsorbing medium for the C_2H_2 molecule [Figure 23].

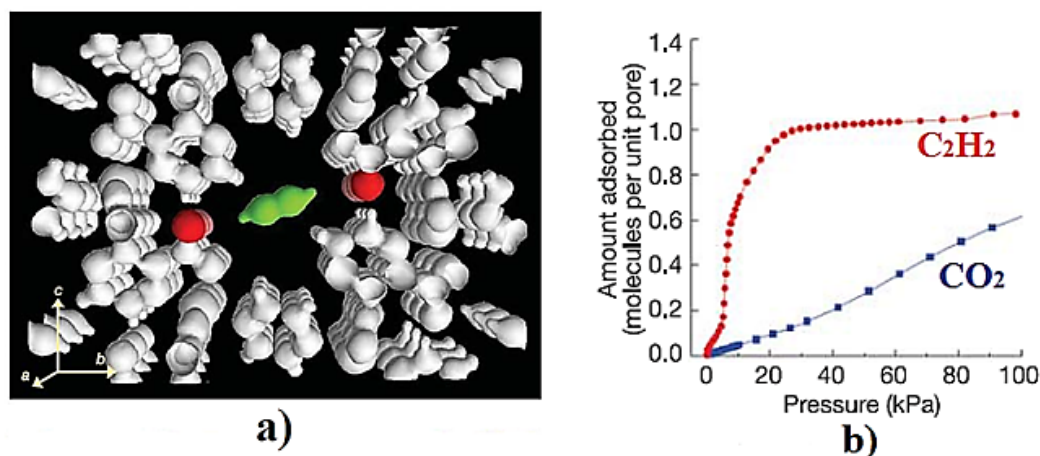


Figure 23. a) MEM electron densities of C_2H_2 adsorbed to $[\text{Cu}_2(\text{pzdc})_2(\text{pyz})]$ complex at 170 K as an equal-density contour surface along the a -axis. b) Adsorption isotherms for C_2H_2 and CO_2 on $[\text{Cu}_2(\text{pzdc})_2(\text{pyz})]$ complex with pressure range of 10^{-4} to 100 kPa and at the temperature of 300K.³⁷

Moreover, due that for each SBUs one molecule of acetylene is retained, this permits the stable storage of acetylene at a calculated density 200 times the safe compression limit of free acetylene at room temperature.

By modulating the characteristics of the framework, such as the surface area of the pores, the free volume, the density of adsorption and the extent of interactions with metal centers it is possible to vary the storage capacity using the same approaches described in Figure 24 for the storage of H₂.³⁸

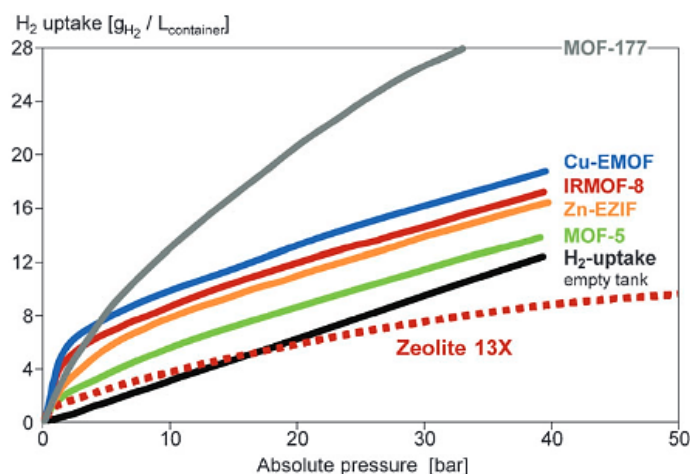


Figure 24. Graph of experimental results for the H₂ storage in containers filled with different MOF and zeolite compared with compression in a vacuum container.³⁸

To obtain a specific interaction with the hydrogen molecule, the interaction between the d orbitals of the transition metals and the antibonding orbital of the H₂ molecule must be employed.³⁹ In this way, energy characteristics depending of the used metal ion are obtained. Overall, the interaction between the framework and the molecule of H₂ must be sufficiently stable to counteract the motions of thermal agitation, yet reversible in order to allow the release of the gas. For this application, the developed materials must therefore present a high concentration of metal ions exposed to the surface of the pores. The pore size is critical to the capacity of gas storage: in structures having very large pores the surface with which the molecules of H₂ can interact is lower than in structures with smaller pores. Increasing the dimension of

pores produces a rise in the amount of adsorbed hydrogen but a decrease in its density.

1.4 Structural determination

The structure–property relationship of natural and synthetic materials has always been an important part of chemical researches.⁴⁰ Crystalline materials such as Coordination Polymers are very attractive because the highly ordered, well defined structures based on non-rigid, rotatable and/or reversible metal–ligand coordination bonds, the weak and changeable supramolecular interactions between multiple coordination networks (either interpenetrated or packed together), and the organic ligands which may be structurally rigid or flexible with various size and characterized by different steric hindrance, conformational freedom and other physical/chemical features, not only produce unique properties but also simplify structural characterizations. Crystalline solids possess property, which is absent in amorphous, liquid, and gaseous states, that is their building blocks arrangement, which develops periodically in the three dimensions.⁴¹ Strict periodicity is an idealization, as a perfect crystal never exists since defects are expected from thermodynamics: indeed, the higher is the disorder the greater is the system entropy and stability. Anyway, periodicity is a good approximation to describe some crystal features.⁴²

In general, it is not possible to predict the structure of even the simplest crystallographic solid from knowledge of their chemical composition, even if many theories have been formulated to describe every energetic contribution that rules matter’s spatial organization.⁴³

Despite theories employ approximations, empirical observations, and deal with idealized models, the prediction of molecules in a crystal needs an enormous amount of variables so calculation become demanding even for the fastest computer beside the fact that they provide an approximate description of the “real things”.

X-ray single crystal diffraction is still the most important and straightforward method for direct visualization of the 3D periodic structures. Quite often, only an X-ray analysis will definitely reveal the composition and three-dimensional arrangement of an unknown compound.

Since Bragg utilized X-ray diffraction to characterize single-crystal structures of simple salts, this technique has been enormously improved in both hardware and software in the past century.

The X-ray diffraction studies and measures the effects of the interaction between an X-ray beam and the crystalline matter. The analysis of the diffraction data allows to determine the crystal structure.

The term *structure* includes the constitutional aspects that are the way the atoms are interconnected one another, i.e. simple or multiple bonds and the spatial organization such as configurations.

Crystallography uses either a single crystal specimen or small amounts of microcrystalline powder.

Generally, exists a unique solution, chemically and physically, consistent with a set of independent reflections obtained for a specific crystal, so the unambiguous interpretation of the structure with SC-XRD is possible.

The structural periodicity of a crystal is represented by translation of the unit cell, which is the smaller unit that maintains all the characteristic of the crystal itself.

The unit cell is defined by six crystallographic parameters which are three non-coplanar vectors a , b , c whose moduli correspond to the lattice periodicity and the three angles α , β , γ between them.

A crystalline sample exposed to a radiation of wavelength (λ) comparable to interatomic distances, origins a discrete diffraction pattern [Figure 25].

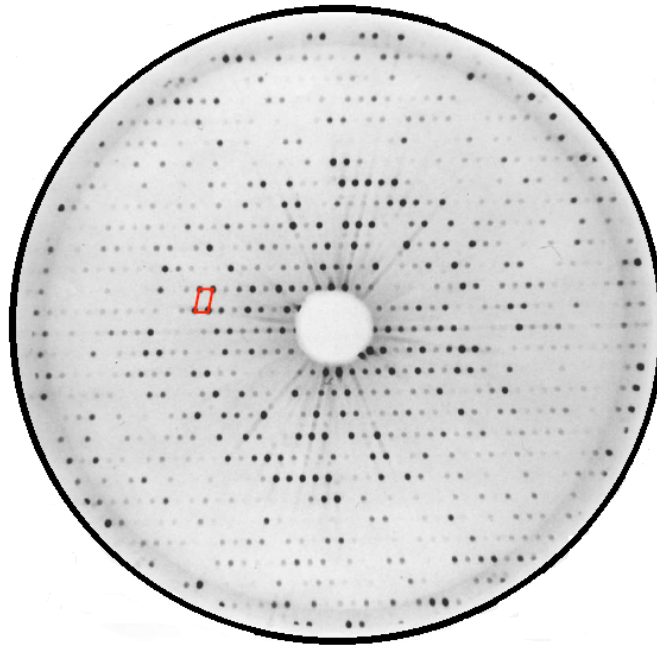


Figure 25. Diffraction pattern obtained by single crystal X-ray diffraction.

The spots (reflections) in fig. 25 are periodically ordinated, according to a geometrical relationship with the crystalline lattice of the specimen. The spacing of atoms in a crystal lattice can be determined by measuring the locations and intensities of spots.

Every reflection arises from the positive interference of the elastically scattered radiation produced by the interaction between electrons and X-ray beam.

The process may be understood at the elementary level by considering how images are generated in a light microscope: i) light from a point source is focused on an object; ii) the light waves are scattered by the object, and iii) these scattered waves are recombined by a series of lenses to generate an enlarged image of the object.

The smaller object whose structure can be determined by such system is established by the wavelength of the visible light. Object smaller than half the wavelength of the incident light cannot be resolved. Therefore, to resolve object as small as molecules X-rays, which have wavelength in the range of 0.7-1.5 Å, are necessary. However, there is no lenses that can recombine X-ray to form an image; instead the pattern of diffracted X-rays is collected directly and an image is reconstructed by mathematical technique.

An electron density of the constitutive unit is obtained from the overall diffraction pattern of spots by using Fourier transform. This allows to build an electron-density map consistent model for the structure.

X-rays are generated by a high-voltage power applied between a cathode (a W or Re filament) and a metal target (usually Cu or Mo) acting as anode. The filament is crossed by current (20-40 mA) and ejects a beam of electrons which are accelerated under vacuum by the high voltage. As the electron beam strikes the anode, X-rays are emitted in form of a characteristic narrow-line spectrum superimposed on a broadband white radiation due to the incoherent collisions between the electron beam and the anode [Figure 26].

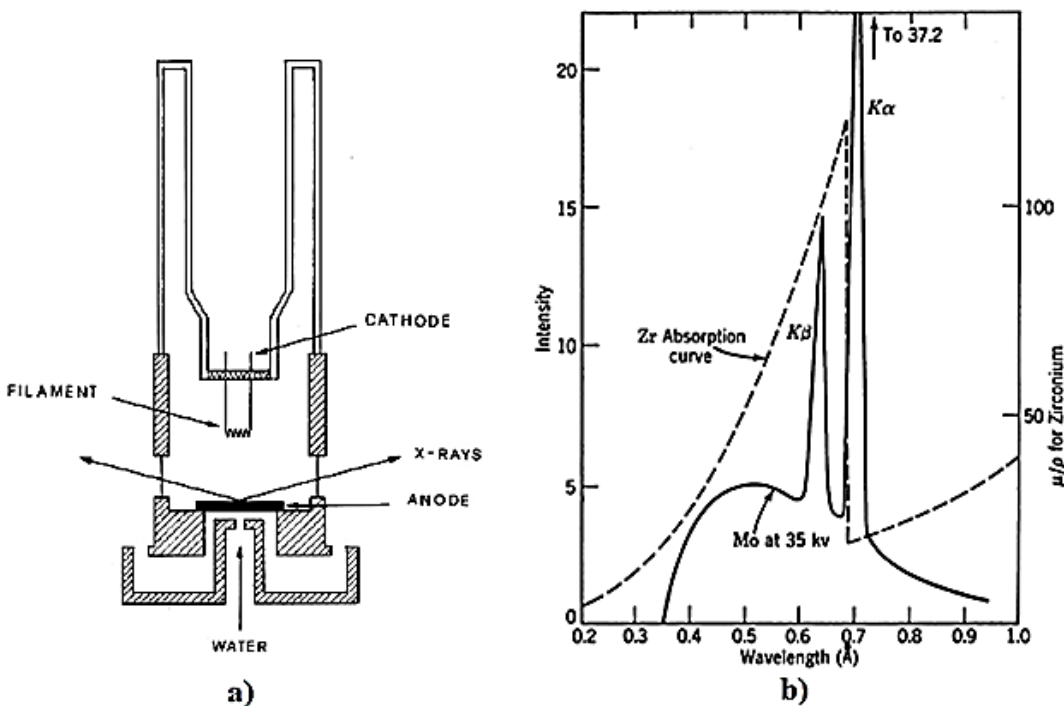


Figure 26. a) Scheme of X-ray source; b) the emitted spectrum for a Mo-anode and the Zr absorption curve.

The X-ray beam coming out from Be windows located on the X-ray tube is then filtered (e.g. Zr crystal filter), in order to select one characteristic line (K α , being this the most intense line). wavelength λ , depending on the metal target (e.g. CuK α = 1.5418 Å, MoK α = 0.7107 Å), is then collimated and sent to the specimen. The

crystal to be analyzed is mounted on a goniometer which rotates it in different orientations with respect to the incident beam. Then, the position and intensities of the diffracted beams are detected.

SC-XRD measured by common X-ray sources can already provide not only precise atomic coordinates, bond lengths and bond angles, but also atomic thermal displacements and occupancies.^{44,45} High-resolution crystal structures are critical for determining the precise atomic positions, so that pore size, pore shape and pore surface structures of CPs can be obtained to understand the structure-property relationship.

A crucial step for using this analysis technique is the formation of suitable single crystals whose dimensions must be in the range of 50-300 μm . Consequently, the structure determination completely depends upon the ability to grow single crystals of sufficient quality and size [Figure 27].

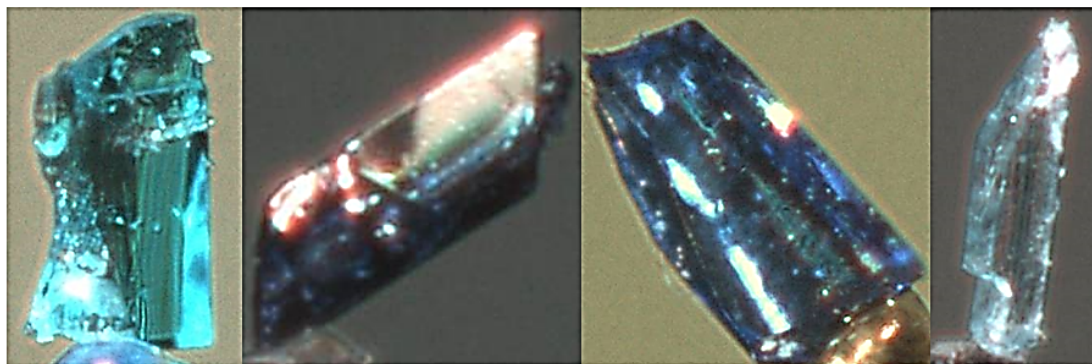


Figure 27. Some of the obtained suitable crystals for SC-XRD.

Several synthetic ways can be adopted for getting crystals which are extended and ordered assemblies of molecules. Different chemical species require different strategies. Some of the most exploited procedures have been described by Jones.⁴⁶

When the compound is soluble the crystallization is possible by *slow cooling of saturated solutions* in order to gradually reduce its solubility. Another strategy for soluble compound consists in *liquid diffusion* of a small amount of solution in a suitable precipitant [Figure 28].

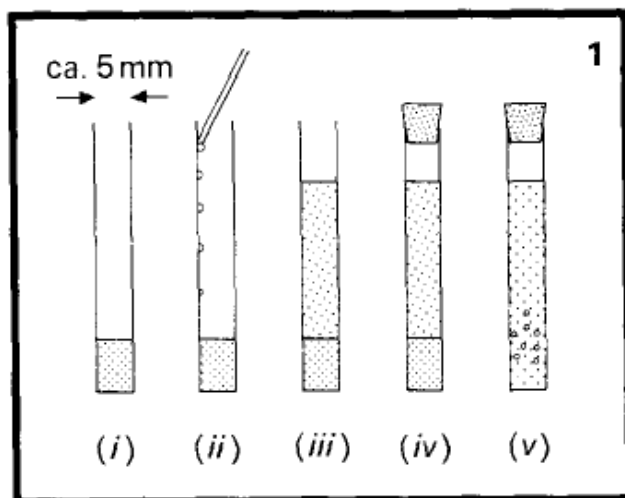


Figure 28. The liquid diffusion method. (i) Solution of compound to be crystallized. (ii)-(iii) Slowly layer on the precipitant. (iv) Stopper and leave overnight: do not disturb. (v) Crystals form at the interface.⁴⁶

Vapor diffusion technique exploits the same principle of the previous method, but the precipitant is allowed to diffuse into the solution from the vapor phase.

Diffusion of reacting solutions is used with compound arising from precipitation of the reaction product between two solutions of reagents. Crystals may be often obtained by layering one reacting solution on the other. Any luck, the crystallization techniques require a slow rate of precipitation or reaction which can be modulated by temperature and solvents.⁴⁷

As previously mentioned, also microcrystalline powders are suitable samples for X-ray analysis. These are composed by a great number of small crystals randomly oriented. The isotropic feature of the sample produces a diffractogram characterized by a series of concentric diffraction cones in place of the discrete spots [Figure 29a] and the output can be plotted in two dimensions as intensity against 2θ angle [Figure 29b].

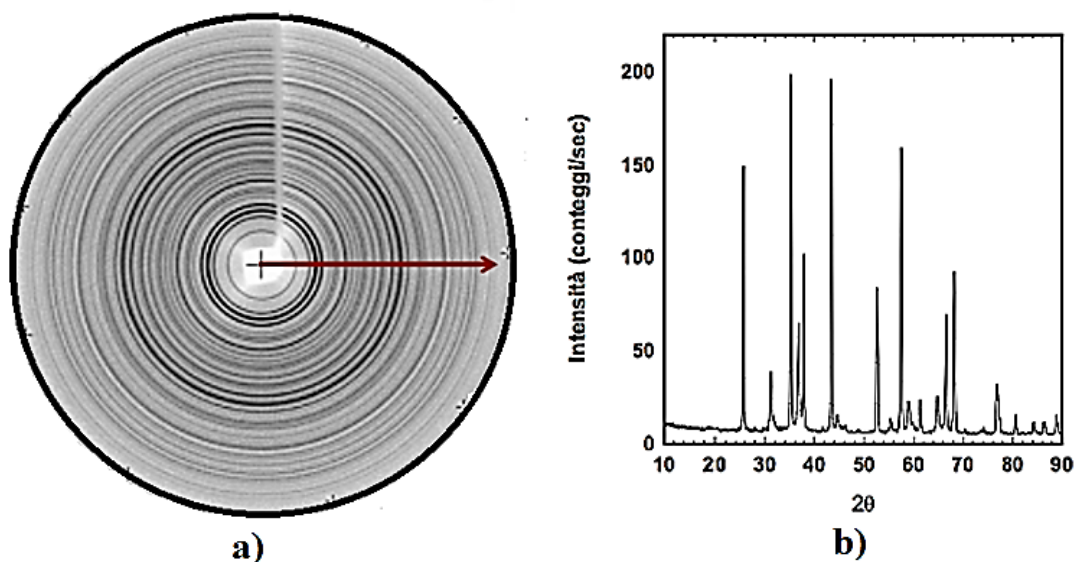


Figure 29. a) Powder diffraction rings. b) Powder diffraction pattern.

The plotted reflections are indexed and cell parameters can be calculated. A complete structure determination from these diffraction patterns is not possible due to poorness of information with respect to the variables. Actually *ab initio* determination from XRPD (X-ray powder diffraction) data is still a very difficult or even impossible challenge.⁴⁸

Nevertheless, this technique provides important qualitative information in relation to phase determination, purity, crystallinity and particle size.

In addition, from the SC-XRD data it is possible to obtain a calculated XRPD diffractogram which, compared with the experimental, allows to establish the similarity or diversity between the structures.

2. OBJECT OF THE THESIS WORK

As previously exposed, Coordination Polymers are being recognized as multifunctional materials thanks to their features and applications. In this context, it is to put in evidence that BASF produced some CPs⁴⁹ which are now commercialized by Sigma-Aldrich under the name Basolite A100, C300, F300, Z1200 and Basosiv M050 and that high throughput strategies to synthesized interesting CPs have been recently proposed.⁵⁰

My thesis work involves two main points:

- a) The synthesis of new CPs, preferably based on the trinuclear triangular SBUs $[\text{Cu}_3(\mu_3\text{-OH})(\mu\text{-pz})_3]$ joined by bicarboxylate anions.
- b) The structural characterization of synthesized compounds by Single Crystal XRD (SCXRD) determination, including the execution of the measurements and the resolution of the structures.

In the laboratories where I developed my thesis work, the synthesis and characterization of CPs, mainly based on the trinuclear triangular fragment $[\text{Cu}_3(\mu_3\text{-OH})(\mu\text{-pz})_3]$, have been pursued in the last years, with the aim to incorporate the $[\text{Cu}_3(\mu_3\text{-OH})(\mu\text{-pz})_3]^{2+}$ metal site in PCPs to enhance the potential storage properties and catalytic performances,^{51,52,53} troughs the design of efficient and mild condition synthetic strategies. Until now, the attention has been directed mainly on CPs obtained with the one-pot reaction of copper(II) mono-carboxylates with pyrazole, carried out in protic solvents. In this conditions the trinuclear moieties self-assembles into 1D or 2D CPs and as hexanuclear cluster and supramolecular networks.^{54,55,56}

In these syntheses a relevant role seems to be played by the basicity of carboxylate ions, that favors the deprotonation of pyrazole and water to produce pyrazolate and hydroxyl ions needed to obtain the trinuclear moiety. This hypothesis is suggested by the fact that the reactions of CuCl_2 or $\text{Cu}(\text{NO}_3)_2$ with Hpz lead to trinuclear triangular species only if an exogenous base as KOH,

NaOH, etc. is added.⁵⁷ Moreover, also the reaction of copper(II) trifluoroacetate with Hpz yielded only the mononuclear $[\text{Cu}(\text{CF}_3\text{COO})_2(\text{Hpz})_2]$ species, being the trifluoroacetate anion unable to efficiently deprotonate water and Hpz.⁵⁵ In this context, with the aim to become familiar with this kind of reactions and to get further insights in the mechanisms connected to the formation of the above mentioned trinuclear triangular copper derivatives, the reaction of Hpz with copper(II) chloroacetate (pK_a of ClCH_2COOH 2.87⁵⁸) has been planned and carried out.

Moreover, in order to obtain structural peculiarities such as porosity and increased framework stability, the syntheses of CPs based on the above mentioned trinuclear fragments joined by bi-carboxylate ions have been performed, by using both rigid (with various sizes) and flexible (with different steric hindrance and conformational freedom) bicarboxylate linkers.

The reactions were first attempted by the usual procedure, i.e. by adding Hpz to solutions of copper bi-carboxylates, but the scarce solubility of the latter, especially those that incorporate large organic anions, limits the efficiency of this reaction. In fact, the required excess of pyrazole favors the formation of mononuclear copper compounds. In addition, since the obtained CPs are normally insoluble, they may result often impure for the unreacted precursor. Therefore, with the purpose of using the reagents in stoichiometric amounts with respect to the desired product and in order to start from soluble reagents, a different synthetic procedure has been also adopted, consisting in the pre-synthesis of a trinuclear node as that present in the $[\text{Cu}_3(\mu_3\text{-OH})(\mu\text{-pz})_3(\text{CH}_3\text{COO})_2(\text{Hpz})]$ species and in the successive substitution of the acetates with desired bi-carboxylate. When it was possible both the two synthetic procedures were adopted to put in evidence any possible differences.

Products (both CPs or discrete complexes) obtained as “stable” crystals of suitable dimensions have been characterized by SC-XRD determinations. Polycrystalline species have been instead characterized through Powder XRD (XRPD) measurements, performed by Dr. Federico Zorzi at the Geosciences Department of the University of Padua.

3. EXPERIMENTAL SECTION

3.1 Materials and Methods

The reagents and solvents used in the following syntheses which are commercially available, were used without further purification. Copper chloroacetate, methylsuccinate and dimethylsuccinate were synthesized according to the procedure described by Dubicki *et al.*⁵⁹ from corresponding dicarboxylic acids and copper carbonate. $[\text{Cu}_3(\mu_3\text{-OH})(\mu\text{-pz})_3(\text{CH}_3\text{COO})_2\text{Hpz}]$ complex was obtained from the synthesis reported in the literature⁶⁰. All reactions were carried out in air.

Elemental analyses (C, H, N) were performed in the Microanalysis Laboratory of the Chemistry Department of Padua University, with a *Fisons Instruments 1108 CHNS-O Elemental Analyzer*.

Infrared Spectra were measured in the range of 4000-600 cm^{-1} with a *Jasco FT/IR-4100 Spectrophotometer* in ATR modality. Spectral bands were always reported in cm^{-1} and the following code was adopted: s = strong, m = medium, w = weak.

The magnetic susceptibility measures were obtained at room temperature with the *Sherwood Scientific MSB-Auto Balance* (Gouy method) using $\text{HgCo}(\text{NCS})_4$ as standard for calibration. The magnetic moments, expressed in B.M. (*Bohr Magneton*), were calculated by the equation $\mu_{\text{eff}} = 2.84 \cdot (\chi_m^{\text{corr}} \text{ T})^{1/2}$, using the correct molar magnetic susceptibility considering the diamagnetic contributions. The latter was calculated, with reference to the reported formula for each compound, employing Pascal constants.⁶¹

XRPD investigations were carried out by Dott. Federico Zorzi at the Department of Geosciences of the Padua University using a Panalytical X'Pert Pro diffractometer.

SC-XRD data for unit cell determinations and whole structure solution were collected at the Department of Geosciences of Padua University using an Agilent Technologies SuperNova diffractometer. The program CryAlis RED⁶² was used to compute and refine unit cell parameters; for further details and structure solution see Section 4.

3.2 Synthetic procedures

- Reaction of [Cu(Clac)₂] with Hpz

To a solution of 1.38 g of [Cu(Clac)₂] (5.52 mmol) in 50 mL of MeOH, a solution of Hpz (618 mg, 9.1 mmol) in 4 mL of MeOH was added under stirring. The resulting deep blue solution was let to evaporate in the air yielding pale-blue platelets of **1a**, suitable for a SC-XRD determination, that were washed with few drops of MeOH and dried in the air. In a second recrystallization fraction, a mixture of light-blue (**1b**) and dark-blue (**1c**) crystals formed. The crystals were manually separated and employed for SC-XRD determinations.

1a. Yield: 1.054 g, 60% (with respect to Hpz). Elem. Anal. Calcd for Cu(Clac)₂(Hpz)₂: C = 31.06; H = 3.13; N = 14.49. Found: C = 30.65, H = 3.09, N = 13.91. IR (ATR, cm⁻¹): 3145, 3118, 2985, 2945, 1574, 1553, 1404, 1364, 1253, 1169, 1152, 1071, 1050, 956, 931, 916, 886, 853, 784, 687, 617. μ_{eff} (293 K) = 2.277 BM (calculated for C₁₀H₁₂Cl₂CuN₄O₄).

- Reaction of [Cu₃(μ_3 -OH)(μ -pz)₃(CH₃COO)₂Hpz] with 1,4-Phenylenediacrylic acid (H₂PheDiAcr)

To a solution of 235 mg ($3.96 \cdot 10^{-4}$ mol) of Cu₃(OH)(pz)₃(CH₃COO)₂Hpz in 100 ml of MeOH a solution of 84 mg ($3.85 \cdot 10^{-4}$ mol) of H₂PheDiAcr in 15 ml of DMF was added under stirring, obtaining a blue-green suspension. A light blue microcrystalline solid (**2a**) was filtered, washed with MeOH and dried under vacuum, yielding 250 mg of product (98%).

2a. Elem. Anal. Calcd for Cu₃(OH)(pz)₃(PheDiAcr)(H₂O)₂ C=38.24; H=3.36; N=12.75. Found: C=38.25; H=3.87; N=12.62. IR (cm⁻¹): 3266w, 1635m, 1552m, 1420m, 1380s, 1280w, 1179m, 1059m, 978m. μ_{eff} (292.15K): 3.306 BM calculated for Cu₃O₇N₆C₂₁H₂₂.

- Synthesis of single crystals from reaction between
[Cu₃(μ₃-OH)(μ-pz)₃(CH₃COO)₂Hpz] with H₂PheDiAcr

Dropping in 24 hours a 25 ml DMF solution of 18 mg ($8.25 \cdot 10^{-5}$ mol) of H₂PheDiAcr acid in a solution of 50 mg ($8.41 \cdot 10^{-5}$ mol) of [Cu₃(OH)(pz)₃(CH₃COO)₂Hpz] in 100 ml of DMF led, after four days, to the formation of single crystals **2b**. The obtained crystals dried in the air, change their nature to polycrystalline material (**2a**). Covering a single crystal with glue the SC-XRD measurement was possible.

- Reaction of [Cu₃(μ₃-OH)(μ-pz)₃(CH₃COO)₂Hpz] with
Biphenyl-4,4'-dicarboxylic acid (H₂BipheDiCarb)

To a solution of 200 mg ($3.36 \cdot 10^{-4}$ mol) of Cu₃(OH)(pz)₃(CH₃COO)₂Hpz in 100 ml of MeOH, a solution of 83 mg ($3.43 \cdot 10^{-4}$ mol) of H₂BipheDiCarb in 30 ml of DMF was added under stirring, obtaining a dark blue suspension. A blue-gray microcrystalline solid (**3a**) was filtered, washed with MeOH and dried under vacuum, yielding 190 mg of product (83%).

3a. Elem. Anal. Calcd for Cu₃(OH)(pz)₃(BipheDiCarb)(H₂O)₂ C=40.32; H=3.24; N=12.27. Found: C=40.30; H=3.29; N=10.97. IR(cm⁻¹): 3350w, 3147w, 1581m, 1536m, 1383s, 1175m, 1059m, 759m. μ_{eff}(292.15K): 3.400 BM calculated for Cu₃O₇N₆C₂₃H₂₂.

- Reaction of [Cu₃(μ₃-OH)(μ-pz)₃(CH₃COO)₂Hpz] with
trans,trans-Muconic acid (H₂Muc)

To a solution of 206 mg ($3.46 \cdot 10^{-4}$ mol) of Cu₃(OH)(pz)₃(CH₃COO)₂Hpz in 100 ml of MeOH, a solution of 50 mg ($3.52 \cdot 10^{-4}$ mol) of H₂Muc in 20 ml of MeOH was

added under stirring, obtaining a blue suspension. A light blue microcrystalline solid (**4a**) was filtered, washed with MeOH and dried under vacuum, yielding 136 mg of product (70%).

By evaporation of mother liquors some light-blue crystals formed (**4b**).

4a. Elem. Anal. Calcd for $\text{Cu}_3(\text{OH})(\text{pz})_3(\text{Muc})(\text{H}_2\text{O})$ C=31.86; H=2.85; N=14.87. Found: C=31.47; H=2.65; N=13.20. IR(cm^{-1}): 3351w, 1615m, 1538m, 1380s, 1180m, 1054m, 1002m, 772m. $\mu_{\text{eff}}(299.15\text{K})$: 2.970 BM calculated for $\text{Cu}_3\text{O}_6\text{N}_6\text{C}_{15}\text{H}_{16}$.

- Reaction of $[\text{Cu}_3(\mu_3\text{-OH})(\mu\text{-pz})_3(\text{CH}_3\text{COO})_2\text{Hpz}]$ with *trans*- β -Hydromuconic acid (H_2HyMuc)

To a solution of 198 mg ($3.33 \cdot 10^{-4}$ mol) of $\text{Cu}_3(\text{OH})(\text{pz})_3(\text{CH}_3\text{COO})_2\text{Hpz}$ in 100 ml of MeOH, a solution of 52 mg ($3.60 \cdot 10^{-4}$ mol) of H_2HyMuc in 10 ml of DMF was added under stirring, obtaining a blue suspension. A light blue microcrystalline solid (**5a**) was filtered after three hours, washed with MeOH and dried under vacuum, yielding 91 mg of product (44%).

5a. Elem. Anal. Calcd for $\text{Cu}_3(\text{OH})(\text{pz})_3(\text{HyMuc})(\text{H}_2\text{O})_2(\text{MeOH})$ C=31.12; H=3.92; N=13.62. Found: C=31.36; H=3.25; N=13.14. IR(cm^{-1}): 3348w, 3140w, 2933w, 1555s, 1419m, 1379s, 1176s, 1060s, 759m. $\mu_{\text{eff}}(292.15\text{K})$: 3.344 BM calculated for $\text{Cu}_3\text{O}_8\text{N}_6\text{C}_{16}\text{H}_{24}$.

By evaporation of light blue mother liquors polycrystalline blue material and some light-blue crystals (**5b**) formed. SC-XRD measurement was performed on **5b**.

In a second synthetic procedure the filtration of the first obtained product was done after 1 h. From mother liquors blue crystals of (**5c**) formed. SC-XRD measurement was performed on (**5c**).

5c. Elem. Anal. Calcd for $\text{Cu}_3(\text{OH})(\text{pz})_3(\text{HyMuc})(\text{DMF})$: C=34.73; H=3.73; N=15.76. Found: C=34.37; H=3.57; N=15.47. IR(cm^{-1}): 3354w, 3124w, 2938w, 1656m, 1551s, 1422m, 1383s, 1178s, 1061s, 751m.

- Reaction of $[\text{Cu}_3(\mu_3\text{-OH})(\mu\text{-pz})_3(\text{CH}_3\text{COO})_2\text{Hpz}]$ with Methylsuccinic acid (H_2MeSuc)

To a solution of 248 mg ($4.16 \cdot 10^{-4}$ mol) of $\text{Cu}_3(\text{OH})(\text{pz})_3(\text{CH}_3\text{COO})_2\text{Hpz}$ in 125 ml of MeOH a solution of 57 mg ($4.31 \cdot 10^{-4}$ mol) of H_2MeSuc in 15 ml of H_2O was added under stirring, obtaining a blue solution. The stirring was interrupted and the becker was covered. After 24h the formation of blue cubic crystals was observed (**6a**). SC-XRD measurement was performed by covering crystals with glue. The obtained crystals dried in vacuum become polycrystalline materials **6b**.

6b. Elem. Anal. Calcd for $\text{Cu}_3(\text{OH})(\text{pz})_3(\text{MeSuc})(\text{H}_2\text{O})(\text{MeOH})$ C=30.67; H=3.78; N=14.31. Found: C=30.20; H=3.20; N=14.45. IR(cm^{-1}): 3421w, 3125w, 2972w, 1543s, 1417m, 1383m, 1280m, 1177m, 1060s, 763s. $\mu_{\text{eff}}(299.15\text{K})$: 3.827 BM calculated for $\text{Cu}_3\text{O}_7\text{N}_6\text{C}_{15}\text{H}_{22}$.

- Reaction of $[\text{Cu}_3(\mu_3\text{-OH})(\mu\text{-pz})_3(\text{CH}_3\text{COO})_2\text{Hpz}]$ with (S)-Methylsuccinic acid (S- H_2MeSuc)

To a solution of 251 mg ($4.22 \cdot 10^{-4}$ mol) of $\text{Cu}_3(\text{OH})(\text{pz})_3(\text{CH}_3\text{COO})_2\text{Hpz}$ in 125 ml of MeOH a solution of 59 mg ($4.31 \cdot 10^{-4}$ mol) of S- H_2MeSuc in 15 ml of H_2O was added under stirring, obtaining a blue solution. The stirring was interrupted and the becker was covered. After 24h the formation of blue cubic crystals was observed (S-**6a**). SC-XRD measurement was performed by covering crystals with glue. The obtained crystals dried in vacuum become polycrystalline materials (S)-**6b**.

(S)-**6b.** Elem. Anal. Calcd for $\text{Cu}_3(\text{OH})(\text{pz})_3(\text{MeSuc})(\text{H}_2\text{O})(\text{MeOH})$ C=30.67; H=3.78; N=14.31. Found: C=32.73; H=2.92; N=13.72. IR(cm^{-1}): 3446w, 3415w, 3140w, 2975w, 1546s, 1413m, 1382m, 1280m, 1178m, 1055s, 764s.

- Reaction of Cu(MeSuc) · 2H₂O with Hpz (MeSuc = Methylsuccinate ion)

To a suspension of 206 mg ($8.89 \cdot 10^{-4}$ mol) of Cu(MeSuc) · 2H₂O in 30 ml of H₂O a solution of 94 mg ($1.38 \cdot 10^{-3}$ mol) of Hpz in 10 ml of H₂O was added under stirring. After four hours a blue-green suspension was filtered. The product (**7a**) was washed with water and dried under vacuum.

7a. Elem. Anal. Calcd for Cu₃(OH)(pz)₃(MeSuc)(H₂O)(MeOH) C=30.67; H=3.78; N=14.31. Found: C=30.24; H=3.02; N=13.46. IR(cm⁻¹): 3429w, 3134w, 2971w, 1544s, 1418m, 1385m, 1281m, 1172m, 1053s, 766s.

- Reaction of Cu(DimeSuc)·2H₂O with Hpz (DimeSuc = 2,2-Dimethylsuccinate ion)

To a suspension of 286 mg ($1.16 \cdot 10^{-3}$ mol) of Cu(DimeSuc) · 2H₂O in 50 ml of H₂O, a solution of 188 mg ($2.76 \cdot 10^{-3}$ mol) of Hpz in 30 ml of H₂O was added under stirring, obtaining a blue solution. Maintaining the solution at a temperature below to 10°C prismatic blue crystals formed (**8a**) while by evaporation at r.t. a blue amorphous film on the surface of the solution was obtained (**8b**).

8a. Elem. Anal. Calcd for Cu₃(OH)(pz)₃(DimeSucc)(H₂O)(Hpz) C=32.74; H=3.56; N=17.98. Found: C=32.80; H=3.99; N=16.53. IR(cm⁻¹): 3384w, 3139w, 2972w, 1544s, 1415m, 1385m, 1284m, 1177m, 1056s, 755s.

8b. Elem. Anal. Found: C=28.22, H=2.95, N=13.54. IR(cm⁻¹): 3391w, 3135w, 2978w, 1591s, 1403s, 1380s, 1249m, 1178m, 1061s, 765s.

- Reaction of $[\text{Cu}_3(\mu_3\text{-OH})(\mu\text{-pz})_3(\text{CH}_3\text{COO})_2\text{Hpz}]$ with 2,2-Dimethylsuccinic acid ($\text{H}_2\text{DimeSuc}$)

To a solution of 227 mg ($3.82 \cdot 10^{-4}$ mol) of $\text{Cu}_3(\text{OH})(\text{pz})_3(\text{CH}_3\text{COO})_2\text{Hpz}$ in 125 ml of MeOH, a solution of 57 mg ($3.90 \cdot 10^{-4}$ mol) of $\text{H}_2\text{DimeSuc}$ in 20 ml of H_2O was added under stirring, obtaining a blue solution. After 24 h the formation of blue needles **9a** was observed. The obtained crystals dried in the air, change their nature to polycrystalline materials (**9b**). SC-XRD measurement was performed by covering **9a** crystals with glue.

9b. Elem. Anal. Calcd for $\text{Cu}_3(\text{OH})(\text{pz})_3(\text{DiMeSucc})(\text{H}_2\text{O})_2$ C=30.67; H=3.78; N=14.31. Found: C=28.14; H=3.40; N=12.45. IR(cm^{-1}): 3596w, 3147w, 1555s, 1420m, 1385m, 1284w, 1180m, 1059m, 797s. $\mu_{\text{eff}}(299.15\text{K})$: 3.010 BM calculated for $\text{Cu}_3\text{O}_7\text{N}_6\text{C}_{16}\text{H}_{22}$.

4. SC-XRD STRUCTURE DETERMINATION

4.1 Data Collection

Single crystal X-ray diffraction, from which intensity data collections are obtained, were performed using Agilent Technologies SuperNova diffractometer, equipped with a Dectris Pilatus 200K detector. A micro X-ray source working at 50 kV and 0.8 mA (40 W) was used to produce $M\alpha$ radiation with beam size of 110 μm . The sample-detector distance was 68 mm. The measures were carried out in the air at room temperature; both to mount the crystal and, in some cases, to cover it in order to prevent single crystal decomposition causes by possible evaporation of solvent molecules included in the structure glue was used.

To set up and control the data collection process the program *CryAlis* PRO 171.37.35e version⁶² was used. The diffracted intensities were acquired up to 55° in 2 θ , using a 1° ω _scan with exposure time range from 20 to 60 s, recording a total of 14 runs and 1245 frames.

4.2 Data Processing

X-ray diffraction data processing consists in the conversion of spots to numbers. For this purpose, indexing and integration program, that is in our case *CryAlis* RED software package,⁶² proceeds according to the following steps. Starting from the position of the reflections of few images an initial estimation of cell parameters and so of the reticular system are obtained. The unit cell dimensions are estimated by finding three non-coplanar vectors that best described the diffraction pattern, ideally allowing indexing of all the reflections. For each unit cell proposed by the software, the percentage indexing of the peaks is provided: for high-quality diffraction data can be close to 100%, while low values may be caused by sample defects such as mosaicity, twinning, or problems occurred during data collection. In fact, from this

process, also a mosaicity estimation is achieved. In addition, from the presence of the systematic extinction which are centering concerning, is estimated the Bravais lattice. Then using a larger number of images Bravais lattice is validated and cell parameter are refined. Established the Bravais lattice and the dimensions of the unit cell in real space, it becomes possible to derive the corresponding reciprocal lattice and, comparing the measured reflections positions, indexing the reflections themselves i.e. assign indices h, k, l , which identify each lattice plane. Resolution of each spot is the distance between these planes. To maximize resolution and completion of data set is important to set up the previously described data collection strategy.

At this point, it is available the peaks integration and, accordingly, intensities determination I_{hkl} . From diffraction image frames intensity peaks are identified by setting a proper intensity threshold value. After background subtraction of the integrated intensities, it is made an initial reduction of data going from partial reflections to those integers and then merging and scaling of multiple measurements of reflections with identical values of h, k, l indices. At this point, Friedel pairs and symmetric reflections are held separate. By scaling a correction of systematic errors occurs, comparing reflections with same indexes measured in more than one frame. These differences can be derived by different crystal volumes, exposure times, radiation damage, different or fluctuating source intensities, different absorption due to different paths through the crystal and other matter and so on.

After the intensities scaling of the integers indexed reflections and therefore known the reciprocal lattice based on symmetry lattice and systematic extinctions it is given the Patterson symmetry. It must be in agreement and so confirm the assumptions made at the beginning of the process on the type of Bravais lattice. Finally, observing the systematic extinctions related to screw axes and glide planes, space group is determined.

At this point, the scaling and merging of intensities of Friedel pairs and symmetry equivalent reflections are possible. This makes the data internally consistent.

Once scaled, the remaining differences between observations can be analyzed to give an indication of data quality, though not necessarily of its absolute correctness.

A further revision to be applied is the Lorentz-polarization correction:

$$L_p = \frac{1 + \cos^2\theta}{2\sin 2\theta}$$

The above formula relates to the different speed at which the points of the reciprocal lattice remain in diffraction conditions and also to the fact that the light is scattered with different intensities which vary with direction output.

Additional instrumental corrections are applied and, for this purpose, the software refers to the parameter files of each specific experiment. It contains information about the instrumental settings such as geometry: kind of source; beam-stop position; sample-to-detector distance and so further. To avoid the integration of too much noise, lowering data quality, it is important to establish the diffraction maximum angle of the sample which in our case is not greater than about 55 degrees. As a fact, the higher is the scattering angle and thus the resolution, the lower is the intensity. Therefore, high resolution intensities, despite containing fine structure details, may be altered by the high noise contribution. The resolution limit is chosen case by case after careful examination of the data.⁶³

Data quality is evaluated from number of collected reflections compared to the theoretical number to that resolution, the redundancy, their mean intensity and mean I/σ , where σ is the standard deviation for the measured intensity, and then from the internal residual index R_{int} .

I/σ should preferably be more than 2 for data to be used in structure solution. R_{int} is a very useful parameter to be checked: it gives an account of the consistence among equivalent reflections intensities in a set. R_{int} is calculated as follows:

$$R_{int} = \frac{\sum_H |F_j^2 - \langle F^2 \rangle|}{\sum_H [\langle F^2 \rangle]}$$

This means we are considering a unique reflections H resulted from averaging of n equivalent reflections, being $\langle F^2 \rangle$ their mean intensity, and for each of them j we

compare its intensity F_j^2 with the mean. The comparison is made for each unique reflection, and divided by the sum of the mean intensities over all the unique reflections.

For structural purposes, data should have a low overall R_{int} , and, by properly limiting the resolution, we have always tried to obtain datasets with R_{int} not exceeding 0.2, as data that are not even consistent with each other cannot be consistent with a molecular model. It is worth noting that a main cause for R_{int} to rise is primarily absorption effects, so absorption correction is always recommended, as it will improve data quality and consistence.

4.3 Data Elaboration

From the data processing step are obtained two type of file: one containing reflection data and the other containing every kind of structural information such as unit cell parameters, space group, chemical composition, atomic coordinates and ADPs, additional geometrical and chemical information and so on. This file also contains some experimental parameters generally including temperature and wavelength λ and, finally, specific program instructions.

There are several software packages to treat this data, obtaining the solution of crystal structure, of which it is used WinGX version 2014.1.⁶⁴ The choice is based on the type of structure to work with, such as small molecules or macromolecules and the operative system in use.

This software contains several crystallographic programs, concerning data analysis such as E-statistics⁶⁵ and space group determination, structure solution (SIR-92⁶⁶) and refinement (SHELXL⁶⁷), and also, some tools for symmetry and structure analysis (PLATON⁶⁸). In addition, during the refinement stage through X-RED⁶⁹ and X-SHAPE⁷⁰ programs numerical absorption correction is obtained using the correct chemical composition and space group. Publication output via the CIF format is fully supported and extensive checking of CIF syntax and IUCr data validation is possible.⁷¹

A WinGX project make use of the atomic scattering factors taken from International Tables for X-Ray Crystallography. After each program cycle, an updated output file is produced.

4.4 Structure Solution by Direct Methods with SIR-92

From the experiment a quantity proportional to the magnitude of structure factor was obtained.

$$I_{hkl} \propto F_0^2$$

The aim is the interpretation of the X-ray diffraction intensities, which is the basis of the methods for crystal structure determination. The aim is the construction of the structure factor as the Fourier transform of the electron density function (ρ) in each point (xyz) within the unit cell, first as a Fourier integral and later as a sum of atomic contribution, and proceed to the electron density function which is re-expressed as a Fourier synthesis, the coefficients of which are the structure factors.

$$\rho(xyz) = \frac{1}{V} \sum_{hkl} F_{hkl} e^{-2\pi(hx+ky+lz)}$$

The relation between the available $|F(\mathbf{h})|$ and the desired $F(\mathbf{h})$ is:

$$F(\mathbf{h}) = |F(\mathbf{h})| \cdot e^{i\varphi(\mathbf{h})}$$

The above relation lead to the phase problem: *to determine the crystal structure is needed both magnitudes and phases of the structure factors, whereas only quantities related to magnitudes are furnished by the experiment.*

Direct methods (DMs) exploit implicit relations between structure factor amplitudes and implicit phase relations to solve the phase problem without any additional

assumptions. These relations are based on the fact that in a real molecular structure, the variables giving rise to the structure factor distribution such as the atomic coordinates are not independent random variables. DMs is a statistical approach relies on the assumption that the electron density in the unit cell can never be less than 0, and the assumption that atoms are discrete entities.

Overall, the application of these methods for the structure solution can be summarized by the following steps:

- 1) Identify the strongest reflections
- 2) Guess the phases of the reflections and determine the appropriate phase relationships
- 3) Use the guesses to calculate an approximate phase angle (α_{hkl}) for each reflection
- 4) Use the approximate α_{hkl} values to calculate $\rho(xyz)$ and plot it
- 5) Interpret the electron density map in chemically sensible way

If the last step is not good the process must be repeat from point 2.

A fundamental necessity for direct methods is that the interatomic distance between the atoms to be found is larger than the spacing d_{\min} corresponding to the resolution of available diffraction data.

E-Statistics module calculates the mean intensities for the reflection data and compares them with theoretical predictions for a random assembly of the given atoms. It produces the Wilson plot from which approximate overall scale factor and overall thermal parameter are estimated, which will be used as initial values for the following calculations.

Then we must confirm the previously determined by data processing space group with *Assign SpaceGroup* or HKL TOOL module. The module reads the reflection data checking for symmetries and systematic extinctions and then proposes one or more possible space groups. The choice is sometimes uncertain, so one may perform different attempts and verify how the structure solution program works using the selected space group. In some cases, when structure solution is difficult, it may be

necessary to work selecting a lower symmetry space group and restore the true symmetry in a subsequent moment.

SIR was developed to solve crystal structures by Direct Methods and contains a fully automated structure determination procedure to solve the phase problem and provides a reasonable model of the structure.

4.5 Structure Refinement with SHELXL-2004

The refinement process begins from the raw structure obtained as solution by SIR output. The software *SHELXL* uses as input files the reflection data and the atoms/cell instructions one.

The least squares refinement is carried out by full-matrix methods against all F^2 -values.

The molecular fragment obtained with *SIR-92* is analyzed and check for incorrectly assigned atoms: those having unreasonable ADPs are deleted and atom types where changed when incorrectly attributed.

After running *SHELXL*, the molecular model is updated and a difference-Fourier map is calculated, which displays new electron density peaks to interpret. Using the chemical knowledge of the sample it is possible to assign new atoms to the peaks and then refine again.

Ongoing it is useful to switch to anisotropic ADPs for possibly all non-hydrogen atoms or at least for the heaviest ones. This usually improves the model in a great extent, and allows for more accurate detection of new electron density peaks.

The refinement process is repeated until all non-hydrogen atoms in the asymmetric unit are found.

In general, it is difficult to locate hydrogen atoms accurately using X-ray data because of their low scattering power, and because the corresponding electron density is smeared out, asymmetrical, and is not centered at the position of the nucleus but shared in the covalent bond. In addition, hydrogen atoms tend to have larger

vibrational amplitudes than other atoms. For most purposes it is thus preferable to calculate the hydrogen positions according to well-established geometrical criteria and then to adopt a refinement procedure which ensures that a sensible geometry is retained. *SHELXL* provides several models to calculate and refine the various kinds of hydrogen atoms (aromatic, primary aliphatic, secondary aliphatic, OH etc.). For our samples we always make use of the so called “riding model” in which H coordinates are calculated from the corresponding C coordinates plus a fixed distance vector, and the isotropic ADP is multiple (1.2 or 1.5 times) of the one of the C it rides on.

During this process same indexes are taken into account to check if the last introduced modifications have improved or worsened the agreement between our model and the experimental data. This exam uses the previously appointed *R*-factor, in addition, to describe the quality of the model with respect to the experimental data the *Goodness of Fit* (GooF) is used:

$$GooF = S = \sqrt{\frac{\sum w(F_O^2 - F_C^2)^2}{n - p}}$$

where n is the number of reflections, p the total number of parameter and w is the weight calculated as $w = \frac{1}{\sigma^2(F_O^2) + (aP)^2 + (bP)}$ where $P = \frac{2F_C^2 + \text{Max}(F_O^2, 0)}{3}$, a and b are adjustable parameters (the program purposes a suitable value for them after each run). GooF value should be close to 1 and this is accomplished by properly adjusting the weighting scheme.⁷²

During refinement it is desirable that a certain over determination of the parameters is maintained, to ensure the reliability of the model. In the practice it is preferable when n/p is 10 or more. Thus, when necessary, constraints and restraints can usefully be applied, in order to add chemical information to the experimental data. A constraint is an exact mathematical condition enabling one or more least squares variables to be expressed exactly in terms of other variables or constants, and hence eliminated reducing p . A restraint instead, takes the form of additional information

that is not exact but is subject to a probability distribution; it is treated as an extra experimental observation, with an appropriate standard deviation, and has the effect of increasing n .

When each atom of the asymmetric unit is assigned, and any further change does not improve the model anymore (*i. e.* R indexes do not decrease) we can claim the refinement is complete.

5. STRUCTURES DESCRIPTION

- $[\text{Cu}(\text{ClCH}_2\text{COO})_2(\text{Hpz})_2]$, **1a**

A SC-XRD determination, carried out on a light-blue crystal of the first, higher yield, isolated product from the reaction between copper chloroacetate and pyrazole, evidenced the formation of the mononuclear species $[\text{Cu}(\text{ClCH}_2\text{COO})_2(\text{Hpz})_2]$, crystallized in the P_{-1} space group.

The molecular structure of **1a** can be described as a mono-dimensional CP on which two chloroacetate ions bridge, with *syn-anti* geometry, two Cu ions generating also an eight-membered metallacycle [Figure 30]. Two inversion centers are present, one of these coincides with the copper atom position and the other one is in the center of metallacycle.

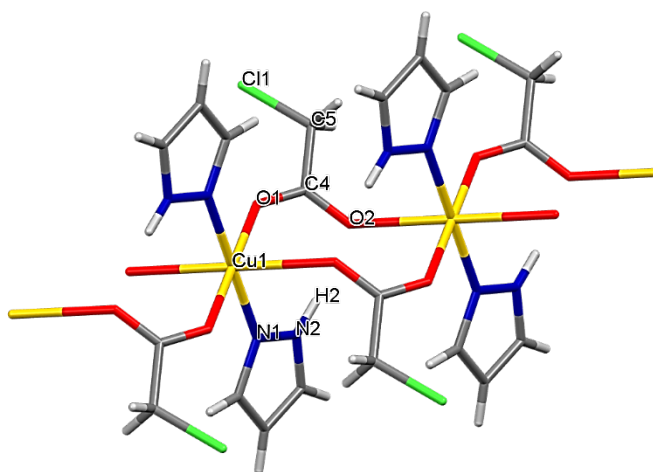


Figure 30. Capped-Stick representation of 1D CP formed by chloroacetate anions bridging $\text{Cu}(\text{Hpz})_2$ moieties.

The length of copper-oxygen bond involving the oxygen atom of the carboxylate group with *anti*-geometry (Cu1-O2), is 2.464 Å while Cu1-O1 distance is 2.004 Å. The latter is comparable with the 1.997 Å of the copper-nitrogen bond length. Accordingly, the resulted coordination geometry of Cu1 is a distorted octahedron, where the elongation of a tetragonal axis is in agreement with the predictions of the

Jahn-Teller theorem for a d^9 electronic configuration. About this, the previously highlighted presence of the inversion center on the copper atom position is crucial.⁷³ Although the unequal distances and the different energy of Cu-O bonds, there is a good electron delocalization in the carboxylate group, evidenced by C4-O1 and C4-O2 distances of 1.256 Å and 1.250 Å, respectively. In this context, it is to be noted that the carboxylate group is involved in a quite strong H-bond interaction with O2-oxygen atom as acceptor and the N2 nitrogen-hydrogen group of pyrazole as donor, with a N \cdots O distance of 2.695 Å and an angle N-H \cdots O of 165.59°. Considering this, the sum of the two weaker interactions, associated to O2, become comparable to the stronger one O1-Cu1, thus justifying the homogeneous delocalization in the carboxylate group. Moreover, this H-bond interaction probably also contributes to the stabilization of the metallacycle.

The mono-dimensional polymer develops in the crystallographic *a*-axis direction. In the crystal packing each chain is isolated from the other ones and not involved in any significant interaction.

- $[\text{Cu}_4(\text{OCH}_2\text{COO})_2(\text{ClCH}_2\text{COO})_2(\text{pz})_2(\text{Hpz})_2(\text{MeOH})_2]$, **1b**

From the second crop of isolated crystals, it was possible to separate two distinct species. A SC-XRD determination carried on one of them, revealed the molecular structure of compound **1b**, whose principal peculiarities can be described observing its asymmetric unit [Figure 31a]. In the dinuclear copper fragment it is possible to recognize some similarities with a portion of a trinuclear triangular Cu^{II} moiety [Figure 31b]. Actually, there are two copper ions connected by a μ -pyrazolate anion and by a central oxygen. Moreover, a pyrazole molecule is coordinate to a copper atom while a carboxylate anion is coordinated to the other one. The most relevant feature of **1b** is the presence of the C7-C8-O2 chain bridging both Cu1 and O1, thus forming a five membered cycle. This bridging structure likely formed through a dehydrochlorination reaction involving a μ -OH group and a second coordinated chloroacetate group, according to the proposed pathway sketched in Scheme 1.

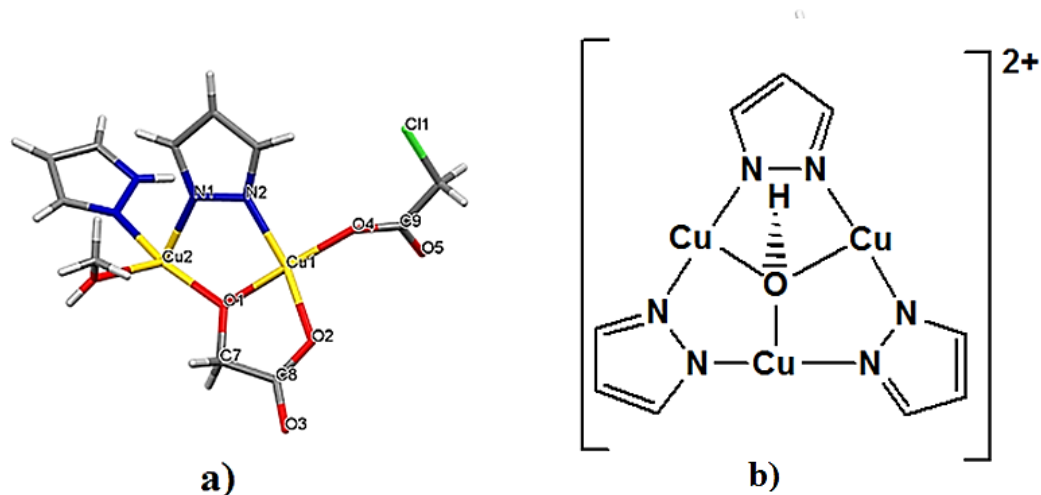
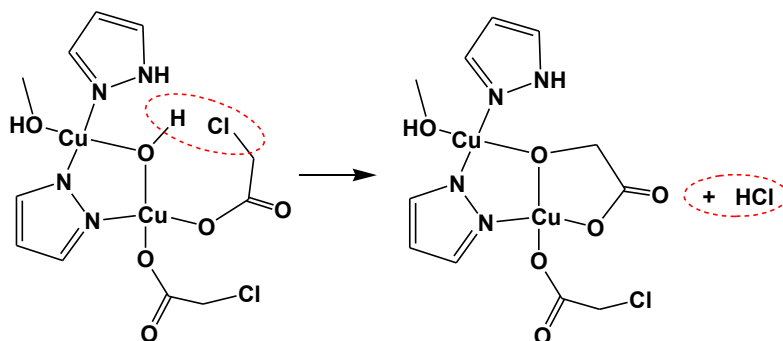


Figure 31. a) Capped-stick representation of the asymmetric unit of compound **1b** with partial atom labeling scheme. b) Schematic representation of the trinuclear triangular $[\text{Cu}_3(\mu_3\text{-OH})(\mu\text{-pz})_3]^{2+}$ moiety.



Scheme 1. Hypothesized de-hydrochlorination reaction pathway.

This formation mechanism seems to be confirmed by DFT calculations⁷⁴ which determine as a possible intermediate in this process the one presenting the chlorine atom of the coordinated chloroacetate group interacting with the same copper atom to which the carboxylate is coordinated [Figure 32]. This interaction likely activates the C-Cl bond that is in close proximity with hydroxyl group.

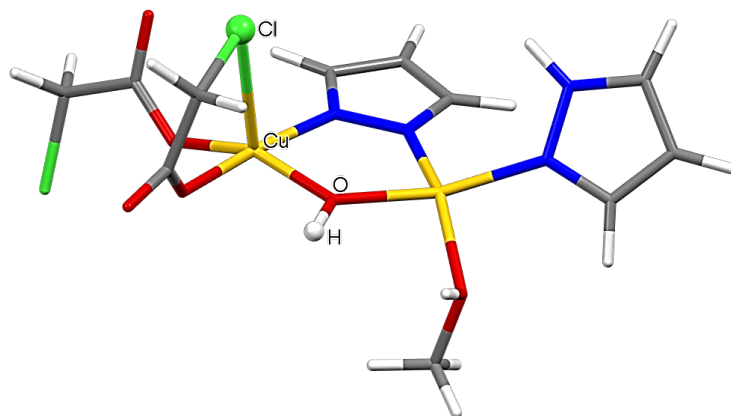


Figure 32. Capped-stick representation of DFT calculated intermediate.

This is not a high energy intermediate compared to the final product, with an energy difference of 3 Kcal/mol; furthermore, the activation energy to de-hydrochlorination is neglectable at room temperature.

Interestingly, this complex may be seen as the result of the first step of the formation of a trinuclear complex which is interrupted by the de-hydrochlorination reaction path above discussed.

The tetranuclear assembly of compound **1b** is obtained through the double *syn-syn* bridging of ClCH₂COO groups pertaining to two asymmetric units likely reinforced by the coordination of O1 to Cu1 of the symmetry related dinuclear unit [Figure 33].

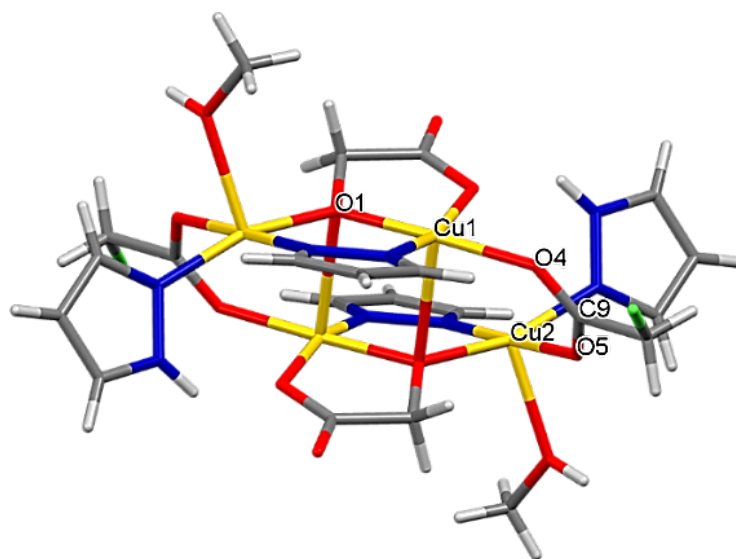


Figure 33. Capped-stick representation tetranuclear complex **1b** with partial atom labeling scheme.

Both copper atoms, individuated in the dinuclear complex, are thus arranged according to a square pyramidal coordination geometry. The pyramid axis is individuated by the longest bond, whereas the other four are approximately equal and arranged in a plane which is orthogonal to the axes. The distances of copper-oxygen and copper-nitrogen bonds of the pyramidal base are similar to those reported in analogue complexes.^{75,76} This coordination geometry is a good compromise between the maximum loss of degeneration of *e* orbitals in a square planar geometry, and the maximum coordination number (the octahedral one), where there is a significant repulsion among ligands. The latter geometry also presents an excessive overcoming of the 18-electron rule, with subsequent occupation of antibonding orbitals. On the other hand, the square planar coordination determines an electronically unsaturated complex. For five-coordinated copper, the electron count is nineteen and the greater energy gain for a d^9 electronic configuration is obtained from a square pyramidal rather than from a trigonal bi-pyramidal geometry. In fact, although compounds with this geometry are also known, they are more rare.⁷⁷

In the stabilization of the structure of **1b** a relevant role is likely played by a quite strong H-bond, which has N-H pyrazole group as donor and O2-oxygen of the carboxylic group pertaining to the symmetry related dinuclear moiety, as acceptor.

Finally, O3 is involved into a strong intermolecular H-bond with O-H group of the coordinated methanol molecule of an adjacent tetranuclear unit. This H-bond is characterized by a length of 2.733 Å and by an angle O-H...O of 171.91° and represents the only significant interaction among the tetranuclear units, generating 1D supramolecular networks.

- $[\{\text{Cu}_3(\mu_3\text{-OH})(\mu\text{-pz})_3(\text{Hpz})_2\}_2(\mu\text{-ClCH}_2\text{COO})_2](\text{Cl})_2$, **1c**

As previously mentioned, from the reaction between copper chloroacetate and pyrazole a third product, **1c**, was isolated. This compound looks like prismatic dark-blue crystals and the structure was solved in the P_{-1} space group. A SC-XRD determination revealed that the hexanuclear compound **1c** is formed by the coupling of two equivalent trinuclear triangular units. In each of them a trihapto oxygen of the hydroxy group and three bridging pyrazolate ligands held together the three copper ions lying at the corners of a triangle, analogously to other trinuclear copper complexes.⁵⁴

Cu1 displays a square pyramidal coordination arrangement and two chloroacetate ions bridge, in a monoatomic fashion, it and its symmetric one, thus generating the hexanuclear complex [Figure 34a]. The charge balance is completed by two chloride ions, both placed at the same distance (3.01 Å) from Cu2 e Cu3 and weakly interacting with pyrazoles N-H through hydrogen bonds. Cu2 and Cu3 adopt a square planar geometry, being coordinated by two nitrogen atoms of two different pyrazolates, one nitrogen from terminal Hpz, and the hydroxyl oxygen. On the other hand, taking into account the symmetrically interacting Cl⁻ counterion, both Cu2 and Cu3 display a square pyramidal coordination with chloride occupying the apical position. It is therefore difficult to classify chlorides as true counterions or weakly coordinated ligands placed in the axial position of square pyramids. The latter hypothesis should be in agreement with the lengths of the Cu-N and Cu-O bonds in the plane, that are longer than those found in pure square planar copper compounds.⁷⁸

Interestingly, almost identical structural features of **1c** have been found on one of the products of the treatment of the $[\{\text{Cu}_3(\mu_3\text{-OH})(\mu\text{-pz})_3(\text{CH}_3\text{COO})_2\text{Hpz}\}_2]$ hexanuclear complex with HCl^{79} [Figure 34b].

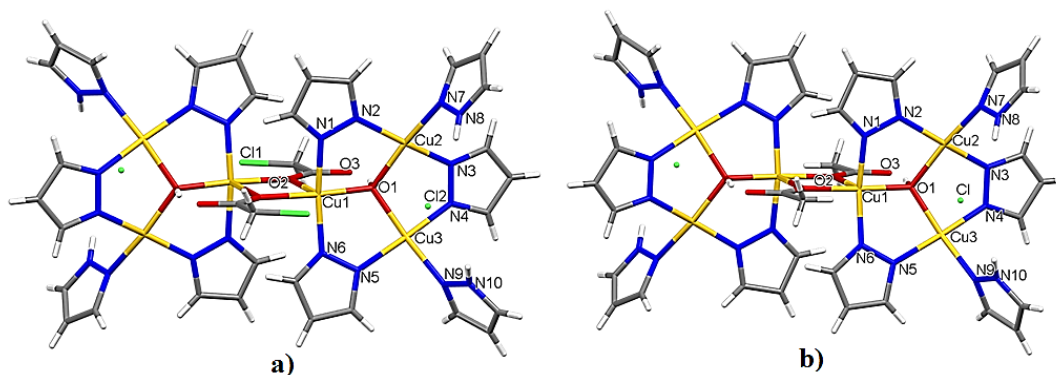


Figure 34. Capped-stick representation of a) compound **1c** and b) $[\{\text{Cu}_3(\mu_3\text{-OH})(\mu\text{-pz})_3(\text{Hpz})_2\}_2(\mu\text{-CH}_3\text{COO})_2](\text{Cl})_2$.

The compared structures have the same space group and very similar cell parameters, besides analogous corresponding bond distances and angles, as shown in Table 1.

| Table 1 | $[\{\text{Cu}_3(\mu_3\text{-OH})(\mu\text{-pz})_3(\text{Hpz})_2\}_2(\mu\text{-ClCH}_2\text{COO})_2](\text{Cl})_2$, 3 | $[\{\text{Cu}_3(\mu_3\text{-OH})(\mu\text{-pz})_3(\text{Hpz})_2\}_2(\mu\text{-CH}_3\text{COO})_2](\text{Cl})_2$ |
|-------------------------------|------------------------------------------------------------------------------------------------------------------------------|-----------------------------------------------------------------------------------------------------------------|
| Space Group | P_{-1} | P_{-1} |
| a, b, c | 8.8168(9); 8.9397(9); c16.8959(16) | 8.889(2); 8.910(2); 16.624(4) |
| α , β , γ | 78.816(8); 78.074(8); 68.557(9) | 79.859(6); 76.747(6); 66.467(6) |

The formation of **1c** supports the hypothesis of the de-hydrochlorination reaction previously proposed. Actually, compound **1c** can be obtained only through the attack to a “pre-synthesized” hexanuclear fragment, possibly $[\{\text{Cu}_3(\mu_3\text{-OH})(\mu\text{-pz})_3(\text{ClCH}_2\text{COO})_2(\text{Hpz})_2\}_2]$, of HCl coming from the formation of compound **1b** via the de-hydrochlorination reaction previously described.

- $[\text{Cu}_3(\mu_3\text{-OH})(\mu\text{-pz})_3(\text{PheDiAcr})]_2$, **2b**

The crystals obtained from the reaction between $[\text{Cu}_3(\mu_3\text{-OH})(\mu\text{-pz})_3(\text{CH}_3\text{COO})_2\text{Hpz}]$

and 1,4-Phenylenediacrylic acid are well defined blue prisms which, dried in the air, change their nature to polycrystalline material. Rapidly covering a single crystal with glue the SC-XRD measure was possible but this technique only slows the fragmentation of the crystal. Therefore a complete data collection was not possible. From the collected data an indicative structure was solved. It was clearly identified the copper trinuclear moieties which are associated in pairs to form hexanuclear nodes by the *syn-anti* bridging of two opposite carboxylate groups involving Cu1 and Cu2 of different trinuclear moieties [Figure 35].

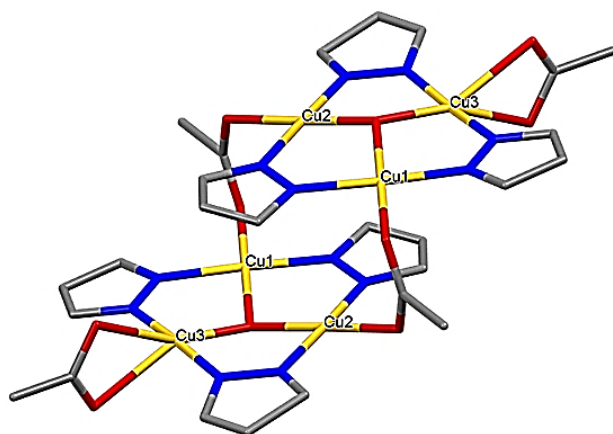


Figure 35. Capped-stick representation of hexanuclear node of compound **2b**.

Cu3 ions are instead chelated by different 1,4-Phenylenediacrylate dianions, thus bridging different hexanuclear nodes [Figure 36].

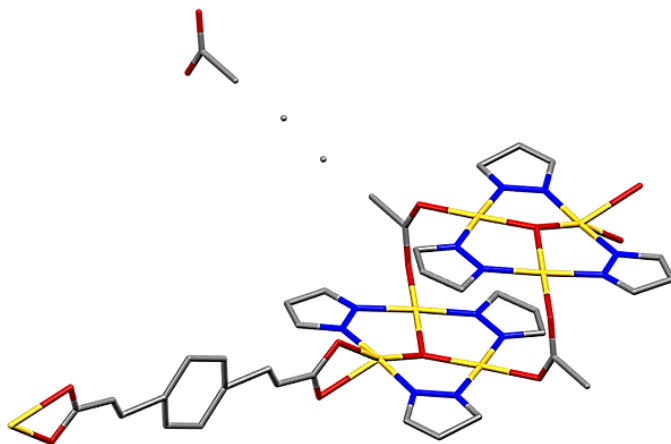


Figure 36. Capped-stick representation of the detected SBU for compound **2b**.

While a 1,4-Phenylenediacrylate was clearly identified and connects Cu₃ of different hexanuclear units, the other one was only partially distinguished. Actually, only the carboxylate groups and some carbon atoms of its chain were identified; in particular in the middle zone of the ligand a disordered electron density was detected. As a matter of fact, the less quality pattern of the diffraction image in this direction attested the more urges crystal direction of fragmentation.

The approximate 3D packing resulting from this connectivity scheme is represented in Figure 37.

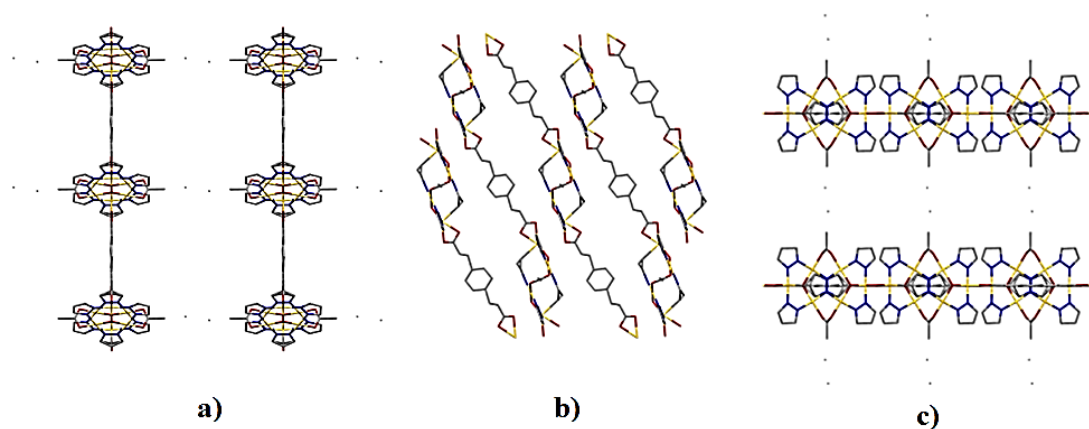


Figure 37. Capped-stick representation of 3D packing of compound **4** view down a) *a*-axes, b) *b*-axes and c) *c*-axes.

The difficulties to solve the structure of **2b** may be probably due to the possible easy elimination of solvent(s) hosted in the large voids, resulting in the collapse of the macroscopic crystal structure. The channels shown in Figure 38 are greater than those obtained by complete assignment of the 1,4-Phenylenediacrylate atoms down *b* axis but anyway it gives a clear idea of the possible voids.

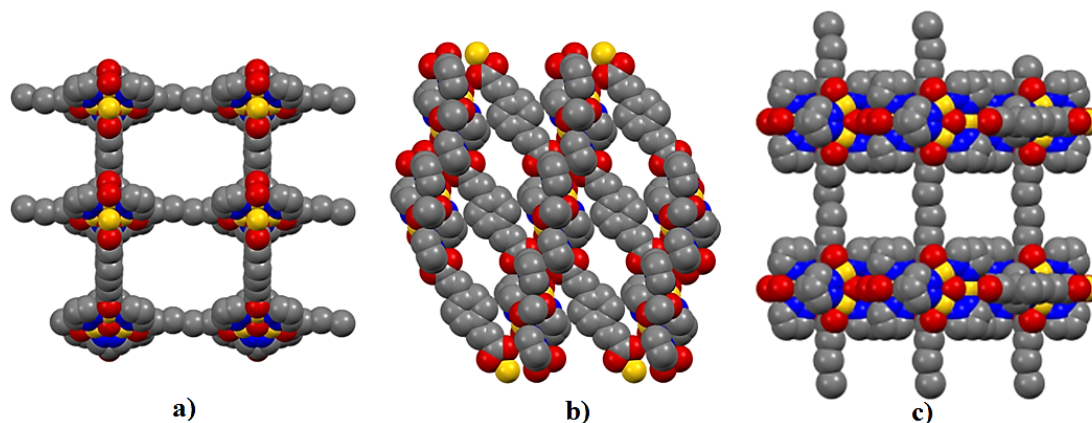


Figure 38. Spacefill representation of 3D packing of compound **2b** view down a) *a* axis, b) *b* axis and c) *c* axis.

When crystals convert to polycrystalline material they become the same of **2a** polycrystalline solid obtained by fast direct reaction. This solid present a crystalline PXRD diffractogram [Appendix_C].

- $[\text{Cu}(\text{Muc})(\text{Hpz})_4]$, **4b**

The reaction between $[\text{Cu}_3(\text{OH})(\text{pz})_3(\text{CH}_3\text{COO})_2\text{Hpz}]$ and Muconic acid produces a trinuclear compound in polycrystalline form which it was impossible to characterized though a SC-XRD determination. By slow evaporation in the air of the mother liquors of this compound few light-blue crystals are obtained.

A SC-XRD structure determination carried on these crystals reveals a CP based on the mononuclear SBU $[\text{Cu}(\text{Muc})(\text{Hpz})_4]$, **4b**.

The structure of **4b** shows that the copper ion sits on a crystallographic inversion center and exhibits a distorted octahedral coordination geometry [Figure 39].

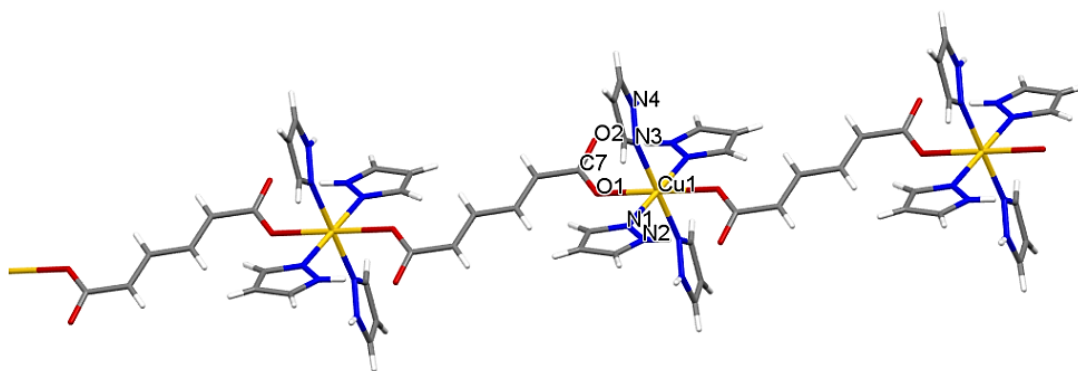


Figure 39. View of 1D CP formed by muconate dianions bridging $\text{Cu}(\text{Hpz})_2$ moieties.

The bi-carboxylate moiety bridges two copper ions attending to elongated apical positions. The four shorter bonds are set by N1 and N3 of coordinated pyrazole molecules and their symmetric equivalents. Although the mono-dentate coordination of carboxylates groups, there is a good electron delocalization in the carboxylate group, evidenced by C7-O1 and C7-O2 lengths of 1.239 Å and 1.267 Å, respectively. In this context, it is to be noted that O2 is involved in two strong H-bond interactions with N-H groups of adjacent pyrazole moieties [Figure 40].

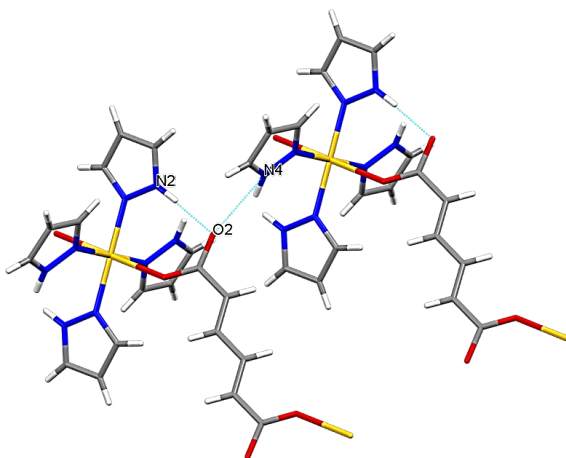


Figure 40. Supramolecular assembly of compound **4b** evidencing in light blue the intra- and intermolecular H-bonds.

One of these H-bond is intramolecular and involves a pyrazole coordinated to the same Cu to which the carboxylate is coordinated [$\text{N2}\cdots\text{O2}$ 2.626 Å, $\text{N2-H}\cdots\text{O2}$

170°]. The second H-bond is intermolecular, involving pyrazole coordinated to an adjacent chain, with a length of 2.777 Å and an angle of 146°. Considering this, the sum of the two weak interactions associated to O2 become comparable to the stronger one O1-Cu1, thus justifying the homogeneous delocalization in the carboxylate group. The intermolecular H-bond is the only significant interaction among chains and imposes a staggered packing [Figure 41].

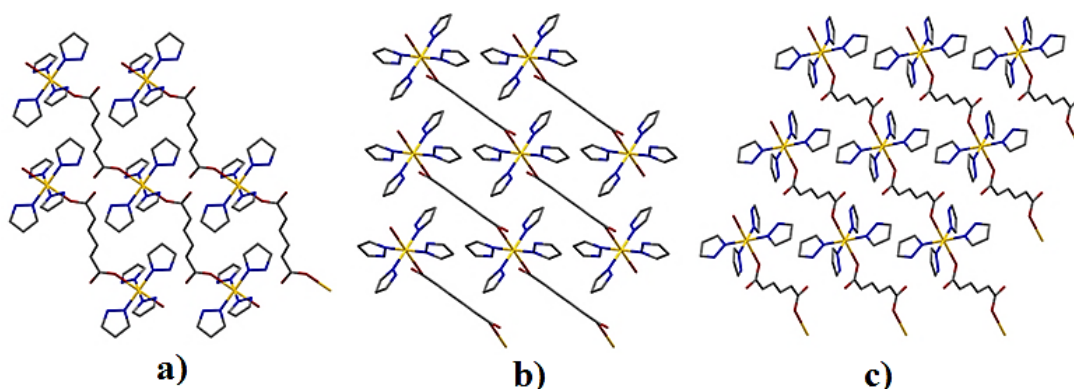


Figure 41. Capped-stick representation of 3D packing of compound **5** view down a) *a*-axes, b) *b*-axes and c) *c*-axes. For sake of clarity the H atoms are omitted.

The overlap of the powder XRD diffractogram of polycrystalline product **4a** with the calculated one of compound **4b** confirms that they are different species [Figure 42].

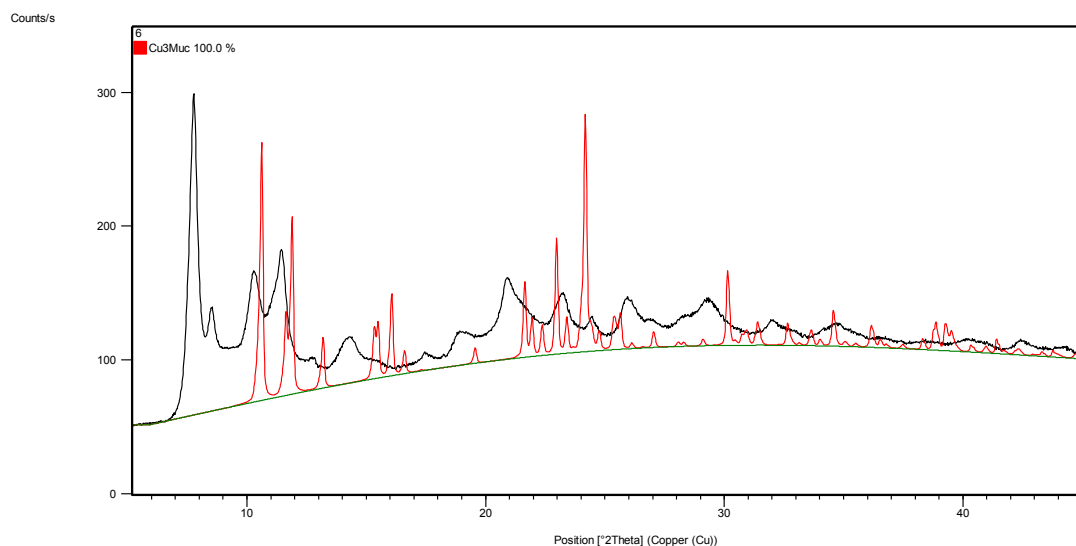


Figure 42. In black the diffractogram of **4a** and in red the calculated one for **4b**.

Moreover, from the reported diffractogram it is evident from the low intensity of reflections and from their width that **4a** is almost a nano-phase.

- [Cu(HyMuc)]·H₂HyMuc, **5b**

Analogously to the Muconic acid case, the major product of reaction between [Cu₃(OH)(pz)₃(CH₃COO)₂Hpz] and Hydromuconic acid is a powder material **5a** whose elemental analysis is in agreement to that of a trinuclear species. This product, filtered after four hours, leaves weakly colored mother liquors, from which, by slow evaporation in the air, few light-blue crystals have been obtained. A SC-XRD determination carried on these prismatic crystals reveals the structure of compound **5b**. It can be described as a mono-dimensional CP on which the Hydromuconate bi-carboxylate group bridges two copper ions, both of them in the mono-dentate coordination modality of the carboxylic group. Copper ion coincides with an inversion center and exhibits distorted octahedral coordination geometry, where carboxylates oxygen are in the apical position while four pyrazole molecules are shorter coordinated in the equatorial plane.

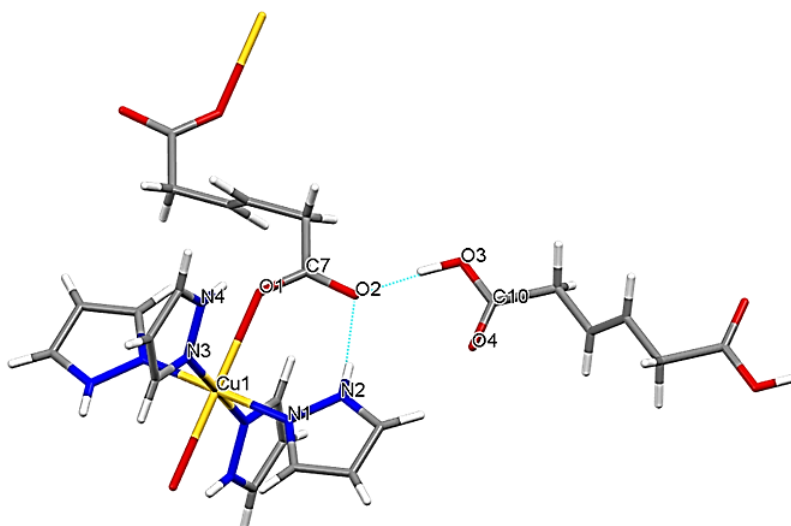


Figure 43. View of intra- and intermolecular H-bonds.

O2 is involved in two strong H-bond [Figure 43]: the first one, having a length of 2.747 Å and an angle of 172°, is with N-H group of a coordinated pyrazole moiety,

while the second one involves the hydroxyl-group of an adjacent molecule of free hydromuconic acid [$O3 \cdots O2$ 2.568 Å, $O3-H \cdots O2$ 173°]. The great energy of these H-bond interactions is attested by the homogeneous delocalization of O1-C7-O2 group.

Overall, there is a mono-dimensional polymeric development due to the repetition of $[Cu(\text{Hydromuconate})(\text{Hpz})_4]$ units. Among parallel polymeric chains, guests molecules of hydromuconic acid form a 2D supramolecular network through the above mentioned strong $O3-H12 \cdots O2$ H-bonds [Figure 44].

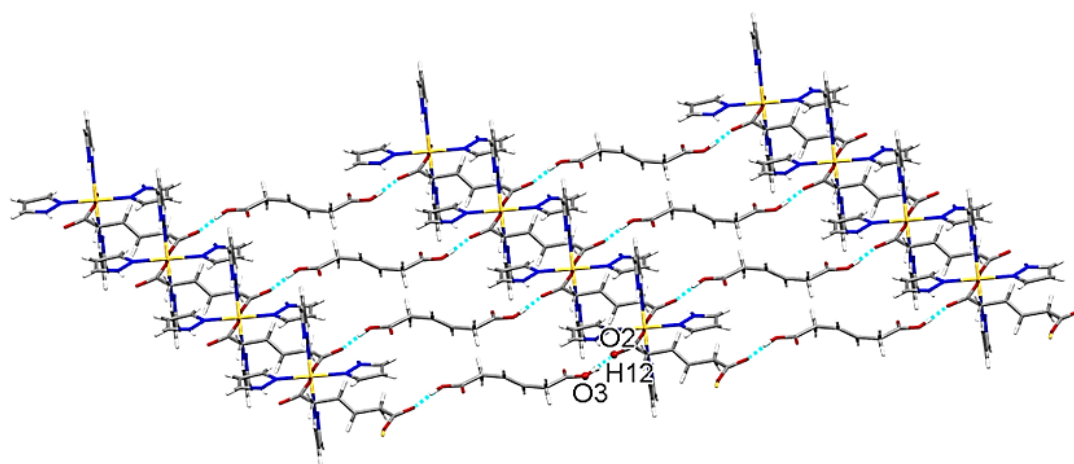


Figure 44. Supramolecular networks.

Although each layer presents holes, the parallel sheets are offset assembled in the third dimension, thus eliminating the accessibility to the cavities [Figure 45].

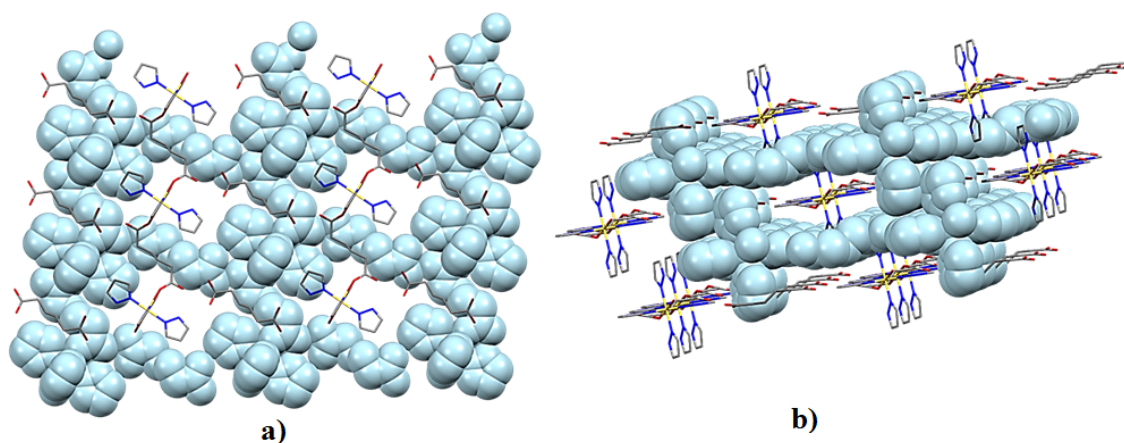


Figure 45. Representing the layers alternatively with space-filling and capped-sticks fashion, is visible a) the offset relation among 2D networks and b) the compact packing of the sheets. For sake of clarity the H atoms are omitted.

- $[\text{Cu}_3(\mu_3\text{-OH})(\mu\text{-pz})_3(\text{HyMuc})(\text{DMF})]$, **5c**

In a second experiment, the reaction procedure between $[\text{Cu}_3(\text{OH})(\text{pz})_3(\text{CH}_3\text{COO})_2\text{Hpz}]$ and hydromuconic acid yielded besides the polycrystalline product **5a**, mother liquors from which blue crystals formed. A SC-XRD determination carried on these prismatic crystals reveals the structure of compound **5c**, formed by two symmetry different trinuclear moieties connected by two hydromuconate di-anions [Figure 46].

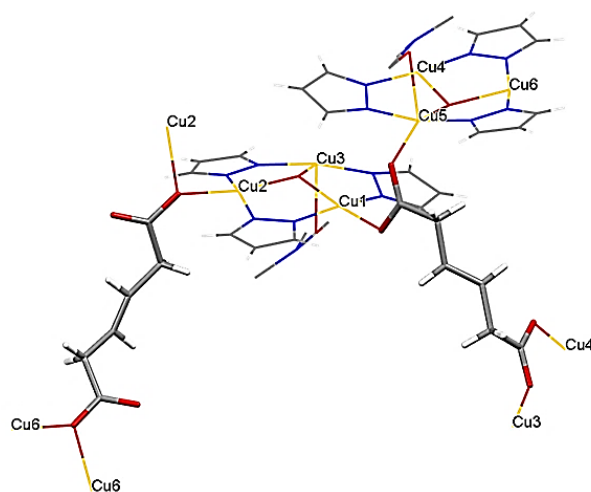


Figure 46. Wireframe representation of the SBU of compound **5c**, with the hydromuconate dianions in capped-sticks fashion.

A carboxylate group connects Cu1 and Cu5 pertaining to the two symmetrically different trinuclear units with *syn-anti* bridge coordination modality. The other carboxylate group of the same hydromuconate ions is bridging Cu3 and Cu4 yet pertaining to another symmetrically different trinuclear units. Then, the second hydromuconate ion presents a carboxylate group which is monoatomic bridging Cu2-Cu2 atoms of two symmetrically equivalent trinuclear units, forming a hexanuclear moiety: the other carboxylate group of the second hydromuconate ion monoatomic bridges Cu6-Cu6 atoms of symmetrically equivalent trinuclear units forming, also in this case, a hexanuclear moiety [Figure 47].

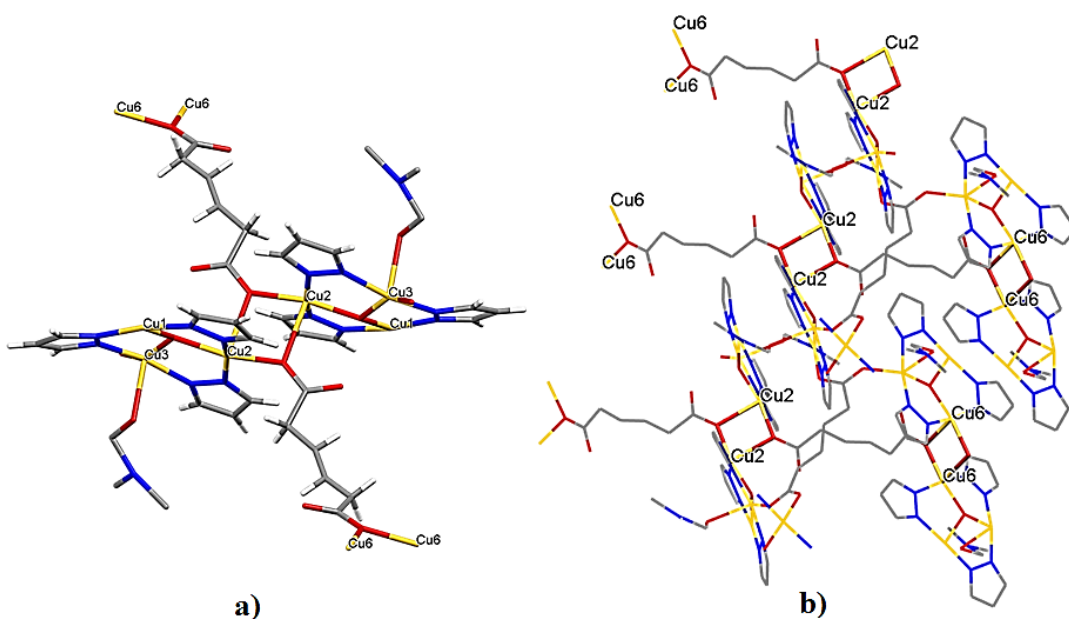


Figure 47. a) Capped-sticks representation of carboxylate group bridging Cu2-Cu2 atoms of symmetrically equivalent trinuclear units forming a hexanuclear moiety; b) wireframe representation of carboxylate bridging both Cu2-Cu2 and Cu6-Cu6 atoms and their corresponding spatial development, for sake of clarity the H atoms are omitted.

These bridges produce a 3D expansion based on different macrocycles which define the backbone of the structure [Figure 48].

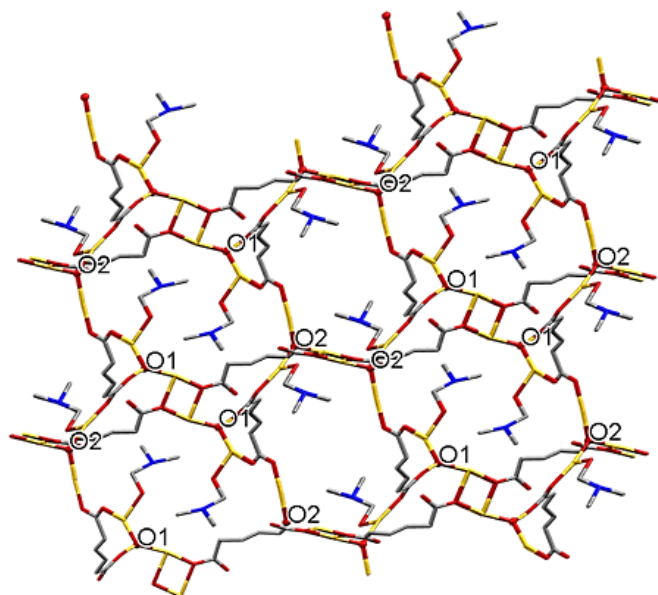


Figure 48. Capped-sticks representation of the alternation of two different macrocycles. O1 and O2 individuate the central oxygen of the two symmetrically different trinuclear units. Hydrogens and pyrazolate ions have been omitted for clarity.

The structure develops as a close packing on which no voids are present. The potential channels are those defined by the macro-cycles and are occupied by coordinated DMF molecules. This is evidenced by the thermal ellipsoid representation of the structure: the greater ellipsoids of the DMF molecules reflect the greater mobility and the higher disorder of the DMF molecules with respect to the other structural components, probably according to a weak coordinating solvents [Figure 49].

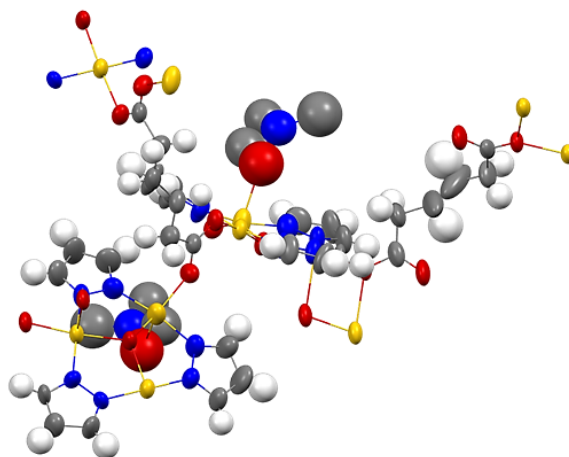


Figure 49. Ellipsoid representation of the SBU of **5c**.

The overlap of the powder XRD diffractograms of **5a** with the calculated ones of **5b** and **5c** shows that they are different species [Figures 50-51]. In particular, **5a** is an amorphous solid that, on the other hand, differs in composition from **5c** by DMF molecules. Likely, the latter have been removed by washing **5a** with MeOH and drying under vacuum (0.1 mmHg).

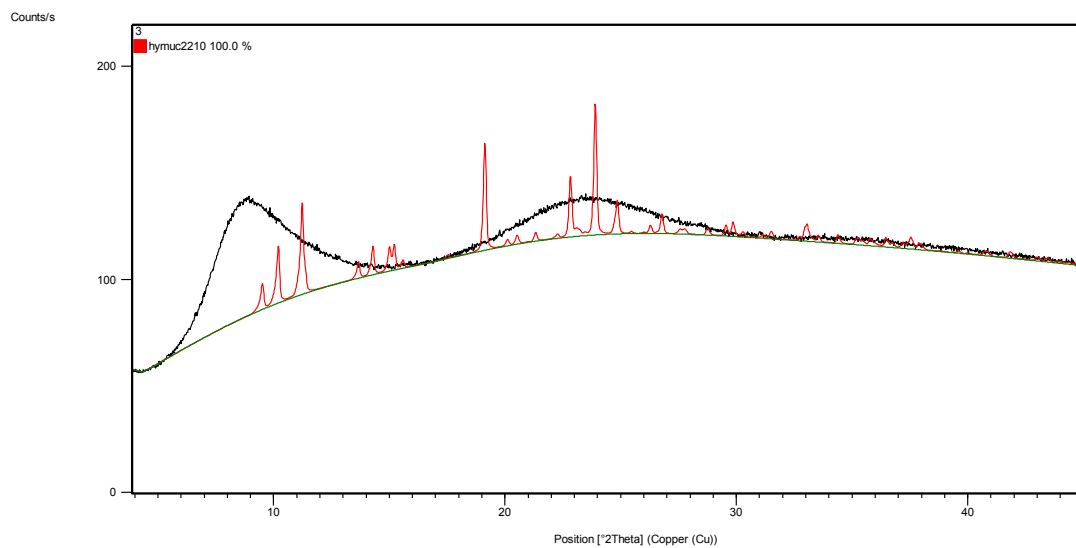


Figure 50. In black the diffractogram of **5a** and in red the calculated one for **5b**.

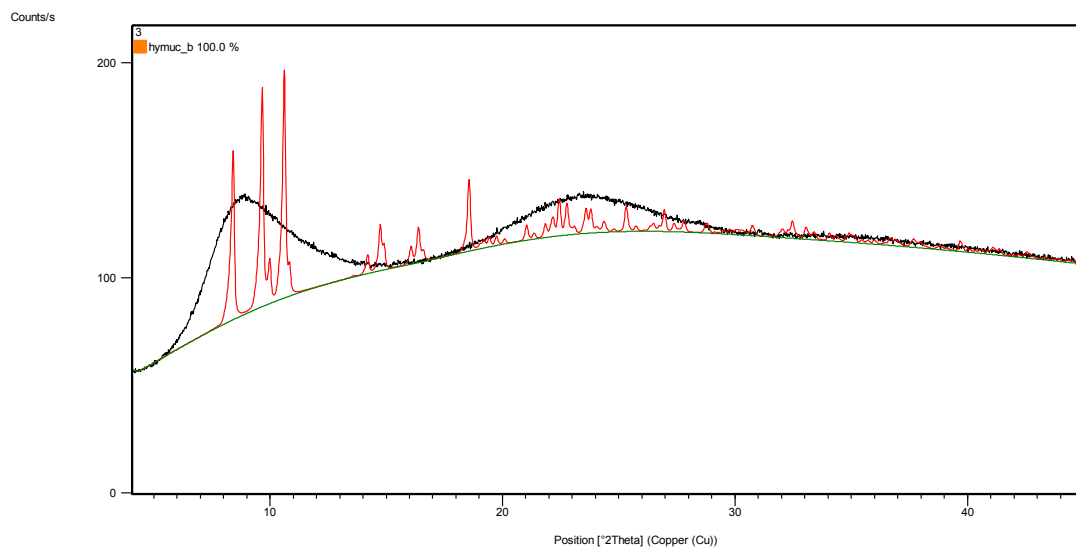


Figure 51. In black the diffractogram of **5a** and in red the calculated one for **5c**.

- $[\text{Cu}_3(\mu_3\text{-OH})(\mu\text{-pz})_3(\text{MeSuc})]$, **6a**

The direct reaction between $[\text{Cu}_3(\mu_3\text{-OH})(\mu\text{-pz})_3(\text{CH}_3\text{COO})_2\text{Hpz}]$ and methylsuccinic acid quantitatively gives a crystalline product **6a**, that dried in vacuum, transforms into the a polycrystalline material **6b**. A SC-XRD determination carried out on **6a** reveals that it presents an asymmetric unit and a spatial development similar to those of a preaviously reported trinuclear copper-pyrazolate structure involving the succinate ion as ligand.⁸⁰ The compared structures have the same space group and very similar cell parameters [Table 2].

| Table 2 | $[\text{Cu}_3(\mu_3\text{-OH})(\mu\text{-pz})_3(\text{Methylsuccinate})$ (MeOH)]·H ₂ O, 6b | $[\text{Cu}_3(\mu_3\text{-OH})(\mu\text{-pz})_3(\text{Succinate})$ (MeOH)]·2H ₂ O |
|-------------------------|-----------------------------------------------------------------------------------------------------------------|-------------------------------------------------------------------------------------------------|
| Space Group | R₃ | R₃ |
| a, b, c | 27.4767(9); 27.4767(9); 20.5399(8) | 26.795(5); 26.795(5); 19.751(4) |
| α, β, γ | 90; 90; 120 | 90; 90; 120 |

Compound **6a** maintains the trinuclear moiety of the reagent. In each asymmetric unit, a methylsuccinate di-anion presents a carboxylate group in chelating and monoatomic coordination modality while the other one shows a chelate behaviour. Both chelating coordinations are asymmetric, presenting Cu-O lengths in the range of 1.9-2.0 Å for the shorter and 2.6-2.7 Å for the longer ones.

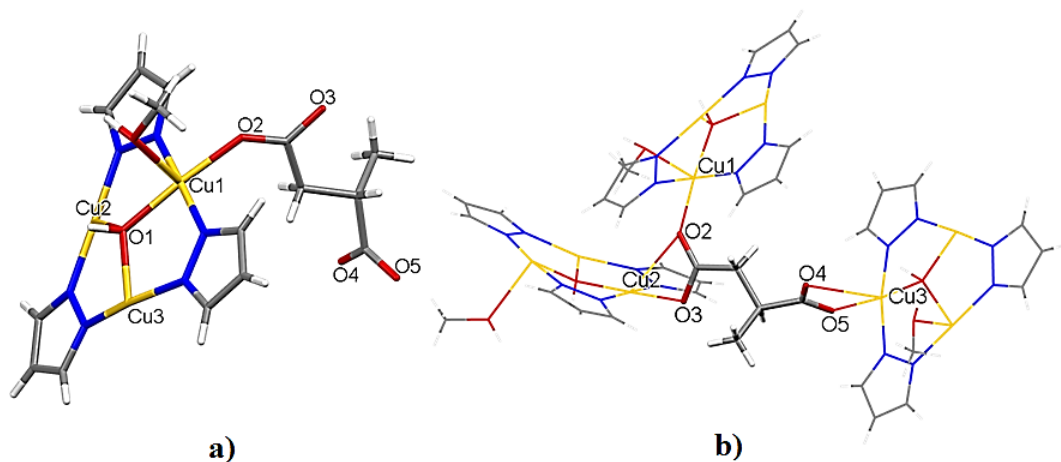


Figure 52. a) Capped-sticks representation of asymmetric unit of **6a**; b) methylsuccinate dianion coordination modes of three different trinuclear moieties.

Thus, the methylsuccinate anion links three different trinuclear moieties: one carboxylate group binds Cu1 of one trinuclear moiety with monoatomic coordination [Figure 52b], and chelates Cu2 of another triangular unit, while the second carboxylate group of the methylsuccinate chelates Cu3 of a third unit.

The repetition of the carboxylates connections joining Cu1 and Cu2 of adjacent trinuclear moieties, generates a macrocycle of six self-assembled asymmetric units [Figure 53a].

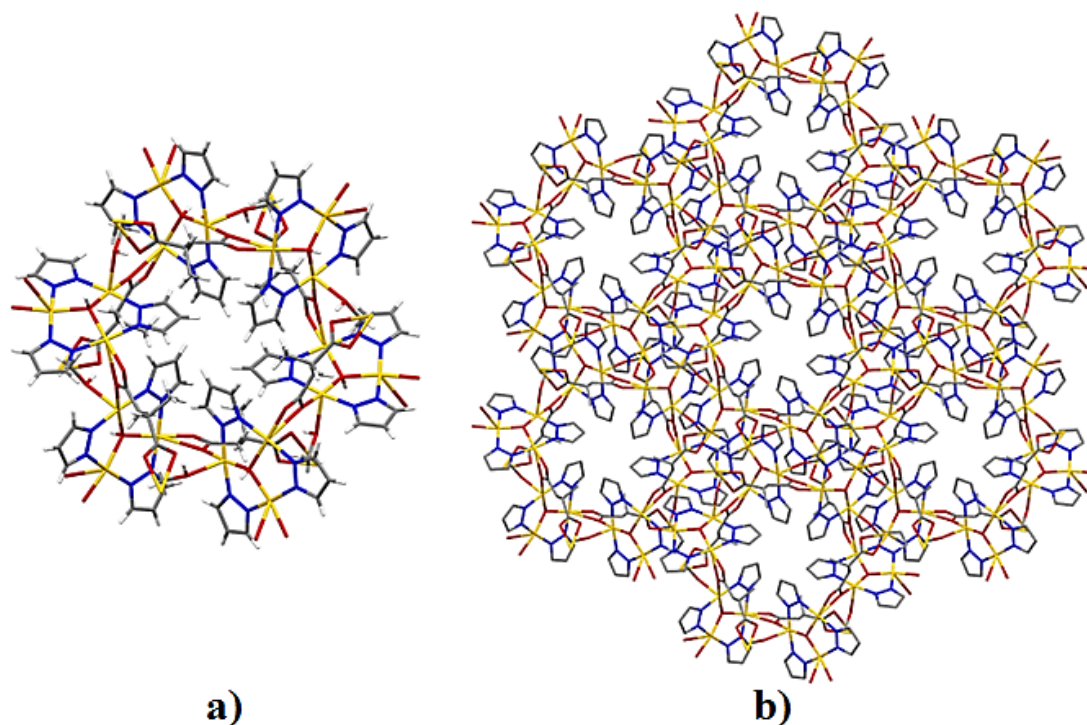


Figure 53. a) Rosette formed by six self-assembled asymmetric units and b) view of 3D CP down the *b*-axis, for sake of clarity the H atoms are omitted.

This rosette can be seen as a sort of tertiary building unit that is repeated in the three-dimensional expansion of the CP. Each unit of this rosette structure presents a methyl succinate moiety, alternatively directed upward and downward from the rosette plane and chelating Cu3 of trinuclear units belonging to another rosette. In the crystal packing various interconnected rosettes result overlapped and distinguishable in the crystallographic *b*-axis direction [Figure 53b].

The overall crystal packing generates, through the above listed coordination interactions, a 3D CP with three intersecting channels of regular micropores [Figure 54].

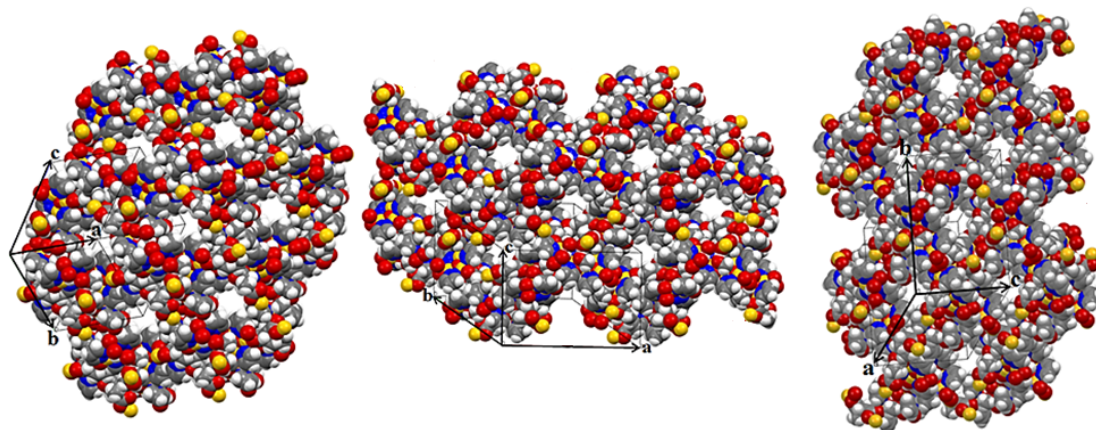


Figure 54. Space-filling representation of the crystal packing of **6a** evidencing the presence of three equivalent intersecting channels.

The pores have a section of ca. $3.81 \times 3.38 \text{ \AA}$, as defined by the distance between two couples of parallel planes as shown in Figure 55. The reported distances are correct V.d.W. radii.

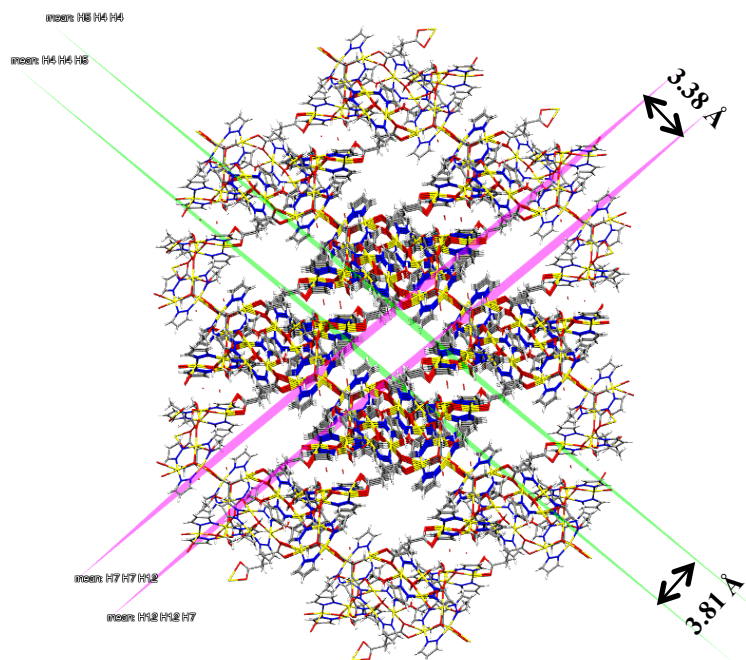


Figure 55. One of the channels individuated by two couple of parallel planes evidencing its dimension as the distance between the planes themselves.

This three-dimensional development comprehensively accounts for a 36% solvent accessible void space as calculated by PLATON/SQUEEZE⁸¹ program with a probe radius of 1.0 Å.

The overlap of powder diffractograms of **6b**, **7a** (polycrystalline product obtained by reaction between CuMeSuc and Hpz) and the calculated one for **6a** shows that the polycrystalline phase (**6b**, **7a**) correspond to the same species [Figure 56] but they are different from **6a** [Figure 57].

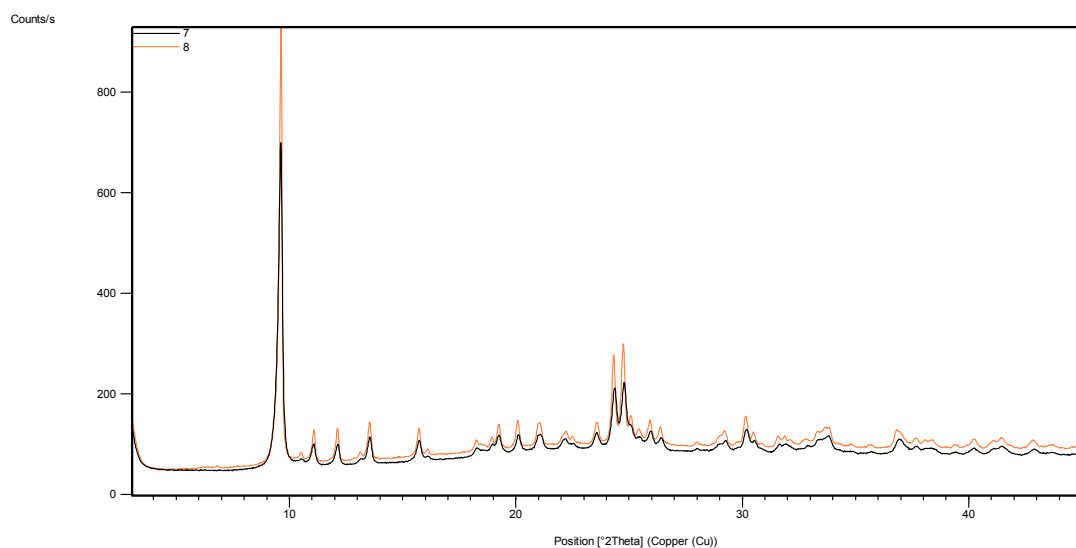


Figure 56. Diffractograms of **7a** (black) and **6b** (orange).

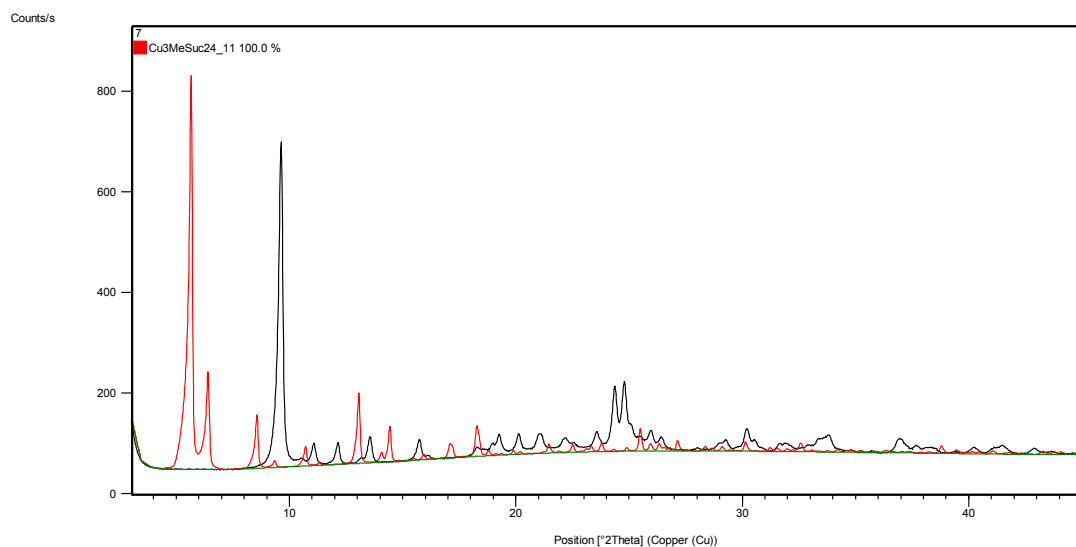


Figure 57. In black the diffractogram of **6b** and in red the calculated one for **6a**.

In particular, **6b** and **7a** present cell parameters analogous to those ones determined for a structure of a compound obtained by drying under vacuum the succinate derivative having the same structure of **6a**⁸⁰ [Table 3].

| Table 3 | [Cu ₃ (μ ₃ -OH)(μ-pz) ₃ (Methylsuccinate) (H ₂ O)(MeOH)], 6b , 7a | [Cu ₃ (μ ₃ -OH)(μ-pz) ₃ (Succinate)] |
|-------------|--------------------------------------------------------------------------------------------------------------------------------|-----------------------------------------------------------------------|
| Space Group | P _{21/n} * | P _{21/n} |
| a, b, c | 9.6291(3); 11.3065(7); 16.0512(8)* | 9.7487(10); 11.0061(15); 15.1631(18) |
| α, β, γ | 90; 92.804 (4); 90* | 90; 94.36(11); 90 |

* cell parameters were determined using Expo software and were refined with HighScorePlus software.

R (profile)/ %: 0.94018

R (weighted profile)/ %: 1.31619

R (Bragg)/ %: 2.45047

- [Cu₃(μ₃-OH)(μ-pz)₃(S-Methylsuccinate)], (**S**)-**6a**

The peculiarity of the just described methylsuccinate linker in structure of **6a**, besides the presence of a certain degree of porosity, is the chiral center of the methylsuccinate anion at the carbon to which the methyl group is linked. In compound **6a**, obtained by the racemic bicarboxylic acid, the carboxylate is present in the both enantiomers.

The direct reaction between [Cu₃(μ₃-OH)(μ-pz)₃(CH₃COO)₂Hpz] and enantiopure S-methylsuccinic acid quantitatively gives a crystalline product analogously to the reaction with the racemic reagent. A SC-XRD determination carried on these crystals reveals the structure of compound (**S**)-**6a**. It has the same composition and spatial development to the previously reported trinuclear copper-pyrazolate structure involving the racemic methylsuccinate ion as ligand. Due to the presence of the enantiopure chiral center the space group is non-centrosymmetric, specifically is the R3 space group. The compared structures have related space group and the same cell parameters [Table 4].

| Table 4 | $[\text{Cu}_3(\mu_3\text{-OH})(\mu\text{-pz})_3(\text{Methylsuccinate}) (\text{MeOH})] \cdot \text{H}_2\text{O}$, 8 | $[\text{Cu}_3(\mu_3\text{-OH})(\mu\text{-pz})_3(\text{S-Methylsuccinate}) (\text{MeOH})] \cdot \text{H}_2\text{O}$, 9 |
|-------------------------|-----------------------------------------------------------------------------------------------------------------------------|-------------------------------------------------------------------------------------------------------------------------------|
| Space Group | R_3 | R_3 |
| a, b, c | 27.4767(9); 27.4767(9); 20.5399(8) | 27.4763(7); 27.4763(7); 19.0861(6) |
| α, β, γ | 90; 90; 120 | 90; 90; 120 |

Due to the absence of the inversion center the asymmetric unit of **(S)-6a** is formed by two trinuclear moieties and the methylsuccinate presents the S-configuration [Figure 58a]. Differently, the inversion center of structure **6a** provides both D- and S-configurations [Figure 58b].

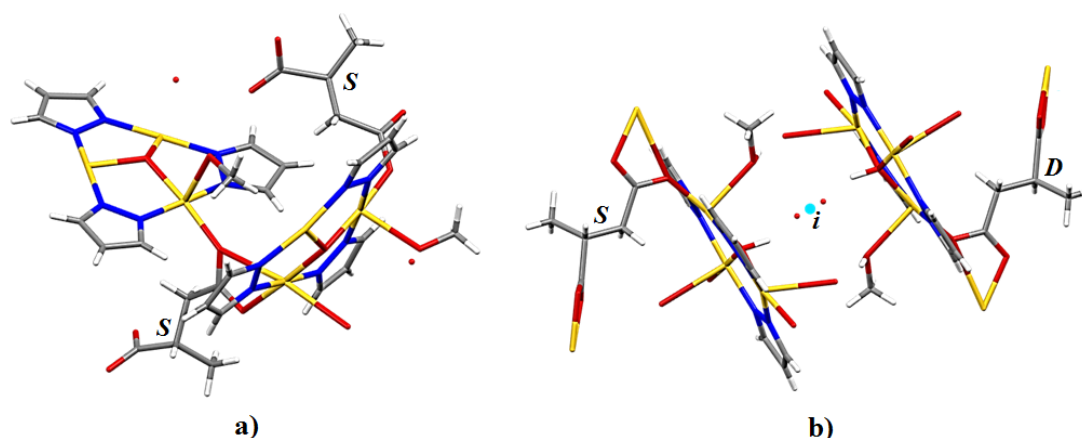


Figure 58. Capped-sticks representation of a) the asymmetric unit of **(S)-6a** and b) two asymmetric units of **6a** related by an inversion center.

- $[\text{Cu}_3(\mu_3\text{-OH})(\mu\text{-pz})_3(\text{DimeSuc})(\text{Hpz})(\text{H}_2\text{O})]$, **8b**

The reaction between $[\text{Cu}(\text{DimeSuc})]$ and Hpz gives a blue solution from which at a temperature below 10° C dark blue cubic crystals are obtained. A SC-XRD determination carried out on these crystals reveals the structure of compound **8b** which shows the presence of the usual copper trinuclear triangular moiety $[\text{Cu}_3(\mu_3\text{-OH})(\text{pz})_3]$ [Figure 59a]. Cu3 exhibits a square pyramidal coordination geometry thanks to the coordination of a pyrazole molecule and the elongated interaction with a H₂O molecule which define the pyramid axis. Cu1 and Cu2 are instead arranged

according to an about regular square planar geometry because of the monoatomic coordination of carboxylic groups belonging to two different dimethylsuccinate dianions. A hexanuclear compound results through double dimethylsuccinate bicarboxylate group bridging Cu1 and Cu2 ions pertaining to two asymmetric units [figure 59b].

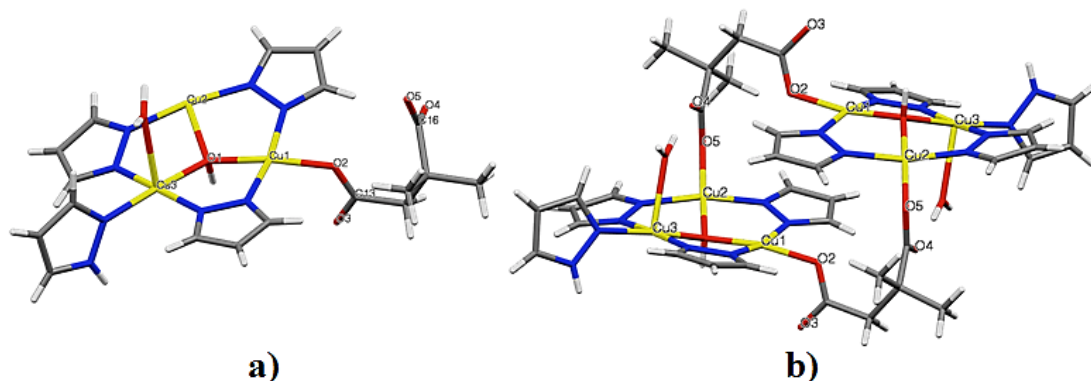


Figure 59. Capped-sticks representation of a) the asymmetric unit of **8b** and b) hexanuclear copper complex derived by the asymmetric unit of **8b**.

Dimethylsuccinate connects the two trinuclear moieties exposing outside the two methyl groups belonging to its chain, probably due to steric factors.

The carboxylate groups despite they are coordinated in a monoatomic modality, present a homogeneous electron delocalization. The very similar C16-O4 and C16-O5 lengths are due to the strong intramolecular H-bond involving O4 as acceptor and the coordinated water molecule [$O6 \cdots O4$ 2.802 Å, $O6-H6A \cdots O4$ 177°]; while the very similar C13-O2 and C13-O3 lengths of the carboxylate are likely due to the strong intermolecular H-bond involving O3 as acceptor and the hydroxyl group of an adjacent hexanuclear unit as donor [$O1 \cdots O3$ 2.623 Å, $O1-H \cdots O2$ 169.5°].

These H-bonds among hexanuclear units are the most relevant interaction and likely determine the close packing of **8b** [Figure 60].

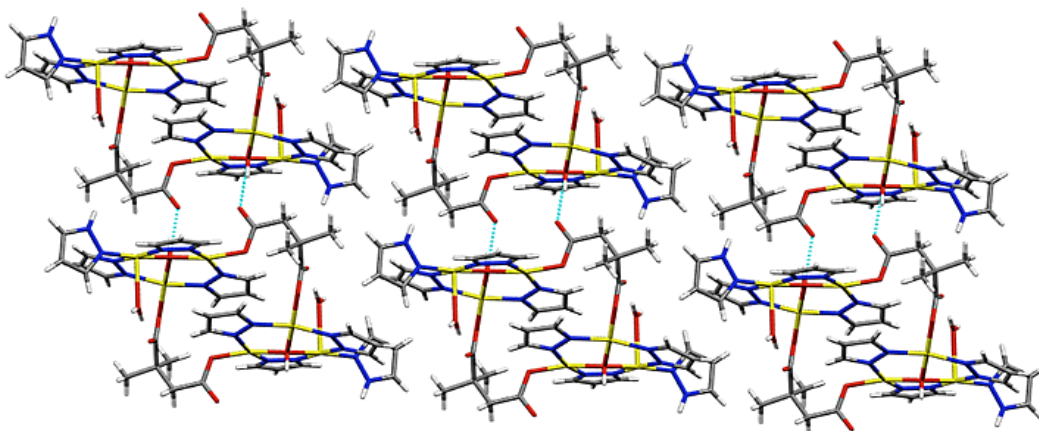


Figure 60. Capped-stick representation of crystal packing of the hexanuclear molecules of **8b** evidencing, the intermolecular H-bonds among these ones (dashed light blue lines).

- $[\text{Cu}_3(\mu_3\text{-OH})(\mu\text{-pz})_3(\text{DimeSuc})(\text{H}_2\text{O})]$, **9a**

The direct reaction between $[\text{Cu}_3(\mu_3\text{-OH})(\mu\text{-pz})_3(\text{CH}_3\text{COO})_2\text{Hpz}]$ and dimethylsuccinic acid gives a blue solution from which blue-purple needles **9a** are obtained, which, dried in the air, quickly transform in a polycrystalline solid **9b**. A SC-XRD determination carried out on **9a**, by covering the crystals with glue, reveals the known trinuclear triangular unit $[\text{Cu}_3(\mu_3\text{-OH})(\mu\text{-pz})_3]$ [Figure 61a].

In each asymmetric unit a dimethylsuccinate di-anion presents a carboxylate group in chelating and monoatomic coordination modality while the other one shows a chelating behavior. Both chelate coordinations are asymmetric, with Cu-O lengths of ca. 2.0 and 2.7 Å for the shorter and the longer one, respectively.

The methylsuccinate anion links three different trinuclear moieties: it binds with monoatomic coordination Cu1 of one trinuclear moiety, while the chelating mode of the same carboxylate group binds Cu2 of another triangular unit and the second carboxylate group of the methylsuccinate binds the Cu3 of a third unit [Figure 61b].

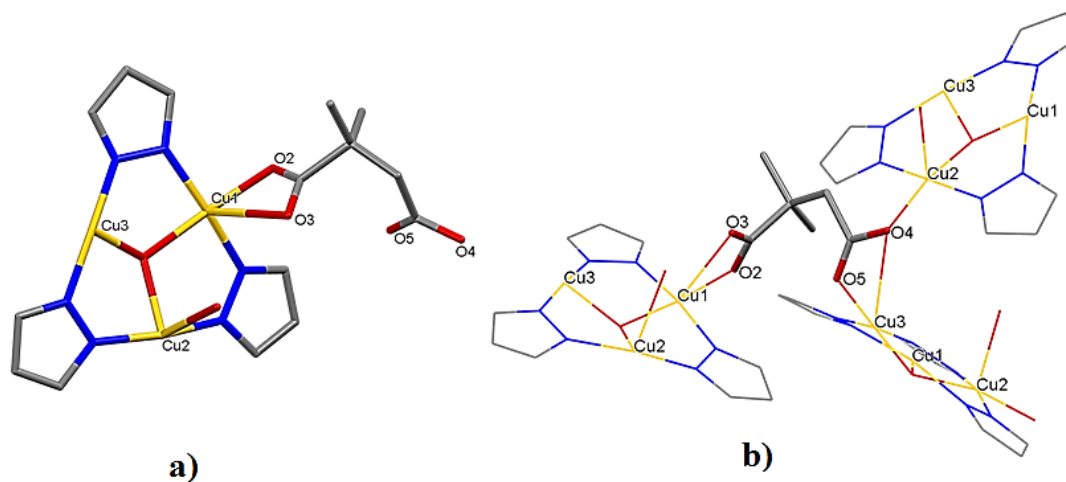


Figure 61. a) Capped-stick representation of the asymmetric unit of **9a** and b) dimethylsuccinate dianion coordination modes of three different trinuclear moieties.

The above indicated connections generate a macrocycle of twelve self-assembled trinuclear moieties. [Figure 62].

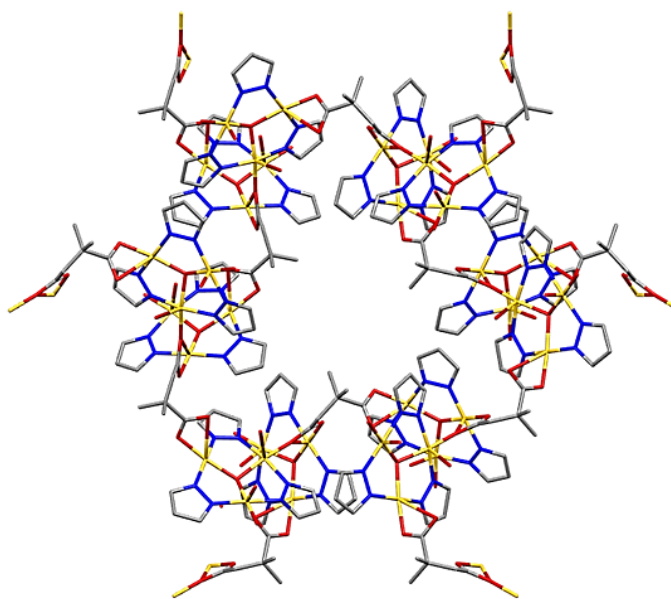


Figure 62. Rosette formed by twelve self-assembled trinuclear moieties.

In the crystal packing interconnected rosettes result overlapped and distinguishable in the crystallographic *b* axes direction, so they generate a 3D CP with parallel channels of regular micro-pores having an approximate triangular section with side of ca. 6 Å [Figure 63].

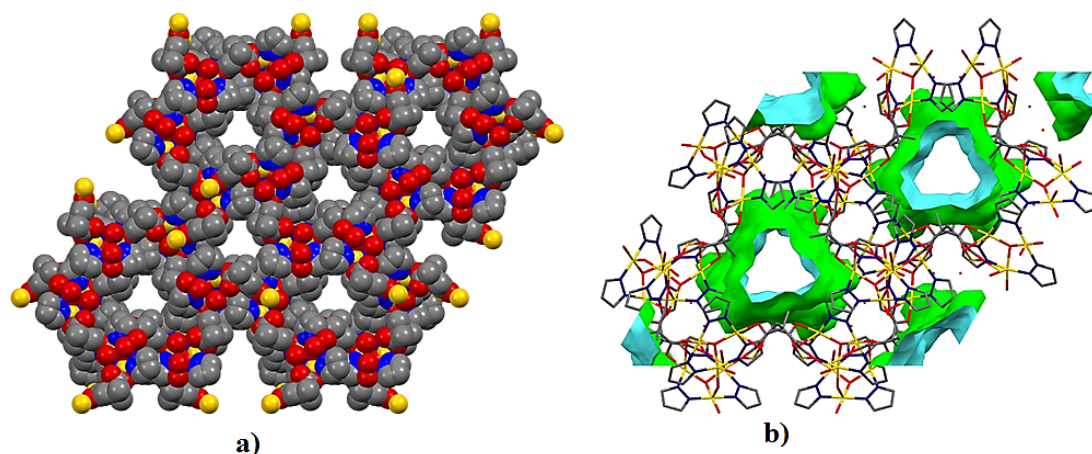


Figure 63. a) Space-filling representation of 3D crystal packing of **9a** evidencing the triangular parallel channels. b) Capped-sticks representation evidencing the void surface.

The overlap of powder XRD diffractograms of **9b** and the calculated one for **9a** shows that they are different crystalline species thus indicating that solvent evaporation from **9a** leads to a structural rearrangement [Figure 64]. The diffractogram of **9b** gives the following cell parameters determined using Expo software and refined with HighScorePlus software (Le Bail method):

Space group: P_{-1}

Lattice parameters:

| | |
|--------------------------|------------|
| $a/\text{Å}$: | 16.390(2) |
| $b/\text{Å}$: | 14.672(2) |
| $c/\text{Å}$: | 12.261(1) |
| $\alpha/^\circ$: | 90.92(1) |
| $\beta/^\circ$: | 108.08(1) |
| $\gamma/^\circ$: | 66.10(1) |
| $V/10^6\text{ pm}^3$ | 2542.30200 |
| R (expected)/ %: | 0.62661 |
| R (profile)/ %: | 2.24297 |
| R (weighted profile)/ %: | 3.90052 |
| R (Bragg)/ %: | 2.60094 |

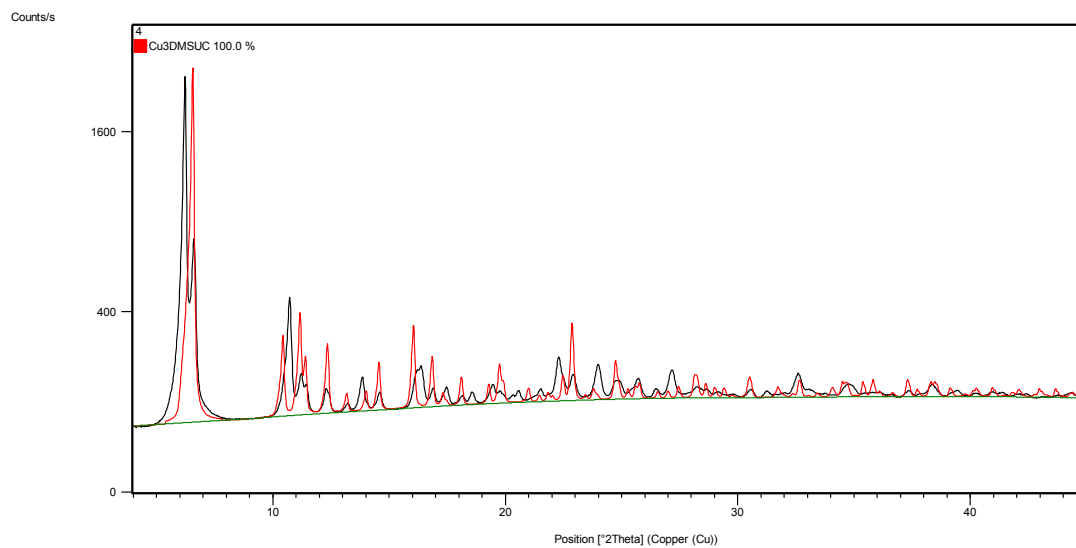


Figure 64. In black the diffractogram of **9b** and in red the calculated one for **9a**.

6. CONCLUSIONS AND FUTURE PERSPECTIVES

As far as the reaction of copper(II) chloroacetate with Hpz in MeOH is concerned, some interesting points are worth to be evidenced. The reaction yields as major product a mononuclear species, **1a**, which, acting as a SBU self-assembles generating a series of parallel 1D CPs. In addition, also a not isolated hexanuclear species is reasonably formed. This compound reacts with HCl released through a peculiar dehydroalogenation reaction, providing the hexanuclear species **1c**. Contemporaneously, the above mentioned dehydrochlorination reaction generate a dinuclear moiety which self-assembles into the tetranuclear species **1b**. Incidentally, also the passible precursor of **1b** has a structure strictly reminiscent of a trinuclear triangular species.

The formation of the mononuclear species as main product is in agreement, with the expectations based on the basicity of chloroacetate anion. On the other hand, the formation of **1b** and **1c** evidenced that minor quantities of trinuclear species can be also obtained due to the fact that the basicity of chloroacetate anion is probably at the border-line value for discriminating between the formation of mono and trinuclear species.

Passing now to the obtaining of CPs including bi-carboxylate anions, an important achievement of this work is related to the new synthetic strategy to insert the trinuclear triangular $[\text{Cu}_3(\mu_3\text{-OH})(\mu\text{-pz})_3]$ node into a polymeric structure, consisting in the reaction of the pre-synthesized trinuclear unit with bicarboxylic acid in stoichiometric amounts. This synthetic method quickly and quantitatively provides trinuclear species, which self-assemble mainly generating CPs. The trinuclear copper structure was structurally solved for **6a**, **9a** and only approximately for **2a**, while for **3a**, **4a** and **5a** it was inferred on the basis of the elemental analyses.

Experiments with the structurally rigid dicarboxylic acids shown a faster product precipitation with respect to the reactions with the flexible ones, a feature which unfavors the single crystals formation. On the other hand, the obtaining of suitable crystals for SC-XRD determination is often a serendipitous issue, even though it

seems that reaction deceleration facilitates this event. Due to the insolubility of the obtained CPs based on the trinuclear moiety, the use of re-crystallization techniques was not possible. On the other hand, the insolubility strongly suggests a stable polymeric nature of these compounds.

The XRPD patterns of **2a**, **3a**, **6b**, **7a** and **9b** confirm that these compounds are pure crystalline phases, while for **4a** it evidences that it has a main nanophase character and, finally, that **5a** is an amorphous phase [Appendix_C].

Anyway, another relevant point is the conservation of the crystal quality and structure after solvent evaporation. This step was crucial only in the cases of porous structures; otherwise, compact structures coincide with stable crystals even after drying.

Of interest, is the peculiar transformation in very mild conditions of **6a** and **9a** into **6b** and **9b**, respectively. This is in agreement to the presence of a first generation porous CPs, according to Kitagawa classification.¹⁵ This behavior may be due to the elimination of guest and/or weakly coordinated solvent molecules which permits structural rearrangements. After guest molecules elimination from PCPs **2a**, **6a** and **9a** a structural rearrangement to a “close” crystalline structure was evidenced in the cases of compounds **6b** and **9b** whose powder diffractograms after drying and calculated ones for the resolved structure were available, while, in the case of **2a** it is only possible to affirm that the dried material is a crystalline phase because the comparison between the structures of **2a** and **2b** was not possible due to the low SC-XRD data quality. On the basis of the previously reported data for the other compounds and on the basis of its macroscopic crystal breaking, probably its structure changes on drying. The structure of **5c** evidences the presence of coordinated DMF molecules, partly occupying the voids, while **5a**, which was washed with MeOH and dried, has analytical data corresponding to those of **5c** minus DMF molecules and an amorphous diffractogram.

The bicarboxylates linkers allow that the trinuclear moieties further self-assemble to generate CPs. In these processes, besides the covalent connections, an important role is likely played by supramolecular interactions that probably favors the formation of strong networks (**5a**) and the close packing of the isolated hexanuclear complexes

(**8b**). Particularly, H-bonds play the principal role as evidenced by the electron charge delocalization on the involved carboxylate groups.

Noteworthy, different reaction conditions may generate different CPs through specific coordination ways of bicarboxylate ions (**8a** vs **9a**).

In this work, it has been further confirmed the ability of Cu(II) ions to easily self-assemble in stable $[\text{Cu}_3(\mu_3\text{-OH})(\mu\text{-pz})_3]^{2+}$ moieties when bicarboxylate Cu(II) compounds are reacted, in suitable conditions, with Hpz, as evidenced by the obtainment of **7a** and **8a**.

Interestingly, the interaction of the preformed trinuclear moiety with muconic and hydromuconic acid gives, besides the trinuclear compounds joined by corresponding bicarboxylates, also neglectable amounts of mononuclear species (**4b**, **5b**) containing coordinated pyrazole molecules. This indicates a partial decomposition process of the starting material $[\text{Cu}_3(\mu_3\text{-OH})(\mu\text{-pz})_3(\text{CH}_3\text{COO})_2\text{Hpz}]$, probably due to the attack of acidic species, similarly to what found in the reactions of $[\text{Cu}_3(\mu_3\text{-OH})(\mu\text{-pz})_3(\text{CH}_3\text{COO})_2\text{Hpz}]$ with strong acids.⁸²

Finally, a homochiral (S)-methylsuccinate based PCP (**S**)-**6a** having the same structural characteristic of **6a**, which involves methylsuccinate in both the enantiomers, was obtained. Work is in progress to test its potential enantioselection power and the operative conditions for gas sorption.

In addition, an interesting future target is the determination of the conditions to obtain stable PCPs after guest molecules elimination.

7. REFERENCES

-
- ¹ H. C. Zhou, S. Kitagawa, *Chem. Soc. Rev.*, **2014**, 43, 5415-5418.
- ² L. J. Stuart, *Chem. Soc. Rev.*, **2003**, 32, 276-288.
- ³ B. F. Hoskins, R. J. Robson, *J. Am. Chem. Soc.*, **1989**, 111, 5962-5964.
- ⁴ W. Lu, Z. Wei, Z. Gu, T. Liu, J. Park, J. Park, J. Tian, M. Zhang, Q. Zhang, T. Gentle III, M. Bosch, H. Zhou, *Chem. Soc. Rev.*, **2014**, 43, 5561-5593.
- ⁵ J. R. Long, O. M. Yaghi, *Chem. Soc. Rev.*, **2009**, 38, 1213-1214.
- ⁶ R. J. Kuppler, D. J. Timmons, Q. R. Fang, J. R. Li, T. A. Makal, M. D. Young, D. Yuan, D. Zhao, W. Zhuang, H. C. Zhou, *Coord. Chem. Rev.*, **2009**, 253, 3042-3066.
- ⁷ K. Biradha, A. Ramanan, J. J. Vittal, *Cryst. Growth Des.*, **2009**, 9, 2069-2970.
- ⁸ S. R. Batten, N. R. Champness, X. M. Chen, J. Garcia-Martinez, S. Kitagawa, L. Öhrström, M. O’Keeffe, M. P. Suh, J. Reedijk, *Pure Appl. Chem.*, **2013**, 85, 1715-1724.
- ⁹ C. Janiak, *Dalton Trans.* **2003**, 2781-2804.
- ¹⁰ A. Y. Robin, K. M. Fromm, *Coord. Chem. Rev.*, **2006**, 250, 2127-2157.
- ¹¹ M. Eddaoudi, J. Kim, N. Rosi, D. Vodak, J. Wachter, M. O’Keeffe, O. M. Yaghi, *Science*, **2002**, 295, 469-472.
- ¹² Q. Ma, C. Abney, L. Wenbin, *Chem. Soc. Rev.* **2009**, 38, 1248-1256.
- ¹³ S. Yenisoy-Karakaş, A. Aygün, M. Güneş, E. Tahtasakal, *Carbon* **2004**, 42, 477-484.
- ¹⁴ O.M. Yaghi, H. Li, C. Davis, D. Richardson, T. L. Groy, *Acc. Chem. Res.* **1998**, 31, 474-484.
- ¹⁵ S. Kitagawa, R. Kitaura, S. Noro *Angew. Chem. Int. Ed.*, **2004**, 43, 2334 –2375.
- ¹⁶ S. Horike, S. Shimomura, S. Kitagawa, *Nat. Chem.* **2009**, 1, 695-704.
- ¹⁷ J. Zhang, P. Liao, H. Zhou, R. Lin, X. Chen, *Chem. Soc. Rev.*, **2014**, 43, 5789-5814.
- ¹⁸ C. Serre, F. Millange, C. Thouvenot, M. Nogues, G. Marsolier, D. Louer, G. Ferey, *J. Am. Chem. Soc.*, **2002**, 124, 13519-13526.
- ¹⁹ Z. Lin, J. Lu, M. Hong, R. Cao, *Chem. Soc. Rev.*, **2014**, 43, 5867-5895.

-
- ²⁰ J. Liu, L. Chen, H. Cui, J. Zhang, L. Zhang, C. Su, *Chem. Soc. Rev.*, **2014**, 43, 6011-6061.
- ²¹ P. T. Anastas, J. C. Warner, *Green Chemistry: Theory and Practice*, Oxford University Press: New York, **1998**, 30.
- ²² C. Copéret, M. Chabanas, R. Petroff Saint-Arroman, J.M. Basset, *Angew. Chem. Int. Ed.*, **2003**, 42, 156-181.
- ²³ G. Rothenberg, *Catalysis: concepts and green applications*, Wiley, VCH, Weinheim, **2008**.
- ²⁴ P. G. Garcia, M. Muller, A. Corma, *Chem. Sci.*, **2014**, 5, 2979-3007.
- ²⁵ J. Lee, O. K. Farha, J. Roberts, K. A. Scheidt, S. T. Nguyen, J. T. Hupp, *Chem. Soc. Rev.*, **2009**, 38, 1450-1459.
- ²⁶ Q. Ma, C. Abney, L. Wenbin, *Chem. Soc. Rev.* **2009**, 38, 1248-1256.
- ²⁷ S. S. Y. Chui, S. M. F. Lo, J. P. H. Charmant, A. G. Orpen, I. D. Williams, *Science*, **1999**, 283, 1148-1150.
- ²⁸ K. Schlichte, T. Kratzke, S. Kaskel, *Microporous Mesoporous Mater.* **2004**, 73, 81-88.
- ²⁹ S. Hasegawa, S. HoriKe, R. Matsuda, S. Furukawa, K. Mochizuki, Y. Kinoshita, S. Kitagawa, *J. Am. Chem. Soc.*, **2007**, 129, 2607-2614.
- ³⁰ J. S. Seo, D. Whang, H. Lee, S. I. Jun, J. Oh, Y. J. Jeon, K. Kim, *Nature*, **2000**, 404, 982-986.
- ³¹ T. Uemura, R. Kitaura, Y. Ohta, M. Nagaoka, and S. Kitagawa, *Angew. Chem. Int. Ed.*, **2006**, 45, 4112–4116.
- ³² S. Su, Y. Zhang, M. Zhu, X. Song, S. Wang, S. Zhao, S. Song, X. Yang, H. Zhang, *Chem. Commun.*, **2012**, 48, 11118-11120.
- ³³ E. Barea, C. Montoro, J. A. R. Navarro, *Chem. Soc. Rev.*, **2014**, 43, 5419-5430.
- ³⁴ Y. He, W. Zhou, G. Qian, B. Chen, *Chem. Soc. Rev.*, **2014**, 43, 5657-5678.
- ³⁵ J. Song, Z. Luo, D. K. Britt, H. Furukawa, O. M. Yaghi, K. I. Hardcastle and C. L. Hill, *J. Am. Chem. Soc.*, **2011**, 133, 16839-16846.

-
- ³⁶ L. Mathivathanan, J. Torres-King, J. N. Primera-Pedrozo, O. J. García-Ricard, A. J. Hernandez-Maldonado, J. A. Santana, R. G. Raptis, *Cryst. Growth Des.* **2013**, 13, 2628–2635.
- ³⁷ R. Matsuda, R. Kitaura, S. Kitagawa, Y. Kubota, R.V. Belosludov, T.C. Kobayashi, H. Sakamoto, T. Chiba, M. Takata, Y. Kawazoe, Y. Mita, *Nature*, **2005**, 436, 238-241.
- ³⁸ A. U. Czaja, N. Trukhan and U. Mueller, *Chem. Soc. Rev.*, **2009**, 38, 1284-1293
- ³⁹ U. Mueller, M. Schubert, F. Teich, H. Puetter, K. Schierle,-Arndt, J. Pastré, *J. Mater. Chem.*, **2006**, 16, 626-636.
- ⁴⁰ D. Farrusseng, S. Aguado, C. Pinel, *Angew. Chem. Int. Ed.*, **2009**, 48, 7502-7513.
- ⁴¹ G. R. Desiraju, *J. Am. Chem. Soc.*, **2013**, 135, 9952-9967.
- ⁴² Theories and Techniques of Crystal Structure Determination; U. Shmueli, IUCr texts on crystallography, 9; Oxford Science Publications **2007**.
- ⁴³ J. Maddox, *Nature*, **1988**, 335, 201.
- ⁴⁴ *Fundamentals of Crystallography*; Giacovazzo, C., Ed.; IUCr texts on crystallography, 7; Oxford University Press: Oxford, UK, **2002**; Ch. 3 and 5.
- ⁴⁵ McKie, D.; C. McKie, C. *Essentials of crystallography*; Blackwell Scientific Publications: Oxford, **1986**; Ch. 6.
- ⁴⁶ P. G. Jones, *Chem. Br.*, **1981**, 17, 5, 222-225.
- ⁴⁷ B. Spingler, S. Schnigrig, T. Todorova, F. Wild, *Cryst. Eng. Comm.*, **2012**, 14, 751-757.
- ⁴⁸ A. Altomare, C. Giacovazzo, A. Grazia, G. Moliterni, R. J. Rizzi, *Res. Nat. Inst. Stand. Technol.* **2004**, 109, 125-132.
- ⁴⁹ A. U. Czaja, N. Trukhan, U. Müller, *Chem. Soc. Rev.*, **2009**, 38, 1284-1293.
- ⁵⁰ M. Rubio-Martinez, M. P. Batten, A. Polyzos, K-C. Carey, J. I. Mardel, K-S. Lim, M. R. Hill, *Sci. Rep.* **2014**, 4, 5443-5447.
- ⁵¹ K. Leus, Y. Y. Liu, P. Van Der Voort, *Cat. Rev.*, **2014**, 56, 1-56.
- ⁵² E. I. Solomon, U. M. Sundaram, T. E. Machonkin, *Chem. Rev.*, **1996**, 96, 2563.
- ⁵³ C. Di Nicola, F. Garau, Y. Y. Karabach, L. M. D. R. S. Martins, M. Monari, L. Pandolfo, C. Pettinari, A. J. L. Pombeiro, *Eur. J. Inorg. Chem.*, **2009**, 666-676.

-
- ⁵⁴ M. Casarin, C. Corvaja, C. di Nicola, D. Falcomer, L. Franco, M. Monari, L. Pandolfo, C. Pettinari, F. Piccinelli, P. Tagliatesta, *Inorg. Chem.*, **2004**, 43, 5865-5876.
- ⁵⁵ M. Casarin, C. Corvaja, C. Di Nicola, D. Falcomer, L. Franco, M. Monari, L. Pandolfo, C. Pettinari, F. Piccinelli, *Inorg. Chem.*, **2005**, 44, 6265-6276.
- ⁵⁶ C. Di Nicola, Y. Yu. Karabach, A. M. Kirillov, M. Monari, L. Pandolfo, C. Pettinari, A. J. L. Pombeiro, *Inorg. Chem.*, **2007**, 46, 221-230.
- ⁵⁷ E. Zangrando, M. Casanova, E. Alessio, *Chem. Rev.* **2008**, 108, 4979-5013.
- ⁵⁸ CRC Handbook of Chemistry and Physics 84th Ed. **2003-2004**.
- ⁵⁹ L. Dubiski, C. M. Harris, E. Kokot and R. L. Martins, *Inorg. Chem.*, **1966**, 5, 93-100.
- ⁶⁰ M. Casarin, C. Corvaja, C. Di Nicola, D. Falcomer, L. Franco, M. Monari, L. Pandolfo, C. Pettinari, F. Piccinelli, *Inorg. Chem.*, **2005**, 44, 6265-6276.
- ⁶¹ G. A. Bain, J. F. Berry, *J. Chem. Ed.* **2008**, 85, 532-536.
- ⁶² Oxford Diffraction Ltd, Abingdon, England, **2006**, *Oxford Diffraction*.
- ⁶³ The CryAlis user manual.
- ⁶⁴ L.J. Farrugia, *J. Appl. Cryst.*, **2012**, 45, 849-854.
- ⁶⁵ D. Schwarzenbach, S. C. Abrahams, H. D. Flack, W. Gonschorek, T. Hahn, K. Huml, R. E. Marsh, E. Prince, B. E. Robertson, J. S. Rollet, A. J. C. Wilson, *Acta Crystallogr., Sect. A: Found. Crystallogr.* **1989**, 45, 63-75.
- ⁶⁶ A. Altomare, M. C. Burla, M. Camalli, G. L. Cascareno, C. Giacovazzo, A. Guagliardi, A. G. G. Moliterni, G. Polidori, R. Spagna, *J. Appl. Cryst.*, **1999**, 32, 115-119.
- ⁶⁷ *SHELX97* [Includes SHELXS97, SHELXL97, CIFTAB, SHELXA] - *Programs for Crystal Structure Analysis (Release 97-2)*. G. M. Sheldrick, Institut für Anorganische Chemie der Universität, Tammanstrasse 4, D-3400 Göttingen, DE, **1998**.
- ⁶⁸ *PLATON, A Multipurpose Crystallographic Tool*. A. L. Spek, Utrecht University, Utrecht, NL, **1998**.
- ⁶⁹ *X-RED. Data Reduction Program*. STOE and Cie GmbH, Darmstadt, DE, **2001**.

-
- ⁷⁰ *X-SHAPE. Crystal Optimisation for Numerical Absorption Correction*. STOE and Cie GmbH, Darmstadt, DE, **1999**.
- ⁷¹ A. L. Speck, *Acta Cryst*, **2009**, D65, 148-155.
- ⁷² The SHELX-97 Manual.
- ⁷³ G. L. Miessler, D. A. Tarr, *Inorganic Chemistry*, 5th ed.
- ⁷⁴ M. Casarin, S. Carlotto, *Personal Communication*.
- ⁷⁵ F. A. Cotton, G. Wilkinson, *Advanced Inorganic Chemistry*, 5th ed., Wiley Interscience, **1988**.
- ⁷⁶ D. J. White, L. Cronin, S. Parsons, N. Robertson, P. A. Tasker, A. P. Bisson, *Chem. Comm.*, **1999**, 1107-1108.
- ⁷⁷ T. A. Albright, J. K. Burdett, M. H. Whangbo, *Orbital Interaction in Chemistry*, **1985**, Wiley ed.
- ⁷⁸ C. Ramakrishnan, Y. S. Geetha, *Chem. Sci.*, **1990**, 102, 481-496.
- ⁷⁹ M. Casarin, A. Cingolani, C. Di Nicola, D. Falcomer, M. Monari, L. Pandolfo, C. Pettinari, *Crys. Growth Des.*, **2007**, 7, 676-685
- ⁸⁰ C. Di Nicola, E. Forlin, F. Garau, M. Gazzano, A. Lanza, M. Monari, F. Nestola, L. Pandolfo, C. Pettinari, A. Zorzi, F. Zorzi, *Cryst. Growth Des.*, **2013**, 13, 126-135.
- ⁸¹ Spek, A. L. PLATON A Multipurpose Crystallographic Tool; Utrecht University: Utrecht, the Netherlands, **2003**.
- ⁸² C. Di Nicola, F. Garau, M. Gazzano, M. Monari, L. Pandolfo, C. Pettinari, R. Pettinari, *Cryst. Growth Des.*, **2010**, 10, 3120.

Appendix A Crystal data and structure refinement

| | |
|-----------------------------------|-------------------------------------------------------------------------------------------------------------|
| Identification code | 1a |
| Empirical formula | C ₅ H ₆ Cl Cu _{0.5} N ₂ O ₂ |
| Formula weight | 192.47 g/mol |
| Temperature | 293(2) K |
| Wavelength | 0.71073 Å |
| Crystal system, space group | Triclinic, P ₁ |
| Unit cell dimensions | a = 5.0783(2) Å α = 73.150(4)° b = 7.5176(4) Å β = 83.485(4)° c = 9.9479(4) Å γ = 77.841(4)° |
| Volume | 354.76(3) Å ³ |
| Z, Calculated density | 2, 1.810 g/cm ³ |
| Absorption coefficient | 1.936 mm ⁻¹ |
| F(000) | 195 |
| Crystal size | 0.1 x 0.1 x 0.1 mm ³ |
| Theta range for data collection | 2.142 to 32.020° |
| Limiting indices | -7 ≤ h ≤ 7, -11 ≤ k ≤ 11, -14 ≤ l ≤ 14 |
| Reflections collected / unique | 8914 / 2279 [R _{int} = 0.0276] |
| Completeness to theta = 25.242 | 100.0 % |
| Refinement method | Full-matrix least-squares on F ² |
| Data / restraints / parameters | 2279 / 0 / 121 |
| Goodness-of-fit on F ² | 0.944 |
| Final R indices [I > 2σ(I)] | R1 = 0.0269, wR2 = 0.0729 |
| R indices (all data) | R1 = 0.0311, wR2 = 0.0765 |
| Extinction coefficient | n/a |
| Largest diff. peak and hole | 0.333 and -0.319 e.Å ⁻³ |

| | |
|-----------------------------------|------------------------------------------------------------------------------------------------|
| Identification code | 1b |
| Empirical formula | C ₂₂ H ₂₄ Cl ₂ Cu ₄ N ₈ O ₁₂ |
| Formula weight | 913.80 g/mol |
| Temperature | 296(2) K |
| Wavelength | 0.71073 Å |
| Crystal system, space group | Monoclinic, P _{21/n} |
| Unit cell dimensions | a = 8.4951(4) Å α = 90° b = 16.0943(7) Å β = 109.077(6)° c = 12.8819(6) Å γ = 90° |
| Volume | 1664.52(14) Å ³ |
| Z, Calculated density | 2, 1.831 g/cm ³ |
| Absorption coefficient | 2.750 mm ⁻¹ |
| F(000) | 916 |
| Crystal size | 0.1 x 0.1 x 0.1 mm ³ |
| Theta range for data collection | 2.097 to 31.882 deg. |
| Limiting indices | -10 ≤ h ≤ 12, -22 ≤ k ≤ 17, - 18 ≤ l ≤ 18 |
| Reflections collected / unique | 6659 / 4309 [R _{int} = 0.0205] |
| Completeness to theta = 25.242 | 89.8 % |
| Refinement method | Full-matrix least-squares on F ² |
| Data / restraints / parameters | 4309 / 1 / 221 |
| Goodness-of-fit on F ² | 1.025 |
| Final R indices [I > 2σ(I)] | R1 = 0.0388, wR2 = 0.1063 |
| R indices (all data) | R1 = 0.0560, wR2 = 0.1155 |
| Extinction coefficient | n/a |
| Largest diff. peak and hole | 0.991 and -0.869 e.Å ⁻³ |

| | |
|-----------------------------------|------------------------------------------------------------------------------------------------------------|
| Identification code | 1c |
| Empirical formula | C ₁₇ Cl ₁ Cu ₃ H ₂₀ N ₁₀ O ₃ |
| Formula weight | 635.93 g/mol |
| Temperature | 296(2) K |
| Wavelength | 0.71073 Å |
| Crystal system, space group | Triclinic, P ₁ |
| Unit cell dimensions | a = 8.8168(9) Å α = 78.816(8)° b = 8.9397(9) Å β = 78.074(8)° c = 16.8959(16) Å γ = 68.557(9)° |
| Volume | 1202.5(2) Å ³ |
| Z, Calculated density | 2, 1.834 g/cm ³ |
| Absorption coefficient | 2.896 mm ⁻¹ |
| F(000) | 662 |
| Crystal size | 0.1 x 0.1 x 0.1 mm ⁻³ |
| Theta range for data collection | 2.469 to 25.998° |
| Limiting indices | -10 ≤ h ≤ 10, -11 ≤ k ≤ 11, - 20 ≤ l ≤ 20 |
| Reflections collected / unique | 17371 / 4713 [R _{int} = 0.0705] |
| Completeness to theta = 25.242 | 99.9 % |
| Refinement method | Full-matrix least-squares on F ² |
| Data / restraints / parameters | 4713 / 2 / 320 |
| Goodness-of-fit on F ² | 1.002 |
| Final R indices [I > 2σ(I)] | R1 = 0.0765, wR2 = 0.2203 |
| R indices (all data) | R1 = 0.1049, wR2 = 0.2433 |
| Extinction coefficient | n/a |
| Largest diff. peak and hole | 1.765 and -0.756 e.Å ⁻³ |

| | |
|-----------------------------------|-----------------------------------------------------------------------------------------------------------|
| Identification code | 4b |
| Empirical formula | C ₁₈ H ₂₀ Cu ₁ N ₈ O ₄ |
| Formula weight | 475.09 g/mol |
| Temperature | 293(2) K |
| Wavelength | 0.71073 Å |
| Crystal system, space group | Triclinic, P ₁ |
| Unit cell dimensions | a = 8.0205(4) Å α = 90.406(4)° b = 8.1821(4) Å β = 94.075(4)° c = 8.3376(4) Å γ = 111.760(4)° |
| Volume | 506.55(4) Å ³ |
| Z, Calculated density | 2, 1.800 g/cm ³ |
| Absorption coefficient | 3.159 mm ⁻¹ |
| F(000) | 273 |
| Crystal size | 0.1 x 0.1 x 0.1 mm |
| Theta range for data collection | 2.451 to 29.910° |
| Limiting indices | -10 ≤ h ≤ 10, -11 ≤ k ≤ 10, -11 ≤ l ≤ 11 |
| Reflections collected / unique | 9785 / 2618 [R _{int} = 0.0229] |
| Completeness to theta = 25.242 | 99.9 % |
| Refinement method | Full-matrix least-squares on F ² |
| Data / restraints / parameters | 2618 / 0 / 142 |
| Goodness-of-fit on F ² | 1.060 |
| Final R indices [I > 2σ(I)] | R1 = 0.0289, wR2 = 0.0710 |
| R indices (all data) | R1 = 0.0335, wR2 = 0.0730 |
| Extinction coefficient | n/a |
| Largest diff. peak and hole | 0.355 and -0.232 e.Å ⁻³ |

| | |
|-----------------------------------|-----------------------------------------------------------------------------------------------------------|
| Identification code | 5b |
| Empirical formula | C ₂₄ H ₃₀ Cu N ₈ O ₈ |
| Formula weight | 621.15 |
| Temperature | 293(2) K |
| Wavelength | 0.71073 Å |
| Crystal system, space group | Triclinic, P ₁ |
| Unit cell dimensions | a = 8.6225(3) Å α = 87.185(3)° b = 8.6600(3) Å β = 65.715(3)° c = 10.1755(3) Å γ = 88.797(3)° |
| Volume | 691.74(4) Å ³ |
| Z, Calculated density | 2, 1.656 g/cm ³ |
| Absorption coefficient | 1.601 mm ⁻¹ |
| F(000) | 356 |
| Crystal size | 0.1 x 0.1 x 0.1 mm |
| Theta range for data collection | 2.198 to 32.067° |
| Limiting indices | -12 ≤ h ≤ 12, -12 ≤ k ≤ 12, -14 ≤ l ≤ 15 |
| Reflections collected / unique | 18343 / 4448 [R _{int} = 0.0256] |
| Completeness to theta = 25.242 | 100.0 % |
| Refinement method | Full-matrix least-squares on F ² |
| Data / restraints / parameters | 4448 / 0 / 187 |
| Goodness-of-fit on F ² | 1.082 |
| Final R indices [I > 2σ(I)] | R1 = 0.0414, wR2 = 0.1147 |
| R indices (all data) | R1 = 0.0459, wR2 = 0.1184 |
| Extinction coefficient | n/a |
| Largest diff. peak and hole | 1.615 and -0.828 e.Å ⁻³ |

| | |
|-----------------------------------|------------------------------------------------------------------------------------------------------------------|
| Identification code | 5c |
| Empirical formula | C ₃₆ H ₄₆ Cu ₆ N ₁₄ O ₁₂ |
| Formula weight | 1243.92 |
| Temperature | 296(2) K |
| Wavelength | 0.71073 Å |
| Crystal system, space group | Triclinic, P ₁ |
| Unit cell dimensions | a = 12.1322(11) Å α = 98.386(6)° b = 12.1456(13) Å β = 101.960(5)° c = 19.7386(8) Å γ = 115.189(10)° |
| Volume | 2483.2(4) Å ³ |
| Z, Calculated density | 2, 1.474 g/cm ³ |
| Absorption coefficient | 2.578 mm ⁻¹ |
| F(000) | 1100 |
| Crystal size | 0.1 x 0.1 x 0.1 mm |
| Theta range for data collection | 1.921 to 25.999 deg. |
| Limiting indices | -14 ≤ h ≤ 14, -14 ≤ k ≤ 14, -24 ≤ l ≤ 24 |
| Reflections collected / unique | 38744 / 9723 [R _{int} = 0.1195] |
| Completeness to theta = 25.242 | 99.9 % |
| Refinement method | Full-matrix least-squares on F ² |
| Data / restraints / parameters | 9723 / 1 / 563 |
| Goodness-of-fit on F ² | 1.039 |
| Final R indices [I > 2σ(I)] | R1 = 0.0920, wR2 = 0.2439 |
| R indices (all data) | R1 = 0.1893, wR2 = 0.3032 |
| Extinction coefficient | n/a |
| Largest diff. peak and hole | 2.180 and -0.772 e.Å ⁻³ |

| | | |
|-----------------------------------|-------------------------------------------------------------------------------|----------|
| Identification code | 6a | |
| Empirical formula | C ₁₅ H ₂₂ Cu ₃ N ₆ O ₇ | |
| Formula weight | 589.00 g/mol | |
| Temperature | 297(2) K | |
| Wavelength | 0.71073 Å | |
| Crystal system | Trigonal | |
| Space group | R -3 :H | |
| Unit cell dimensions | a = 27.4767(9) Å | α = 90° |
| | b = 27.4767(9) Å | β = 90° |
| | c = 20.5399(8) Å | γ = 120° |
| Volume | 13429.4(10) Å ³ | |
| Z | 18 | |
| Density (calculated) | 1.311 g/cm ³ | |
| Absorption coefficient | 2.154 mm ⁻¹ | |
| F(000) | 5346 | |
| Crystal size | 0.226 x 0.162 x 0.138 mm ³ | |
| Theta range for data collection | 1.482 to 29.940°. | |
| Index ranges | -38 ≤ h ≤ 37, -36 ≤ k ≤ 38, - | |
| | 28 ≤ l ≤ 28 | |
| Reflections collected | 98586 | |
| Independent reflections | 8152 [R(int) = 0.1435] | |
| Completeness to theta = 25.242° | 100.0 % | |
| Absorption correction | Gaussian | |
| Max. and min. transmission | 0.736 and 0.647 | |
| Refinement method | Full-matrix least-squares on F ² | |
| Data / restraints / parameters | 8152 / 4 / 286 | |
| Goodness-of-fit on F ² | 1.000 | |
| Final R indices [I > 2σ(I)] | R1 = 0.0736, wR2 = 0.2459 | |
| R indices (all data) | R1 = 0.1732, wR2 = 0.3061 | |
| Extinction coefficient | n/a | |
| Largest diff. peak and hole | 1.416 and -0.420 e.Å ⁻³ | |

| | |
|-----------------------------------|--------------------------------------------------------------------------------------------|
| Identification code | (S)-6a |
| Empirical formula | C ₁₅ H ₂₂ Cu ₃ N ₆ O ₇ |
| Formula weight | 589.00 g/mol |
| Temperature | 298(2) K |
| Wavelength | 0.71073 Å |
| Crystal system, space group | Trigonal, R ₃ |
| Unit cell dimensions | a = 27.4763(7) Å α = 90° b = 27.4763(7) Å β = 90° c = 19.0861(6) Å γ = 120° |
| Volume | 12478.5(7) Å ³ |
| Z, Calculated density | 3, 1.881 g/cm ³ |
| Absorption coefficient | 3.091 mm ⁻¹ |
| F(000) | 7128 |
| Crystal size | 0.1 x 0.1 x 0.1 mm |
| Theta range for data collection | 1.482 to 30.168 deg. |
| Limiting indices | -36<=h<=35, -38<=k<=37, -26<=l<=26 |
| Reflections collected / unique | 78746 / 14733 [R _{int} = 0.0702] |
| Completeness to theta = 25.242 | 100.0 % |
| Refinement method | Full-matrix least-squares on F ² |
| Data / restraints / parameters | 14733 / 49 / 559 |
| Goodness-of-fit on F ² | 0.996 |
| Final R indices [I>2sigma(I)] | R1 = 0.0593, wR2 = 0.1560 |
| R indices (all data) | R1 = 0.1191, wR2 = 0.1821 |
| Absolute structure parameter | 0.111(17) |
| Extinction coefficient | n/a |
| Largest diff. peak and hole | 0.663 and -0.327 e.Å ⁻³ |

| | |
|-----------------------------------|--------------------------------------------------------------------------------------------------------------|
| Identification code | 8b |
| Empirical formula | C ₁₈ H ₂₈ Cu ₃ N ₈ O ₈ |
| Formula weight | 672.99 |
| Temperature | 293(2) K |
| Wavelength | 0.71073 Å |
| Crystal system | Triclinic |
| Space group | P -1 |
| Unit cell dimensions | a = 9.0103(3) Å α = 76.257(2)° b = 9.4673(3) Å β = 77.300(2)° c = 15.6095(4) Å γ = 89.281(2)° |
| Volume | 1260.67(7) Å ³ |
| Z | 2 |
| Density (calculated) | 1.537 g/cm ³ |
| Absorption coefficient | 1.737 mm ⁻¹ |
| F(000) | 604 |
| Crystal size | 0.1 x 0.1 x 0.1 mm ³ |
| Theta range for data collection | 2.217 to 32.034°. |
| Index ranges | -13 ≤ h ≤ 12, -13 ≤ k ≤ 13, -23 ≤ l ≤ 22 |
| Reflections collected | 34399 |
| Independent reflections | 8109 [R _{int} = 0.0333] |
| Completeness to theta = 25.242° | 100.0 % |
| Refinement method | Full-matrix least-squares on F ² |
| Data / restraints / parameters | 8109 / 4 / 349 |
| Goodness-of-fit on F ² | 1.035 |
| Final R indices [I > 2σ(I)] | R1 = 0.0361, wR2 = 0.0937 |
| R indices (all data) | R1 = 0.0538, wR2 = 0.1027 |
| Extinction coefficient | n/a |
| Largest diff. peak and hole | 1.127 and -0.702 e.Å ⁻³ |

| | |
|-----------------------------------|--------------------------------------------------------------------------------------|
| Identification code | 9a |
| Empirical formula | C ₁₅ H ₁₈ Cu ₃ N ₆ O ₆ |
| Formula weight | 599.92 g/mol |
| Temperature | 298(2) K |
| Wavelength | 0.71073 Å |
| Crystal system, space group | Trigonal, R _{3c} |
| Unit cell dimensions | a = 26.820(4) Å α = 90° b = 26.820(4) Å β = 90° c = 18.147(2) Å γ = 120° |
| Volume | 11305(4) Å ³ |
| Z, Calculated density | 6, 0.975 g/cm ³ |
| Absorption coefficient | 1.699 mm ⁻¹ |
| F(000) | 3324 |
| Crystal size | 0.1 x 0.1 x 0.1 mm ³ |
| Theta range for data collection | 1.518 to 25.999° |
| Limiting indices | -33 ≤ h ≤ 32, -33 ≤ k ≤ 33, -22 ≤ l ≤ 22 |
| Reflections collected / unique | 24393 / 4459 [R _{int} = 0.3287] |
| Completeness to theta = 25.242 | 100.0 % |
| Refinement method | Full-matrix least-squares on F ² |
| Data / restraints / parameters | 4459 / 1 / 280 |
| Goodness-of-fit on F ² | 1.050 |
| Final R indices [I > 2σ(I)] | R1 = 0.1227, wR2 = 0.2113 |
| R indices (all data) | R1 = 0.2738, wR2 = 0.2631 |
| Absolute structure parameter | 0.95(4) |
| Extinction coefficient | n/a |
| Largest diff. peak and hole | 0.517 and -0.513 e.Å ⁻³ |

Appendix B Bond lengths and angles

Table 1. Bond lengths [Å] and angles [°] for **1a**.

| | | | |
|------------------------------------------------------------------------------|------------|-------------------|------------|
| Cu(01)-N(006) | 1.9968(12) | Cu(2)-O(1) | 1.933(2) |
| Cu(01)-N(006)#1 | 1.9968(12) | Cu(2)-O(2) | 1.934(2) |
| Cu(01)-O(004) | 2.0040(11) | Cu(2)-N(2) | 1.937(3) |
| Cu(01)-O(004)#1 | 2.0040(11) | Cu(2)-O(5)#1 | 1.965(2) |
| Cl(02)-C(009) | 1.767(2) | Cl(1)-C(10) | 1.752(4) |
| O(003)-C(010) | 1.2507(19) | O(3)-C(8) | 1.231(4) |
| O(004)-C(010) | 1.2563(18) | O(2)-C(8) | 1.292(4) |
| N(005)-C(007) | 1.341(2) | O(5)-C(9) | 1.235(4) |
| N(005)-N(006) | 1.3495(17) | O(5)-Cu(2)#1 | 1.965(2) |
| N(006)-C(008) | 1.342(2) | O(1)-C(7) | 1.416(3) |
| C(007)-C(011) | 1.368(3) | O(4)-C(9) | 1.240(4) |
| C(008)-C(011) | 1.389(2) | O(6)-C(11) | 1.393(5) |
| C(009)-C(010) | 1.522(2) | O(6)-H(6M) | 0.878(19) |
| N(006)-Cu(01)-N(006)#1 | 180.0 | N(4)-C(6) | 1.337(5) |
| N(006)-Cu(01)-O(004) | 94.93(5) | N(4)-N(3) | 1.339(4) |
| N(006)#1-Cu(01)-O(004) | 85.07(5) | N(4)-H(4) | 0.8600 |
| N(006)-Cu(01)-O(004)#1 | 85.07(5) | N(2)-C(3) | 1.338(4) |
| N(006)#1-Cu(01)-O(004)#1 | 94.93(5) | N(2)-N(1) | 1.363(4) |
| O(004)-Cu(01)-O(004)#1 | 180.0 | C(8)-C(7) | 1.517(4) |
| C(010)-O(004)-Cu(01) | 136.04(11) | N(1)-C(1) | 1.349(4) |
| C(007)-N(005)-N(006) | 111.11(14) | C(4)-N(3) | 1.313(4) |
| C(008)-N(006)-N(005) | 105.34(13) | C(4)-C(5) | 1.392(6) |
| C(008)-N(006)-Cu(01) | 130.76(11) | C(4)-H(4A) | 0.9300 |
| N(005)-N(006)-Cu(01) | 123.72(10) | C(7)-H(7A) | 0.9700 |
| N(005)-C(007)-C(011) | 107.84(15) | C(7)-H(7B) | 0.9700 |
| N(006)-C(008)-C(011) | 110.69(15) | C(9)-C(10) | 1.539(4) |
| C(010)-C(009)-Cl(02) | 114.81(13) | C(3)-C(2) | 1.370(5) |
| O(003)-C(010)-O(004) | 126.77(15) | C(3)-H(3) | 0.9300 |
| O(003)-C(010)-C(009) | 114.96(14) | C(10)-H(10A) | 0.9700 |
| O(004)-C(010)-C(009) | 118.26(15) | C(10)-H(10B) | 0.9700 |
| C(007)-C(011)-C(008) | 105.03(15) | C(1)-C(2) | 1.387(5) |
| Symmetry transformations used to generate equivalent atoms: #1 -x+2,-y,-z | | C(1)-H(1) | 0.9300 |
| Table 2. Bond lengths [Å] and angles [°] for 1b . | | C(2)-H(2) | 0.9300 |
| Cu(1)-N(1) | 1.959(3) | C(6)-C(5) | 1.331(6) |
| Cu(1)-O(1) | 1.962(2) | C(6)-H(6) | 0.9300 |
| Cu(1)-O(4) | 1.981(2) | C(5)-H(5) | 0.9300 |
| Cu(1)-N(3) | 2.008(3) | C(11)-H(11A) | 0.9600 |
| Cu(1)-O(6) | 2.271(3) | C(11)-H(11B) | 0.9600 |
| | | C(11)-H(11C) | 0.9600 |
| | | N(1)-Cu(1)-O(1) | 87.62(10) |
| | | N(1)-Cu(1)-O(4) | 178.70(11) |
| | | O(1)-Cu(1)-O(4) | 92.07(9) |
| | | N(1)-Cu(1)-N(3) | 90.86(11) |
| | | O(1)-Cu(1)-N(3) | 163.91(11) |
| | | O(4)-Cu(1)-N(3) | 89.09(11) |
| | | N(1)-Cu(1)-O(6) | 97.05(11) |
| | | O(1)-Cu(1)-O(6) | 101.38(11) |
| | | O(4)-Cu(1)-O(6) | 84.25(10) |
| | | N(3)-Cu(1)-O(6) | 94.71(12) |
| | | O(1)-Cu(2)-O(2) | 84.42(9) |
| | | O(1)-Cu(2)-N(2) | 90.10(10) |
| | | O(2)-Cu(2)-N(2) | 164.82(11) |
| | | O(1)-Cu(2)-O(5)#1 | 177.25(10) |

| | |
|---------------------|------------|
| O(2)-Cu(2)-O(5)#1 | 94.58(10) |
| N(2)-Cu(2)-O(5)#1 | 91.49(10) |
| C(8)-O(2)-Cu(2) | 114.19(19) |
| C(9)-O(5)-Cu(2)#1 | 130.9(2) |
| C(7)-O(1)-Cu(2) | 111.43(17) |
| C(7)-O(1)-Cu(1) | 125.80(17) |
| Cu(2)-O(1)-Cu(1) | 119.11(10) |
| C(9)-O(4)-Cu(1) | 127.3(2) |
| C(11)-O(6)-Cu(1) | 124.5(3) |
| C(11)-O(6)-H(6M) | 113(3) |
| Cu(1)-O(6)-H(6M) | 121(3) |
| C(6)-N(4)-N(3) | 110.6(3) |
| C(6)-N(4)-H(4) | 124.7 |
| N(3)-N(4)-H(4) | 124.7 |
| C(3)-N(2)-N(1) | 108.3(3) |
| C(3)-N(2)-Cu(2) | 132.0(2) |
| N(1)-N(2)-Cu(2) | 119.39(18) |
| O(3)-C(8)-O(2) | 123.0(3) |
| O(3)-C(8)-C(7) | 120.8(3) |
| O(2)-C(8)-C(7) | 116.1(3) |
| C(1)-N(1)-N(2) | 107.2(3) |
| C(1)-N(1)-Cu(1) | 130.8(2) |
| N(2)-N(1)-Cu(1) | 121.99(19) |
| N(3)-C(4)-C(5) | 109.9(3) |
| N(3)-C(4)-H(4A) | 125.1 |
| C(5)-C(4)-H(4A) | 125.1 |
| O(1)-C(7)-C(8) | 110.1(2) |
| O(1)-C(7)-H(7A) | 109.6 |
| C(8)-C(7)-H(7A) | 109.6 |
| O(1)-C(7)-H(7B) | 109.6 |
| C(8)-C(7)-H(7B) | 109.6 |
| H(7A)-C(7)-H(7B) | 108.2 |
| C(4)-N(3)-N(4) | 105.9(3) |
| C(4)-N(3)-Cu(1) | 130.4(3) |
| N(4)-N(3)-Cu(1) | 123.0(2) |
| O(5)-C(9)-O(4) | 128.5(3) |
| O(5)-C(9)-C(10) | 118.2(3) |
| O(4)-C(9)-C(10) | 113.3(3) |
| N(2)-C(3)-C(2) | 110.1(3) |
| N(2)-C(3)-H(3) | 125.0 |
| C(2)-C(3)-H(3) | 125.0 |
| C(9)-C(10)-Cl(1) | 113.7(3) |
| C(9)-C(10)-H(10A) | 108.8 |
| Cl(1)-C(10)-H(10A) | 108.8 |
| C(9)-C(10)-H(10B) | 108.8 |
| Cl(1)-C(10)-H(10B) | 108.8 |
| H(10A)-C(10)-H(10B) | 107.7 |
| N(1)-C(1)-C(2) | 109.7(3) |
| N(1)-C(1)-H(1) | 125.1 |
| C(2)-C(1)-H(1) | 125.1 |
| C(3)-C(2)-C(1) | 104.7(3) |
| C(3)-C(2)-H(2) | 127.7 |
| C(1)-C(2)-H(2) | 127.7 |
| C(5)-C(6)-N(4) | 107.8(4) |
| C(5)-C(6)-H(6) | 126.1 |
| N(4)-C(6)-H(6) | 126.1 |
| C(6)-C(5)-C(4) | 105.7(4) |
| C(6)-C(5)-H(5) | 127.1 |
| C(4)-C(5)-H(5) | 127.1 |
| O(6)-C(11)-H(11A) | 109.5 |

| | |
|---------------------|-------|
| O(6)-C(11)-H(11B) | 109.5 |
| H(11A)-C(11)-H(11B) | 109.5 |
| O(6)-C(11)-H(11C) | 109.5 |
| H(11A)-C(11)-H(11C) | 109.5 |
| H(11B)-C(11)-H(11C) | 109.5 |

Symmetry transformations used to generate equivalent atoms:

#1 -x+1,-y+1,-z+1

Table 3. Bond lengths [Å] and angles [°] for **1c**.

| | |
|-------------|-----------|
| Cu(1)-N(1) | 1.948(7) |
| Cu(1)-N(6) | 1.958(7) |
| Cu(1)-O(2) | 1.980(6) |
| Cu(1)-O(1) | 1.975(6) |
| Cu(2)-N(2) | 1.947(7) |
| Cu(2)-N(3) | 1.955(8) |
| Cu(2)-O(1) | 1.962(6) |
| Cu(2)-N(7) | 2.000(8) |
| Cu(3)-N(4) | 1.953(8) |
| Cu(3)-N(5) | 1.960(7) |
| Cu(3)-O(1) | 1.974(6) |
| Cu(3)-N(9) | 2.015(8) |
| Cl(1)-C(17) | 1.760(11) |
| C(5)-C(4) | 1.351(15) |
| C(5)-C(6) | 1.404(15) |
| C(5)-H(5) | 0.9300 |
| O(2)-C(16) | 1.246(10) |
| O(3)-C(16) | 1.249(10) |
| O(1)-H(18) | 0.90(2) |
| N(1)-N(2) | 1.344(10) |
| N(1)-C(1) | 1.359(12) |
| N(2)-C(3) | 1.350(12) |
| N(5)-C(7) | 1.337(12) |
| N(5)-N(6) | 1.360(10) |
| N(6)-C(9) | 1.300(12) |
| N(4)-N(3) | 1.341(11) |
| N(4)-C(6) | 1.362(12) |
| N(7)-N(8) | 1.316(11) |
| N(7)-C(10) | 1.326(13) |
| N(3)-C(4) | 1.343(11) |
| N(8)-C(12) | 1.322(13) |
| N(8)-H(8) | 0.8600 |
| N(9)-C(13) | 1.301(13) |
| N(9)-N(10) | 1.341(12) |
| C(16)-C(17) | 1.529(13) |
| C(2)-C(1) | 1.340(15) |
| C(2)-C(3) | 1.371(15) |
| C(2)-H(2) | 0.9300 |
| C(4)-H(4) | 0.9300 |
| N(10)-C(15) | 1.335(16) |
| N(10)-H(13) | 0.8600 |
| C(3)-H(3) | 0.9300 |

| | | | |
|------------------|-----------|--------------------|-----------|
| C(10)-C(11) | 1.399(15) | N(3)-N(4)-C(6) | 108.0(8) |
| C(10)-H(10) | 0.9300 | N(3)-N(4)-Cu(3) | 118.9(6) |
| C(8)-C(7) | 1.386(14) | C(6)-N(4)-Cu(3) | 132.3(7) |
| C(8)-C(9) | 1.403(14) | N(8)-N(7)-C(10) | 106.3(8) |
| C(8)-H(8) | 0.9300 | N(8)-N(7)-Cu(2) | 118.1(6) |
| C(11)-C(12) | 1.393(17) | C(10)-N(7)-Cu(2) | 135.4(8) |
| C(11)-H(11) | 0.9300 | C(4)-N(3)-N(4) | 108.3(8) |
| C(6)-H(6) | 0.9300 | C(4)-N(3)-Cu(2) | 133.3(7) |
| C(7)-H(7) | 0.9300 | N(4)-N(3)-Cu(2) | 117.9(6) |
| C(13)-C(14) | 1.367(16) | N(7)-N(8)-C(12) | 113.9(9) |
| C(13)-H(10A) | 0.9300 | N(7)-N(8)-H(8) | 123.0 |
| C(12)-H(12) | 0.9300 | C(12)-N(8)-H(8) | 123.0 |
| C(1)-H(1) | 0.9300 | C(13)-N(9)-N(10) | 104.9(9) |
| C(9)-H(9) | 0.9300 | C(13)-N(9)-Cu(3) | 135.0(8) |
| C(17)-H(17A) | 0.9700 | N(10)-N(9)-Cu(3) | 118.5(7) |
| C(17)-H(17B) | 0.9700 | O(2)-C(16)-O(3) | 123.6(8) |
| C(14)-C(15) | 1.32(2) | O(2)-C(16)-C(17) | 123.0(8) |
| C(14)-H(15) | 0.9300 | O(3)-C(16)-C(17) | 113.4(7) |
| C(15)-H(14) | 0.9300 | C(1)-C(2)-C(3) | 106.8(9) |
| N(1)-Cu(1)-N(6) | 168.8(3) | C(1)-C(2)-H(2) | 126.6 |
| N(1)-Cu(1)-O(2) | 92.5(3) | C(3)-C(2)-H(2) | 126.6 |
| N(6)-Cu(1)-O(2) | 92.0(3) | N(3)-C(4)-C(5) | 110.7(9) |
| N(1)-Cu(1)-O(1) | 88.6(3) | N(3)-C(4)-H(4) | 124.6 |
| N(6)-Cu(1)-O(1) | 89.6(3) | C(5)-C(4)-H(4) | 124.6 |
| O(2)-Cu(1)-O(1) | 164.9(3) | C(15)-N(10)-N(9) | 111.2(11) |
| N(2)-Cu(2)-N(3) | 170.6(3) | C(15)-N(10)-H(13) | 124.4 |
| N(2)-Cu(2)-O(1) | 89.1(3) | N(9)-N(10)-H(13) | 124.4 |
| N(3)-Cu(2)-O(1) | 89.0(3) | N(2)-C(3)-C(2) | 108.3(8) |
| N(2)-Cu(2)-N(7) | 92.8(3) | N(2)-C(3)-H(3) | 125.9 |
| N(3)-Cu(2)-N(7) | 90.6(3) | C(2)-C(3)-H(3) | 125.9 |
| O(1)-Cu(2)-N(7) | 170.7(3) | N(7)-C(10)-C(11) | 109.1(10) |
| N(4)-Cu(3)-N(5) | 168.5(3) | N(7)-C(10)-H(10) | 125.5 |
| N(4)-Cu(3)-O(1) | 88.2(3) | C(11)-C(10)-H(10) | 125.5 |
| N(5)-Cu(3)-O(1) | 89.7(3) | C(7)-C(8)-C(9) | 102.9(8) |
| N(4)-Cu(3)-N(9) | 90.3(3) | C(7)-C(8)-H(8) | 128.6 |
| N(5)-Cu(3)-N(9) | 93.6(3) | C(9)-C(8)-H(8) | 128.6 |
| O(1)-Cu(3)-N(9) | 170.7(3) | C(12)-C(11)-C(10) | 105.7(9) |
| C(4)-C(5)-C(6) | 104.7(9) | C(12)-C(11)-H(11) | 127.2 |
| C(4)-C(5)-H(5) | 127.6 | C(10)-C(11)-H(11) | 127.2 |
| C(6)-C(5)-H(5) | 127.6 | N(4)-C(6)-C(5) | 108.2(9) |
| C(16)-O(2)-Cu(1) | 135.5(6) | N(4)-C(6)-H(6) | 125.9 |
| Cu(2)-O(1)-Cu(1) | 116.6(3) | C(5)-C(6)-H(6) | 125.9 |
| Cu(2)-O(1)-Cu(3) | 108.8(3) | N(5)-C(7)-C(8) | 110.0(8) |
| Cu(1)-O(1)-Cu(3) | 115.8(3) | N(5)-C(7)-H(7) | 125.0 |
| Cu(2)-O(1)-H(18) | 101(3) | C(8)-C(7)-H(7) | 125.0 |
| Cu(1)-O(1)-H(18) | 110(7) | N(9)-C(13)-C(14) | 110.4(11) |
| Cu(3)-O(1)-H(18) | 103(8) | N(9)-C(13)-H(10A) | 124.8 |
| N(2)-N(1)-C(1) | 107.7(7) | C(14)-C(13)-H(10A) | 124.8 |
| N(2)-N(1)-Cu(1) | 120.7(6) | N(8)-C(12)-C(11) | 104.9(9) |
| C(1)-N(1)-Cu(1) | 131.2(7) | N(8)-C(12)-H(12) | 127.5 |
| C(3)-N(2)-N(1) | 108.0(7) | C(11)-C(12)-H(12) | 127.5 |
| C(3)-N(2)-Cu(2) | 130.8(6) | C(2)-C(1)-N(1) | 109.1(9) |
| N(1)-N(2)-Cu(2) | 121.1(6) | C(2)-C(1)-H(1) | 125.5 |
| C(7)-N(5)-N(6) | 107.8(7) | N(1)-C(1)-H(1) | 125.5 |
| C(7)-N(5)-Cu(3) | 131.8(6) | N(6)-C(9)-C(8) | 110.8(9) |
| N(6)-N(5)-Cu(3) | 120.4(5) | N(6)-C(9)-H(9) | 124.6 |
| C(9)-N(6)-N(5) | 108.5(7) | C(8)-C(9)-H(9) | 124.6 |
| C(9)-N(6)-Cu(1) | 131.0(6) | C(16)-C(17)-Cl(1) | 116.4(7) |
| N(5)-N(6)-Cu(1) | 120.5(5) | C(16)-C(17)-H(17A) | 108.2 |
| | | Cl(1)-C(17)-H(17A) | 108.2 |

| | |
|---------------------|-----------|
| C(16)-C(17)-H(17B) | 108.2 |
| Cl(1)-C(17)-H(17B) | 108.2 |
| H(17A)-C(17)-H(17B) | 107.3 |
| C(15)-C(14)-C(13) | 107.0(11) |
| C(15)-C(14)-H(15) | 126.5 |
| C(13)-C(14)-H(15) | 126.5 |
| C(14)-C(15)-N(10) | 106.4(12) |
| C(14)-C(15)-H(14) | 126.8 |
| N(10)-C(15)-H(14) | 126.8 |

Table 4. Bond lengths [\AA] and angles [$^\circ$] for **4b**.

| | |
|---------------------|------------|
| Cu(1)-N(1) | 2.0090(12) |
| Cu(1)-N(1)#1 | 2.0090(12) |
| Cu(1)-N(3) | 2.0312(13) |
| Cu(1)-N(3)#1 | 2.0312(13) |
| O(1)-C(7) | 1.2392(19) |
| C(6)-N(4) | 1.336(2) |
| C(6)-C(5) | 1.359(3) |
| C(6)-H(6) | 0.9300 |
| O(2)-C(7) | 1.2671(19) |
| N(4)-N(3) | 1.3482(18) |
| N(4)-H(4) | 0.8600 |
| N(2)-C(3) | 1.330(2) |
| N(2)-N(1) | 1.3520(19) |
| N(2)-H(2) | 0.8600 |
| N(3)-C(4) | 1.331(2) |
| N(1)-C(1) | 1.329(2) |
| C(9)-C(8) | 1.325(2) |
| C(9)-C(9)#2 | 1.453(3) |
| C(9)-H(9) | 0.9300 |
| C(1)-C(2) | 1.386(2) |
| C(1)-H(1) | 0.9300 |
| C(2)-C(3) | 1.366(3) |
| C(2)-H(2A) | 0.9300 |
| C(4)-C(5) | 1.387(2) |
| C(4)-H(4A) | 0.9300 |
| C(7)-C(8) | 1.492(2) |
| C(5)-H(5) | 0.9300 |
| C(8)-H(8) | 0.9300 |
| C(3)-H(3) | 0.9300 |
| N(1)-Cu(1)-N(1)#1 | 180.0 |
| N(1)-Cu(1)-N(3) | 88.50(5) |
| N(1)#1-Cu(1)-N(3) | 91.50(5) |
| N(1)-Cu(1)-N(3)#1 | 91.50(5) |
| N(1)#1-Cu(1)-N(3)#1 | 88.50(5) |
| N(3)-Cu(1)-N(3)#1 | 180.0 |
| N(4)-C(6)-C(5) | 107.33(16) |
| N(4)-C(6)-H(6) | 126.3 |
| C(5)-C(6)-H(6) | 126.3 |
| C(6)-N(4)-N(3) | 111.64(15) |
| C(6)-N(4)-H(4) | 124.2 |
| N(3)-N(4)-H(4) | 124.2 |
| C(3)-N(2)-N(1) | 110.56(14) |

| | |
|------------------|------------|
| C(3)-N(2)-H(2) | 124.7 |
| N(1)-N(2)-H(2) | 124.7 |
| C(4)-N(3)-N(4) | 104.88(14) |
| C(4)-N(3)-Cu(1) | 128.99(11) |
| N(4)-N(3)-Cu(1) | 126.02(11) |
| C(1)-N(1)-N(2) | 105.93(13) |
| C(1)-N(1)-Cu(1) | 128.95(11) |
| N(2)-N(1)-Cu(1) | 123.38(10) |
| C(8)-C(9)-C(9)#2 | 124.8(2) |
| C(8)-C(9)-H(9) | 117.6 |
| C(9)#2-C(9)-H(9) | 117.6 |
| N(1)-C(1)-C(2) | 110.37(15) |
| N(1)-C(1)-H(1) | 124.8 |
| C(2)-C(1)-H(1) | 124.8 |
| C(3)-C(2)-C(1) | 105.07(15) |
| C(3)-C(2)-H(2A) | 127.5 |
| C(1)-C(2)-H(2A) | 127.5 |
| N(3)-C(4)-C(5) | 110.87(16) |
| N(3)-C(4)-H(4A) | 124.6 |
| C(5)-C(4)-H(4A) | 124.6 |
| O(1)-C(7)-O(2) | 124.74(15) |
| O(1)-C(7)-C(8) | 119.83(14) |
| O(2)-C(7)-C(8) | 115.43(14) |
| C(6)-C(5)-C(4) | 105.29(16) |
| C(6)-C(5)-H(5) | 127.4 |
| C(4)-C(5)-H(5) | 127.4 |
| C(9)-C(8)-C(7) | 124.45(15) |
| C(9)-C(8)-H(8) | 117.8 |
| C(7)-C(8)-H(8) | 117.8 |
| N(2)-C(3)-C(2) | 108.07(16) |
| N(2)-C(3)-H(3) | 126.0 |
| C(2)-C(3)-H(3) | 126.0 |

Symmetry transformations used to generate equivalent atoms:

#1 -x+2,-y,-z+2 #2 -x+1,-y-1,-z+1

Table 5. Bond lengths [\AA] and angles [$^\circ$] for **5a**.

| | |
|--------------|------------|
| Cu(1)-N(3) | 2.0069(14) |
| Cu(1)-N(3)#1 | 2.0069(14) |
| Cu(1)-N(1) | 2.0250(13) |
| Cu(1)-N(1)#1 | 2.0250(13) |
| O(1)-C(7) | 1.2439(18) |
| O(3)-C(10) | 1.320(2) |
| O(2)-C(7) | 1.261(2) |
| O(4)-C(10) | 1.201(2) |
| N(2)-C(3) | 1.336(2) |
| N(2)-N(1) | 1.3441(18) |
| N(4)-C(6) | 1.338(3) |
| N(4)-N(3) | 1.340(2) |
| N(3)-C(4) | 1.331(2) |
| N(1)-C(1) | 1.328(2) |
| C(10)-C(11) | 1.510(2) |
| C(11)-C(12) | 1.499(3) |

| | | | |
|---------------------|------------|---------------|-----------|
| C(2)-C(3) | 1.366(3) | Cu(6)-N(11) | 1.931(10) |
| C(2)-C(1) | 1.391(2) | Cu(6)-N(10) | 1.952(11) |
| C(7)-C(8) | 1.519(2) | Cu(6)-O(9) | 2.000(8) |
| C(12)-C(12)#2 | 1.312(4) | Cu(6)-O(2) | 2.006(7) |
| C(8)-C(9) | 1.497(3) | Cu(2)-N(2) | 1.939(10) |
| C(4)-C(5) | 1.387(3) | Cu(2)-N(3) | 1.955(11) |
| C(5)-C(6) | 1.360(3) | Cu(2)-O(7) | 1.988(8) |
| C(9)-C(9)#3 | 1.263(5) | Cu(2)-O(1) | 1.998(7) |
| | | Cu(2)-O(7)#2 | 2.437(9) |
| N(3)-Cu(1)-N(3)#1 | 180.0 | Cu(5)-N(8) | 1.894(11) |
| N(3)-Cu(1)-N(1) | 90.28(6) | Cu(5)-N(9) | 1.956(12) |
| N(3)#1-Cu(1)-N(1) | 89.72(6) | Cu(5)-O(2) | 1.978(8) |
| N(3)-Cu(1)-N(1)#1 | 89.72(6) | Cu(5)-O(6) | 2.040(9) |
| N(3)#1-Cu(1)-N(1)#1 | 90.28(6) | Cu(3)-N(5) | 1.905(11) |
| N(1)-Cu(1)-N(1)#1 | 180.0 | Cu(3)-N(4) | 1.957(12) |
| C(3)-N(2)-N(1) | 111.43(13) | Cu(3)-O(1) | 1.967(8) |
| C(6)-N(4)-N(3) | 111.53(15) | Cu(3)-O(3) | 2.046(9) |
| C(4)-N(3)-N(4) | 105.12(14) | Cu(3)-O(13) | 2.37(3) |
| C(4)-N(3)-Cu(1) | 134.04(13) | C(19)-O(3) | 1.243(15) |
| N(4)-N(3)-Cu(1) | 120.80(11) | C(19)-O(4) | 1.248(14) |
| C(1)-N(1)-N(2) | 105.46(13) | C(19)-C(20) | 1.528(18) |
| C(1)-N(1)-Cu(1) | 128.75(12) | C(24)-O(5) | 1.251(14) |
| N(2)-N(1)-Cu(1) | 125.78(10) | C(24)-O(6) | 1.272(14) |
| O(4)-C(10)-O(3) | 123.54(17) | C(24)-C(23) | 1.535(17) |
| O(4)-C(10)-C(11) | 123.24(18) | O(7)-C(25) | 1.304(15) |
| O(3)-C(10)-C(11) | 113.21(15) | O(7)-Cu(2)#2 | 2.437(9) |
| C(12)-C(11)-C(10) | 112.31(16) | O(9)-C(30) | 1.275(13) |
| C(3)-C(2)-C(1) | 104.89(15) | C(9)-N(6) | 1.310(16) |
| O(1)-C(7)-O(2) | 123.77(15) | C(9)-C(8) | 1.40(2) |
| O(1)-C(7)-C(8) | 119.71(14) | C(9)-H(9) | 0.9300 |
| O(2)-C(7)-C(8) | 116.49(14) | O(10)-C(30) | 1.224(15) |
| C(12)#2-C(12)-C(11) | 124.2(3) | N(6)-N(5) | 1.354(13) |
| C(9)-C(8)-C(7) | 114.49(14) | O(8)-C(25) | 1.211(16) |
| N(1)-C(1)-C(2) | 110.75(15) | N(2)-C(3) | 1.336(15) |
| N(2)-C(3)-C(2) | 107.48(15) | N(2)-N(1) | 1.343(13) |
| N(3)-C(4)-C(5) | 110.88(17) | N(1)-C(1) | 1.320(16) |
| C(6)-C(5)-C(4) | 104.96(17) | O(2)-Cu(4)#3 | 1.963(8) |
| N(4)-C(6)-C(5) | 107.50(17) | N(7)-C(10) | 1.319(16) |
| C(9)#3-C(9)-C(8) | 127.8(4) | N(7)-N(8) | 1.351(14) |
| | | N(7)-Cu(4)#3 | 1.952(10) |
| | | N(3)-C(4) | 1.322(17) |
| | | N(3)-N(4) | 1.371(14) |
| | | N(10)-C(15) | 1.319(16) |
| | | N(10)-N(9) | 1.345(15) |
| | | N(5)-C(7) | 1.373(17) |
| | | N(12)-C(18) | 1.297(17) |
| | | N(12)-N(11)#1 | 1.347(13) |
| | | C(21)-C(22) | 1.322(17) |
| | | C(21)-C(20)#4 | 1.506(19) |
| | | C(21)-H(21) | 0.9300 |
| | | N(11)-C(16) | 1.326(15) |
| | | N(11)-N(12)#3 | 1.347(13) |
| | | C(26)-C(27) | 1.47(3) |
| | | C(26)-C(25) | 1.49(2) |
| | | C(26)-H(26A) | 0.9700 |
| | | C(26)-H(26B) | 0.9700 |
| | | N(4)-C(6) | 1.329(17) |
| | | N(8)-C(12) | 1.348(18) |
| | | C(10)-C(11) | 1.37(2) |
| | | C(10)-H(10) | 0.9300 |

Symmetry transformations used to generate equivalent atoms:
#1 -x,-y,-z #2 -x+1,-y+1,-z+1 #3 -x+1,-y+2,-z+1

Table 6. Bond lengths [Å] and angles [°] for **5c**.

| | |
|--------------|-----------|
| Cu(1)-N(1) | 1.929(9) |
| Cu(1)-N(6) | 1.945(9) |
| Cu(1)-O(1) | 1.964(8) |
| Cu(1)-O(5) | 1.980(8) |
| Cu(4)-N(12) | 1.941(10) |
| Cu(4)-N(7)#1 | 1.952(10) |
| Cu(4)-O(2)#1 | 1.963(8) |
| Cu(4)-O(4) | 1.982(8) |

| | | | |
|--------------------|-----------|---------------------|-----------|
| C(22)-C(23) | 1.495(18) | N(7)#1-Cu(4)-O(2)#1 | 89.6(4) |
| C(22)-H(22) | 0.9300 | N(12)-Cu(4)-O(4) | 91.3(4) |
| C(30)-C(29)#5 | 1.473(19) | N(7)#1-Cu(4)-O(4) | 90.9(4) |
| C(4)-C(5) | 1.39(2) | O(2)#1-Cu(4)-O(4) | 173.2(4) |
| C(4)-H(4) | 0.9300 | N(11)-Cu(6)-N(10) | 166.2(5) |
| C(20)-C(21)#6 | 1.506(19) | N(11)-Cu(6)-O(9) | 92.3(4) |
| C(20)-H(20A) | 0.9700 | N(10)-Cu(6)-O(9) | 92.2(4) |
| C(20)-H(20B) | 0.9700 | N(11)-Cu(6)-O(2) | 88.4(4) |
| C(16)-C(17) | 1.360(19) | N(10)-Cu(6)-O(2) | 89.8(4) |
| C(16)-H(16) | 0.9300 | O(9)-Cu(6)-O(2) | 168.5(4) |
| N(9)-C(13) | 1.340(16) | N(2)-Cu(2)-N(3) | 166.5(5) |
| C(2)-C(3) | 1.335(19) | N(2)-Cu(2)-O(7) | 92.2(4) |
| C(2)-C(1) | 1.36(2) | N(3)-Cu(2)-O(7) | 92.0(4) |
| C(2)-H(2) | 0.9300 | N(2)-Cu(2)-O(1) | 88.7(4) |
| C(5)-C(6) | 1.29(2) | N(3)-Cu(2)-O(1) | 89.7(4) |
| C(5)-H(5) | 0.9300 | O(7)-Cu(2)-O(1) | 168.6(4) |
| C(27)-C(28) | 1.233(17) | N(2)-Cu(2)-O(7)#2 | 94.0(4) |
| C(27)-H(27) | 0.9300 | N(3)-Cu(2)-O(7)#2 | 99.4(4) |
| C(3)-H(3) | 0.9300 | O(7)-Cu(2)-O(7)#2 | 79.3(3) |
| C(18)-C(17)#1 | 1.40(2) | O(1)-Cu(2)-O(7)#2 | 89.3(3) |
| C(18)-H(18) | 0.9300 | N(8)-Cu(5)-N(9) | 167.7(6) |
| C(8)-C(7) | 1.35(2) | N(8)-Cu(5)-O(2) | 89.7(4) |
| C(8)-H(8) | 0.9300 | N(9)-Cu(5)-O(2) | 90.0(4) |
| C(23)-H(23A) | 0.9700 | N(8)-Cu(5)-O(6) | 92.0(4) |
| C(23)-H(23B) | 0.9700 | N(9)-Cu(5)-O(6) | 94.3(4) |
| C(29)-C(28) | 1.31(3) | O(2)-Cu(5)-O(6) | 150.0(4) |
| C(29)-C(30)#7 | 1.47(2) | N(5)-Cu(3)-N(4) | 169.2(6) |
| C(29)-H(29A) | 0.9700 | N(5)-Cu(3)-O(1) | 89.8(4) |
| C(29)-H(29B) | 0.9700 | N(4)-Cu(3)-O(1) | 90.6(4) |
| C(1)-H(1) | 0.9300 | N(5)-Cu(3)-O(3) | 92.1(4) |
| C(17)-C(18)#3 | 1.40(2) | N(4)-Cu(3)-O(3) | 92.9(4) |
| C(17)-H(17) | 0.9300 | O(1)-Cu(3)-O(3) | 150.3(4) |
| C(7)-H(7) | 0.9300 | N(5)-Cu(3)-O(13) | 86.4(9) |
| C(14)-C(13) | 1.33(2) | N(4)-Cu(3)-O(13) | 82.9(9) |
| C(14)-C(15) | 1.39(2) | O(1)-Cu(3)-O(13) | 97.1(8) |
| C(14)-H(14) | 0.9300 | O(3)-Cu(3)-O(13) | 112.6(9) |
| C(6)-H(6) | 0.9300 | O(3)-C(19)-O(4) | 125.3(12) |
| C(15)-H(15) | 0.9300 | O(3)-C(19)-C(20) | 117.1(12) |
| C(11)-C(12) | 1.35(2) | O(4)-C(19)-C(20) | 117.6(13) |
| C(11)-H(11) | 0.9300 | O(5)-C(24)-O(6) | 123.9(12) |
| C(12)-H(12) | 0.9300 | O(5)-C(24)-C(23) | 117.9(12) |
| C(13)-H(13) | 0.9300 | O(6)-C(24)-C(23) | 118.2(12) |
| C(28)-H(28) | 0.9300 | C(24)-O(5)-Cu(1) | 114.8(8) |
| O(11)-C(51) | 1.53(4) | C(25)-O(7)-Cu(2) | 135.3(10) |
| O(13)-C(61) | 1.62(4) | C(25)-O(7)-Cu(2)#2 | 123.9(9) |
| N(50)-C(45) | 1.46(4) | Cu(2)-O(7)-Cu(2)#2 | 100.7(3) |
| N(50)-C(51) | 1.49(4) | C(19)-O(3)-Cu(3) | 128.1(8) |
| N(50)-C(46) | 1.58(5) | C(19)-O(4)-Cu(4) | 114.1(8) |
| N(60)-C(61) | 1.49(5) | C(30)-O(9)-Cu(6) | 135.1(9) |
| N(60)-C(62) | 1.49(4) | N(6)-C(9)-C(8) | 109.4(14) |
| N(60)-C(63) | 1.64(6) | N(6)-C(9)-H(9) | 125.3 |
| | | C(8)-C(9)-H(9) | 125.3 |
| N(1)-Cu(1)-N(6) | 172.5(5) | C(24)-O(6)-Cu(5) | 126.8(8) |
| N(1)-Cu(1)-O(1) | 88.5(4) | C(9)-N(6)-N(5) | 109.4(10) |
| N(6)-Cu(1)-O(1) | 89.7(4) | C(9)-N(6)-Cu(1) | 130.4(9) |
| N(1)-Cu(1)-O(5) | 91.6(4) | N(5)-N(6)-Cu(1) | 120.2(8) |
| N(6)-Cu(1)-O(5) | 90.9(4) | C(3)-N(2)-N(1) | 107.9(10) |
| O(1)-Cu(1)-O(5) | 173.7(4) | C(3)-N(2)-Cu(2) | 131.0(9) |
| N(12)-Cu(4)-N(7)#1 | 172.3(5) | N(1)-N(2)-Cu(2) | 120.9(7) |
| N(12)-Cu(4)-O(2)#1 | 89.1(4) | C(1)-N(1)-N(2) | 106.7(10) |

| | | | |
|----------------------|-----------|----------------------|-----------|
| C(1)-N(1)-Cu(1) | 130.9(9) | C(19)-C(20)-H(20B) | 108.4 |
| N(2)-N(1)-Cu(1) | 122.0(7) | H(20A)-C(20)-H(20B) | 107.5 |
| Cu(4)#3-O(2)-Cu(5) | 115.7(4) | N(11)-C(16)-C(17) | 109.5(12) |
| Cu(4)#3-O(2)-Cu(6) | 116.4(4) | N(11)-C(16)-H(16) | 125.3 |
| Cu(5)-O(2)-Cu(6) | 116.4(4) | C(17)-C(16)-H(16) | 125.3 |
| C(10)-N(7)-N(8) | 110.3(11) | C(13)-N(9)-N(10) | 107.8(12) |
| C(10)-N(7)-Cu(4)#3 | 129.6(10) | C(13)-N(9)-Cu(5) | 130.3(11) |
| N(8)-N(7)-Cu(4)#3 | 120.0(8) | N(10)-N(9)-Cu(5) | 121.8(9) |
| C(4)-N(3)-N(4) | 106.9(11) | C(3)-C(2)-C(1) | 104.8(13) |
| C(4)-N(3)-Cu(2) | 131.8(10) | C(3)-C(2)-H(2) | 127.6 |
| N(4)-N(3)-Cu(2) | 121.3(8) | C(1)-C(2)-H(2) | 127.6 |
| Cu(1)-O(1)-Cu(3) | 115.9(4) | C(6)-C(5)-C(4) | 105.2(14) |
| Cu(1)-O(1)-Cu(2) | 116.7(4) | C(6)-C(5)-H(5) | 127.4 |
| Cu(3)-O(1)-Cu(2) | 117.1(4) | C(4)-C(5)-H(5) | 127.4 |
| C(15)-N(10)-N(9) | 107.2(12) | C(28)-C(27)-C(26) | 155(2) |
| C(15)-N(10)-Cu(6) | 131.6(10) | C(28)-C(27)-H(27) | 102.7 |
| N(9)-N(10)-Cu(6) | 121.1(8) | C(26)-C(27)-H(27) | 102.7 |
| N(6)-N(5)-C(7) | 106.5(11) | C(2)-C(3)-N(2) | 109.9(12) |
| N(6)-N(5)-Cu(3) | 120.4(8) | C(2)-C(3)-H(3) | 125.1 |
| C(7)-N(5)-Cu(3) | 130.5(11) | N(2)-C(3)-H(3) | 125.1 |
| C(18)-N(12)-N(11)#1 | 108.9(10) | N(12)-C(18)-C(17)#1 | 109.2(12) |
| C(18)-N(12)-Cu(4) | 130.4(9) | N(12)-C(18)-H(18) | 125.4 |
| N(11)#1-N(12)-Cu(4) | 120.6(8) | C(17)#1-C(18)-H(18) | 125.4 |
| C(22)-C(21)-C(20)#4 | 126.5(12) | C(7)-C(8)-C(9) | 104.8(14) |
| C(22)-C(21)-H(21) | 116.7 | C(7)-C(8)-H(8) | 127.6 |
| C(20)#4-C(21)-H(21) | 116.7 | C(9)-C(8)-H(8) | 127.6 |
| C(16)-N(11)-N(12)#3 | 108.0(10) | C(22)-C(23)-C(24) | 114.4(11) |
| C(16)-N(11)-Cu(6) | 129.6(9) | C(22)-C(23)-H(23A) | 108.7 |
| N(12)#3-N(11)-Cu(6) | 122.2(8) | C(24)-C(23)-H(23A) | 108.7 |
| C(27)-C(26)-C(25) | 111.1(15) | C(22)-C(23)-H(23B) | 108.7 |
| C(27)-C(26)-H(26A) | 109.4 | C(24)-C(23)-H(23B) | 108.7 |
| C(25)-C(26)-H(26A) | 109.4 | H(23A)-C(23)-H(23B) | 107.6 |
| C(27)-C(26)-H(26B) | 109.4 | C(28)-C(29)-C(30)#7 | 112.8(17) |
| C(25)-C(26)-H(26B) | 109.4 | C(28)-C(29)-H(29A) | 109.0 |
| H(26A)-C(26)-H(26B) | 108.0 | C(30)#7-C(29)-H(29A) | 109.0 |
| C(6)-N(4)-N(3) | 106.2(13) | C(28)-C(29)-H(29B) | 109.0 |
| C(6)-N(4)-Cu(3) | 133.2(12) | C(30)#7-C(29)-H(29B) | 109.0 |
| N(3)-N(4)-Cu(3) | 120.5(9) | H(29A)-C(29)-H(29B) | 107.8 |
| C(12)-N(8)-N(7) | 106.4(12) | N(1)-C(1)-C(2) | 110.8(13) |
| C(12)-N(8)-Cu(5) | 130.7(11) | N(1)-C(1)-H(1) | 124.6 |
| N(7)-N(8)-Cu(5) | 121.4(8) | C(2)-C(1)-H(1) | 124.6 |
| N(7)-C(10)-C(11) | 107.3(14) | C(16)-C(17)-C(18)#3 | 104.4(13) |
| N(7)-C(10)-H(10) | 126.4 | C(16)-C(17)-H(17) | 127.8 |
| C(11)-C(10)-H(10) | 126.4 | C(18)#3-C(17)-H(17) | 127.8 |
| O(8)-C(25)-O(7) | 119.9(14) | C(8)-C(7)-N(5) | 109.9(14) |
| O(8)-C(25)-C(26) | 122.8(13) | C(8)-C(7)-H(7) | 125.1 |
| O(7)-C(25)-C(26) | 117.0(13) | N(5)-C(7)-H(7) | 125.1 |
| C(21)-C(22)-C(23) | 126.0(12) | C(13)-C(14)-C(15) | 104.5(13) |
| C(21)-C(22)-H(22) | 117.0 | C(13)-C(14)-H(14) | 127.8 |
| C(23)-C(22)-H(22) | 117.0 | C(15)-C(14)-H(14) | 127.8 |
| O(10)-C(30)-O(9) | 119.5(13) | C(5)-C(6)-N(4) | 112.4(15) |
| O(10)-C(30)-C(29)#5 | 121.7(11) | C(5)-C(6)-H(6) | 123.8 |
| O(9)-C(30)-C(29)#5 | 118.4(12) | N(4)-C(6)-H(6) | 123.8 |
| N(3)-C(4)-C(5) | 109.1(13) | N(10)-C(15)-C(14) | 110.0(14) |
| N(3)-C(4)-H(4) | 125.5 | N(10)-C(15)-H(15) | 125.0 |
| C(5)-C(4)-H(4) | 125.5 | C(14)-C(15)-H(15) | 125.0 |
| C(21)#6-C(20)-C(19) | 115.3(12) | C(12)-C(11)-C(10) | 107.0(14) |
| C(21)#6-C(20)-H(20A) | 108.4 | C(12)-C(11)-H(11) | 126.5 |
| C(19)-C(20)-H(20A) | 108.4 | C(10)-C(11)-H(11) | 126.5 |
| C(21)#6-C(20)-H(20B) | 108.4 | N(8)-C(12)-C(11) | 109.0(15) |

| | | | |
|-------------------|-----------|--------------|-----------|
| N(8)-C(12)-H(12) | 125.5 | N(4)-C(6) | 1.334(11) |
| C(11)-C(12)-H(12) | 125.5 | C(13)-O(5)#4 | 1.241(10) |
| C(14)-C(13)-N(9) | 110.4(15) | C(13)-C(12) | 1.519(11) |
| C(14)-C(13)-H(13) | 124.8 | C(10)-C(11) | 1.526(10) |
| N(9)-C(13)-H(13) | 124.8 | C(12)-C(11) | 1.513(12) |
| C(27)-C(28)-C(29) | 151(3) | C(12)-C(14) | 1.525(14) |
| C(27)-C(28)-H(28) | 104.5 | C(12)-H(12) | 0.9800 |
| C(29)-C(28)-H(28) | 104.5 | C(11)-H(11A) | 0.9700 |
| C(61)-O(13)-Cu(3) | 95(2) | C(11)-H(11B) | 0.9700 |
| C(45)-N(50)-C(51) | 94(3) | C(1)-C(2) | 1.337(11) |
| C(45)-N(50)-C(46) | 100(3) | C(1)-H(1) | 0.9300 |
| C(51)-N(50)-C(46) | 160(3) | C(3)-C(2) | 1.398(12) |
| C(61)-N(60)-C(62) | 89(3) | C(3)-H(3) | 0.9300 |
| C(61)-N(60)-C(63) | 165(3) | C(2)-H(2) | 0.9300 |
| C(62)-N(60)-C(63) | 104(3) | C(8)-C(9) | 1.339(13) |
| N(60)-C(61)-O(13) | 92(3) | C(8)-C(7) | 1.360(15) |
| N(50)-C(51)-O(11) | 93(3) | C(8)-H(8) | 0.9300 |

Symmetry transformations used to generate equivalent atoms:

#1 $x+1, y+1, z$ #2 $-x+2, -y, -z+2$ #3 $x-1, y-1, z$
#4 $x-1, y, z$ #5 $x-1, y-1, z-1$ #6 $x+1, y, z$
#7 $x+1, y+1, z+1$

Table 7. Bond lengths [Å] and angles [°] for **6a**.

| | | | |
|--------------|-----------|-------------------|----------|
| Cu(1)-N(6) | 1.939(7) | N(6)-Cu(1)-N(1) | 174.7(3) |
| Cu(1)-N(1) | 1.950(6) | N(6)-Cu(1)-O(2) | 91.6(3) |
| Cu(1)-O(2) | 1.988(5) | N(1)-Cu(1)-O(2) | 90.6(2) |
| Cu(1)-O(1) | 1.995(5) | N(6)-Cu(1)-O(1) | 88.7(3) |
| Cu(1)-O(6) | 2.394(6) | N(1)-Cu(1)-O(1) | 88.5(2) |
| Cu(2)-N(3) | 1.927(7) | O(2)-Cu(1)-O(1) | 173.6(2) |
| Cu(2)-N(2) | 1.942(6) | N(6)-Cu(1)-O(6) | 90.0(3) |
| Cu(2)-O(3)#1 | 1.994(5) | N(1)-Cu(1)-O(6) | 94.8(2) |
| Cu(2)-O(1) | 2.010(5) | O(2)-Cu(1)-O(6) | 90.9(2) |
| Cu(3)-N(4) | 1.924(8) | O(1)-Cu(1)-O(6) | 95.6(2) |
| Cu(3)-N(5) | 1.961(7) | N(3)-Cu(2)-N(2) | 176.3(3) |
| Cu(3)-O(1) | 1.977(5) | N(3)-Cu(2)-O(3)#1 | 92.3(3) |
| Cu(3)-O(5) | 1.980(6) | N(2)-Cu(2)-O(3)#1 | 91.1(2) |
| O(6)-C(15) | 1.433(12) | N(3)-Cu(2)-O(1) | 89.0(3) |
| O(6)-H(16) | 0.95(2) | N(2)-Cu(2)-O(1) | 87.7(2) |
| O(1)-H(10) | 0.952(19) | O(3)#1-Cu(2)-O(1) | 177.8(2) |
| O(3)-C(10) | 1.281(9) | N(4)-Cu(3)-N(5) | 167.6(3) |
| O(3)-Cu(2)#2 | 1.994(5) | N(4)-Cu(3)-O(1) | 90.1(3) |
| O(2)-C(10) | 1.237(9) | N(5)-Cu(3)-O(1) | 88.9(2) |
| O(4)-C(13) | 1.242(10) | N(4)-Cu(3)-O(5) | 91.7(3) |
| O(5)-C(13)#3 | 1.241(10) | N(5)-Cu(3)-O(5) | 91.9(3) |
| N(5)-C(7) | 1.321(11) | O(1)-Cu(3)-O(5) | 167.7(2) |
| N(5)-N(6) | 1.334(10) | C(15)-O(6)-Cu(1) | 123.3(6) |
| N(1)-C(1) | 1.310(10) | C(15)-O(6)-H(16) | 108(6) |
| N(1)-N(2) | 1.358(8) | Cu(1)-O(6)-H(16) | 107(6) |
| N(2)-C(3) | 1.344(10) | Cu(3)-O(1)-Cu(1) | 117.1(2) |
| N(6)-C(9) | 1.334(11) | Cu(3)-O(1)-Cu(2) | 115.7(2) |
| N(3)-C(4) | 1.350(11) | Cu(1)-O(1)-Cu(2) | 115.3(2) |
| N(3)-N(4) | 1.370(10) | Cu(3)-O(1)-H(10) | 88(4) |

| | | | |
|---------------------|-----------|-----------------------------------------------------------------|-----------------------------|
| Cu(1)-O(1)-H(10) | 119(5) | C(12)-C(14)-H(14B) | 109.5 |
| Cu(2)-O(1)-H(10) | 98(4) | H(14A)-C(14)-H(14B) | 109.5 |
| C(10)-O(3)-Cu(2)#2 | 109.5(5) | C(12)-C(14)-H(14C) | 109.5 |
| C(10)-O(2)-Cu(1) | 130.0(5) | H(14A)-C(14)-H(14C) | 109.5 |
| C(13)#3-O(5)-Cu(3) | 106.0(6) | H(14B)-C(14)-H(14C) | 109.5 |
| C(7)-N(5)-N(6) | 110.1(8) | N(4)-C(6)-C(5) | 110.4(10) |
| C(7)-N(5)-Cu(3) | 128.7(7) | N(4)-C(6)-H(6) | 124.8 |
| N(6)-N(5)-Cu(3) | 121.1(5) | C(5)-C(6)-H(6) | 124.8 |
| C(1)-N(1)-N(2) | 108.0(6) | O(6)-C(15)-H(15A) | 109.5 |
| C(1)-N(1)-Cu(1) | 130.7(5) | O(6)-C(15)-H(15B) | 109.5 |
| N(2)-N(1)-Cu(1) | 121.1(5) | H(15A)-C(15)-H(15B) | 109.5 |
| C(3)-N(2)-N(1) | 107.9(7) | O(6)-C(15)-H(15C) | 109.5 |
| C(3)-N(2)-Cu(2) | 130.8(6) | H(15A)-C(15)-H(15C) | 109.5 |
| N(1)-N(2)-Cu(2) | 121.2(5) | H(15B)-C(15)-H(15C) | 109.5 |
| N(5)-N(6)-C(9) | 106.1(7) | C(6)-C(5)-C(4) | 106.4(10) |
| N(5)-N(6)-Cu(1) | 122.4(5) | C(6)-C(5)-H(5) | 126.8 |
| C(9)-N(6)-Cu(1) | 131.4(7) | C(4)-C(5)-H(5) | 126.8 |
| C(4)-N(3)-N(4) | 108.8(8) | N(3)-C(4)-C(5) | 107.8(10) |
| C(4)-N(3)-Cu(2) | 129.6(7) | N(3)-C(4)-H(4) | 126.1 |
| N(4)-N(3)-Cu(2) | 121.5(5) | C(5)-C(4)-H(4) | 126.1 |
| C(6)-N(4)-N(3) | 106.5(8) | | |
| C(6)-N(4)-Cu(3) | 132.3(7) | | |
| N(3)-N(4)-Cu(3) | 121.2(5) | | |
| O(5)#4-C(13)-O(4) | 123.4(8) | | |
| O(5)#4-C(13)-C(12) | 115.8(8) | | |
| O(4)-C(13)-C(12) | 120.7(8) | | |
| O(2)-C(10)-O(3) | 122.7(7) | | |
| O(2)-C(10)-C(11) | 119.6(7) | | |
| O(3)-C(10)-C(11) | 117.6(7) | | |
| C(11)-C(12)-C(13) | 109.2(7) | | |
| C(11)-C(12)-C(14) | 110.9(9) | | |
| C(13)-C(12)-C(14) | 110.1(8) | | |
| C(11)-C(12)-H(12) | 108.9 | | |
| C(13)-C(12)-H(12) | 108.9 | | |
| C(14)-C(12)-H(12) | 108.9 | | |
| C(12)-C(11)-C(10) | 118.4(7) | | |
| C(12)-C(11)-H(11A) | 107.7 | | |
| C(10)-C(11)-H(11A) | 107.7 | | |
| C(12)-C(11)-H(11B) | 107.7 | | |
| C(10)-C(11)-H(11B) | 107.7 | | |
| H(11A)-C(11)-H(11B) | 107.1 | | |
| N(1)-C(1)-C(2) | 111.1(7) | | |
| N(1)-C(1)-H(1) | 124.4 | | |
| C(2)-C(1)-H(1) | 124.4 | | |
| N(2)-C(3)-C(2) | 107.6(8) | | |
| N(2)-C(3)-H(3) | 126.2 | | |
| C(2)-C(3)-H(3) | 126.2 | | |
| C(1)-C(2)-C(3) | 105.3(8) | | |
| C(1)-C(2)-H(2) | 127.3 | | |
| C(3)-C(2)-H(2) | 127.3 | | |
| C(9)-C(8)-C(7) | 106.3(9) | | |
| C(9)-C(8)-H(8) | 126.9 | | |
| C(7)-C(8)-H(8) | 126.9 | | |
| N(6)-C(9)-C(8) | 110.0(10) | | |
| N(6)-C(9)-H(9) | 125.0 | | |
| C(8)-C(9)-H(9) | 125.0 | | |
| N(5)-C(7)-C(8) | 107.5(9) | | |
| N(5)-C(7)-H(7) | 126.3 | | |
| C(8)-C(7)-H(7) | 126.3 | | |
| C(12)-C(14)-H(14A) | 109.5 | | |
| | | | |
| | | Symmetry transformations used to generate equivalent atoms: | |
| | | #1 y+1/3,-x+y+2/3,-z+5/3 | #2 x-y+1/3,x- 1/3,-z+5/3 |
| | | #3 -x+y+2/3,-x+1/3,z+1/3 | #4 -y+1/3,x-y- 1/3,z-1/3 |
| | | | |
| | | Table 8. Bond lengths [Å] and angles [°] for (S)-6a . | |
| | | | |
| | | | |
| | | Cu(4)-N(7) | 1.890(10) |
| | | Cu(4)-N(12) | 1.930(11) |
| | | Cu(4)-O(2) | 2.012(8) |
| | | Cu(4)-O(4) | 2.024(9) |
| | | Cu(1)-N(1) | 1.900(10) |
| | | Cu(1)-N(6) | 1.939(10) |
| | | Cu(1)-O(1) | 2.001(10) |
| | | Cu(1)-O(3) | 2.031(9) |
| | | Cu(1)-O(11) | 2.408(12) |
| | | Cu(5)-N(9) | 1.938(12) |
| | | Cu(5)-O(7) | 1.945(9) |
| | | Cu(5)-N(8) | 1.965(9) |
| | | Cu(5)-O(2) | 1.997(8) |
| | | Cu(5)-O(12) | 2.365(10) |
| | | Cu(2)-N(3) | 1.942(13) |
| | | Cu(2)-N(2) | 1.966(11) |
| | | Cu(2)-O(1) | 1.990(10) |
| | | Cu(2)-O(8)#1 | 1.990(9) |
| | | Cu(6)-N(11) | 1.902(13) |
| | | Cu(6)-N(10) | 1.932(13) |
| | | Cu(6)-O(10)#2 | 1.949(9) |
| | | Cu(6)-O(2) | 1.986(8) |
| | | Cu(3)-N(5) | 1.934(12) |
| | | Cu(3)-N(4) | 1.975(13) |
| | | Cu(3)-O(1) | 1.989(9) |
| | | Cu(3)-O(5) | 1.989(10) |

| | | | |
|---------------|-----------|-------------------|-----------|
| C(27)-O(9) | 1.21(2) | C(5)-C(4) | 1.364(19) |
| C(27)-O(10) | 1.29(2) | C(5)-H(5) | 0.9300 |
| C(27)-C(26) | 1.61(2) | C(13)-H(13) | 0.9300 |
| O(3)-C(19) | 1.237(13) | C(29)-H(29A) | 0.9600 |
| N(3)-N(4) | 1.306(15) | C(29)-H(29B) | 0.9600 |
| N(3)-C(4) | 1.354(15) | C(29)-H(29C) | 0.9600 |
| N(1)-C(1) | 1.353(13) | C(26)-C(25) | 1.30(2) |
| N(1)-N(2) | 1.397(13) | C(26)-C(28) | 1.53(2) |
| O(12)-C(30) | 1.32(2) | C(26)-H(26) | 0.9800 |
| O(8)-C(24) | 1.242(15) | C(25)-H(25A) | 0.9700 |
| O(8)-Cu(2)#3 | 1.990(9) | C(25)-H(25B) | 0.9700 |
| N(9)-C(13) | 1.347(14) | C(23)-H(23A) | 0.9600 |
| N(9)-N(10) | 1.361(14) | C(23)-H(23B) | 0.9600 |
| O(7)-C(24) | 1.292(16) | C(23)-H(23C) | 0.9600 |
| N(10)-C(15) | 1.318(14) | C(30)-H(30A) | 0.9600 |
| C(15)-C(14) | 1.356(19) | C(30)-H(30B) | 0.9600 |
| C(15)-H(15) | 0.9300 | C(30)-H(30C) | 0.9600 |
| N(7)-N(8) | 1.339(12) | C(16)-C(17) | 1.361(19) |
| N(7)-C(10) | 1.353(12) | C(16)-H(16) | 0.9300 |
| O(4)-C(19) | 1.250(15) | C(17)-H(17) | 0.9300 |
| O(11)-C(29) | 1.491(18) | C(28)-H(28A) | 0.9600 |
| O(5)-C(22) | 1.224(16) | C(28)-H(28B) | 0.9600 |
| N(11)-C(16) | 1.345(16) | C(28)-H(28C) | 0.9600 |
| N(11)-N(12) | 1.377(14) | C(8)-H(8) | 0.9300 |
| C(20)-C(19) | 1.454(17) | O(6)-C(22) | 1.273(15) |
| C(20)-C(21) | 1.55(2) | C(22)-C(21)#6 | 1.474(19) |
| C(20)-H(20A) | 0.9700 | C(4)-H(4) | 0.9300 |
| C(20)-H(20B) | 0.9700 | | |
| N(2)-C(3) | 1.299(16) | N(7)-Cu(4)-N(12) | 176.3(4) |
| C(24)-C(25) | 1.563(18) | N(7)-Cu(4)-O(2) | 87.7(3) |
| N(8)-C(12) | 1.325(13) | N(12)-Cu(4)-O(2) | 88.5(4) |
| N(4)-C(6) | 1.347(15) | N(7)-Cu(4)-O(4) | 91.2(4) |
| O(10)-Cu(6)#4 | 1.949(9) | N(12)-Cu(4)-O(4) | 92.5(4) |
| N(5)-C(7) | 1.336(17) | O(2)-Cu(4)-O(4) | 176.6(4) |
| N(5)-N(6) | 1.339(13) | N(1)-Cu(1)-N(6) | 176.2(4) |
| C(6)-C(5) | 1.326(18) | N(1)-Cu(1)-O(1) | 89.8(4) |
| C(6)-H(6) | 0.9300 | N(6)-Cu(1)-O(1) | 87.9(4) |
| C(3)-C(2) | 1.385(17) | N(1)-Cu(1)-O(3) | 90.3(4) |
| C(3)-H(3) | 0.9300 | N(6)-Cu(1)-O(3) | 91.7(4) |
| C(12)-C(11) | 1.365(15) | O(1)-Cu(1)-O(3) | 173.2(4) |
| C(12)-H(12) | 0.9300 | N(1)-Cu(1)-O(11) | 92.2(4) |
| C(21)-C(22)#5 | 1.473(19) | N(6)-Cu(1)-O(11) | 90.8(5) |
| C(21)-C(23) | 1.52(2) | O(1)-Cu(1)-O(11) | 92.5(4) |
| C(21)-H(21) | 0.9800 | O(3)-Cu(1)-O(11) | 94.3(4) |
| C(1)-C(2) | 1.362(16) | N(9)-Cu(5)-O(7) | 92.4(5) |
| C(1)-H(1) | 0.9300 | N(9)-Cu(5)-N(8) | 174.4(5) |
| C(14)-C(13) | 1.372(16) | O(7)-Cu(5)-N(8) | 91.4(4) |
| C(14)-H(14) | 0.9300 | N(9)-Cu(5)-O(2) | 88.8(4) |
| C(2)-H(2) | 0.9300 | O(7)-Cu(5)-O(2) | 174.9(3) |
| C(9)-N(6) | 1.291(16) | N(8)-Cu(5)-O(2) | 87.1(4) |
| C(9)-C(8) | 1.391(17) | N(9)-Cu(5)-O(12) | 90.7(4) |
| C(9)-H(9) | 0.9300 | O(7)-Cu(5)-O(12) | 92.2(4) |
| N(12)-C(18) | 1.340(15) | N(8)-Cu(5)-O(12) | 93.2(4) |
| C(10)-C(11) | 1.354(15) | O(2)-Cu(5)-O(12) | 92.8(4) |
| C(10)-H(10) | 0.9300 | N(3)-Cu(2)-N(2) | 176.2(5) |
| C(11)-H(11) | 0.9300 | N(3)-Cu(2)-O(1) | 87.9(5) |
| C(7)-C(8) | 1.363(17) | N(2)-Cu(2)-O(1) | 88.6(4) |
| C(7)-H(7) | 0.9300 | N(3)-Cu(2)-O(8)#1 | 92.9(5) |
| C(18)-C(17) | 1.367(16) | N(2)-Cu(2)-O(8)#1 | 90.8(4) |
| C(18)-H(18) | 0.9300 | O(1)-Cu(2)-O(8)#1 | 173.9(5) |

| | | | |
|---------------------|-----------|---------------------|-----------|
| N(11)-Cu(6)-N(10) | 170.0(5) | N(7)-N(8)-Cu(5) | 121.5(7) |
| N(11)-Cu(6)-O(10)#2 | 93.8(5) | N(3)-N(4)-C(6) | 107.5(15) |
| N(10)-Cu(6)-O(10)#2 | 89.2(5) | N(3)-N(4)-Cu(3) | 120.5(8) |
| N(11)-Cu(6)-O(2) | 89.5(4) | C(6)-N(4)-Cu(3) | 131.9(13) |
| N(10)-Cu(6)-O(2) | 89.3(4) | Cu(3)-O(1)-Cu(2) | 116.9(5) |
| O(10)#2-Cu(6)-O(2) | 169.2(4) | Cu(3)-O(1)-Cu(1) | 116.7(5) |
| N(5)-Cu(3)-N(4) | 170.9(5) | Cu(2)-O(1)-Cu(1) | 115.2(4) |
| N(5)-Cu(3)-O(1) | 88.7(4) | C(27)-O(10)-Cu(6)#4 | 107.9(11) |
| N(4)-Cu(3)-O(1) | 88.5(5) | C(7)-N(5)-N(6) | 107.8(12) |
| N(5)-Cu(3)-O(5) | 93.8(5) | C(7)-N(5)-Cu(3) | 130.9(10) |
| N(4)-Cu(3)-O(5) | 90.8(5) | N(6)-N(5)-Cu(3) | 121.3(8) |
| O(1)-Cu(3)-O(5) | 167.1(5) | C(5)-C(6)-N(4) | 109.7(15) |
| O(9)-C(27)-O(10) | 123.6(15) | C(5)-C(6)-H(6) | 125.2 |
| O(9)-C(27)-C(26) | 126.4(18) | N(4)-C(6)-H(6) | 125.2 |
| O(10)-C(27)-C(26) | 109.7(17) | O(3)-C(19)-O(4) | 119.8(11) |
| C(19)-O(3)-Cu(1) | 130.5(9) | O(3)-C(19)-C(20) | 117.4(12) |
| N(4)-N(3)-C(4) | 109.1(14) | O(4)-C(19)-C(20) | 122.8(12) |
| N(4)-N(3)-Cu(2) | 123.5(9) | N(2)-C(3)-C(2) | 109.1(13) |
| C(4)-N(3)-Cu(2) | 127.0(13) | N(2)-C(3)-H(3) | 125.4 |
| C(1)-N(1)-N(2) | 104.3(10) | C(2)-C(3)-H(3) | 125.4 |
| C(1)-N(1)-Cu(1) | 133.1(9) | N(8)-C(12)-C(11) | 109.7(11) |
| N(2)-N(1)-Cu(1) | 122.1(7) | N(8)-C(12)-H(12) | 125.1 |
| C(30)-O(12)-Cu(5) | 116.6(11) | C(11)-C(12)-H(12) | 125.1 |
| C(24)-O(8)-Cu(2)#3 | 111.3(9) | C(22)#5-C(21)-C(23) | 113.7(12) |
| C(13)-N(9)-N(10) | 106.9(11) | C(22)#5-C(21)-C(20) | 111.3(12) |
| C(13)-N(9)-Cu(5) | 131.7(10) | C(23)-C(21)-C(20) | 105.9(12) |
| N(10)-N(9)-Cu(5) | 121.5(9) | C(22)#5-C(21)-H(21) | 108.6 |
| Cu(6)-O(2)-Cu(5) | 116.2(4) | C(23)-C(21)-H(21) | 108.6 |
| Cu(6)-O(2)-Cu(4) | 116.0(4) | C(20)-C(21)-H(21) | 108.6 |
| Cu(5)-O(2)-Cu(4) | 115.7(3) | N(1)-C(1)-C(2) | 111.0(12) |
| C(24)-O(7)-Cu(5) | 130.3(8) | N(1)-C(1)-H(1) | 124.5 |
| C(15)-N(10)-N(9) | 108.8(13) | C(2)-C(1)-H(1) | 124.5 |
| C(15)-N(10)-Cu(6) | 129.4(11) | C(15)-C(14)-C(13) | 105.9(14) |
| N(9)-N(10)-Cu(6) | 121.5(9) | C(15)-C(14)-H(14) | 127.1 |
| N(10)-C(15)-C(14) | 109.6(14) | C(13)-C(14)-H(14) | 127.1 |
| N(10)-C(15)-H(15) | 125.2 | C(1)-C(2)-C(3) | 105.1(13) |
| C(14)-C(15)-H(15) | 125.2 | C(1)-C(2)-H(2) | 127.4 |
| N(8)-N(7)-C(10) | 104.0(9) | C(3)-C(2)-H(2) | 127.4 |
| N(8)-N(7)-Cu(4) | 122.3(7) | N(6)-C(9)-C(8) | 112.2(14) |
| C(10)-N(7)-Cu(4) | 133.3(8) | N(6)-C(9)-H(9) | 123.9 |
| C(19)-O(4)-Cu(4) | 110.5(8) | C(8)-C(9)-H(9) | 123.9 |
| C(29)-O(11)-Cu(1) | 115.7(11) | C(18)-N(12)-N(11) | 107.9(11) |
| C(22)-O(5)-Cu(3) | 109.4(8) | C(18)-N(12)-Cu(4) | 131.4(10) |
| C(16)-N(11)-N(12) | 106.6(14) | N(11)-N(12)-Cu(4) | 120.7(8) |
| C(16)-N(11)-Cu(6) | 130.9(12) | N(7)-C(10)-C(11) | 112.6(10) |
| N(12)-N(11)-Cu(6) | 122.5(8) | N(7)-C(10)-H(10) | 123.7 |
| C(19)-C(20)-C(21) | 119.2(12) | C(11)-C(10)-H(10) | 123.7 |
| C(19)-C(20)-H(20A) | 107.5 | C(9)-N(6)-N(5) | 107.6(11) |
| C(21)-C(20)-H(20A) | 107.5 | C(9)-N(6)-Cu(1) | 129.4(10) |
| C(19)-C(20)-H(20B) | 107.5 | N(5)-N(6)-Cu(1) | 122.8(9) |
| C(21)-C(20)-H(20B) | 107.5 | C(10)-C(11)-C(12) | 103.2(10) |
| H(20A)-C(20)-H(20B) | 107.0 | C(10)-C(11)-H(11) | 128.4 |
| C(3)-N(2)-N(1) | 110.2(11) | C(12)-C(11)-H(11) | 128.4 |
| C(3)-N(2)-Cu(2) | 130.7(10) | N(5)-C(7)-C(8) | 110.7(14) |
| N(1)-N(2)-Cu(2) | 118.8(8) | N(5)-C(7)-H(7) | 124.6 |
| O(8)-C(24)-O(7) | 121.1(11) | C(8)-C(7)-H(7) | 124.6 |
| O(8)-C(24)-C(25) | 120.3(14) | N(12)-C(18)-C(17) | 109.5(14) |
| O(7)-C(24)-C(25) | 118.4(12) | N(12)-C(18)-H(18) | 125.3 |
| C(12)-N(8)-N(7) | 110.4(9) | C(17)-C(18)-H(18) | 125.3 |
| C(12)-N(8)-Cu(5) | 127.9(9) | C(6)-C(5)-C(4) | 106.5(15) |

| | |
|---------------------|-----------|
| C(6)-C(5)-H(5) | 126.8 |
| C(4)-C(5)-H(5) | 126.8 |
| N(9)-C(13)-C(14) | 108.8(14) |
| N(9)-C(13)-H(13) | 125.6 |
| C(14)-C(13)-H(13) | 125.6 |
| O(11)-C(29)-H(29A) | 109.5 |
| O(11)-C(29)-H(29B) | 109.5 |
| H(29A)-C(29)-H(29B) | 109.5 |
| O(11)-C(29)-H(29C) | 109.5 |
| H(29A)-C(29)-H(29C) | 109.5 |
| H(29B)-C(29)-H(29C) | 109.5 |
| C(25)-C(26)-C(28) | 125(2) |
| C(25)-C(26)-C(27) | 110.5(14) |
| C(28)-C(26)-C(27) | 112.1(14) |
| C(25)-C(26)-H(26) | 101.7 |
| C(28)-C(26)-H(26) | 101.7 |
| C(27)-C(26)-H(26) | 101.7 |
| C(26)-C(25)-C(24) | 120.4(14) |
| C(26)-C(25)-H(25A) | 107.2 |
| C(24)-C(25)-H(25A) | 107.2 |
| C(26)-C(25)-H(25B) | 107.2 |
| C(24)-C(25)-H(25B) | 107.2 |
| H(25A)-C(25)-H(25B) | 106.8 |
| C(21)-C(23)-H(23A) | 109.5 |
| C(21)-C(23)-H(23B) | 109.5 |
| H(23A)-C(23)-H(23B) | 109.5 |
| C(21)-C(23)-H(23C) | 109.5 |
| H(23A)-C(23)-H(23C) | 109.5 |
| H(23B)-C(23)-H(23C) | 109.5 |
| O(12)-C(30)-H(30A) | 109.5 |
| O(12)-C(30)-H(30B) | 109.5 |
| H(30A)-C(30)-H(30B) | 109.5 |
| O(12)-C(30)-H(30C) | 109.5 |
| H(30A)-C(30)-H(30C) | 109.5 |
| H(30B)-C(30)-H(30C) | 109.5 |
| N(11)-C(16)-C(17) | 110.2(16) |
| N(11)-C(16)-H(16) | 124.9 |
| C(17)-C(16)-H(16) | 124.9 |
| C(16)-C(17)-C(18) | 105.7(15) |
| C(16)-C(17)-H(17) | 127.2 |
| C(18)-C(17)-H(17) | 127.2 |
| C(26)-C(28)-H(28A) | 109.5 |
| C(26)-C(28)-H(28B) | 109.5 |
| H(28A)-C(28)-H(28B) | 109.5 |
| C(26)-C(28)-H(28C) | 109.5 |
| H(28A)-C(28)-H(28C) | 109.5 |
| H(28B)-C(28)-H(28C) | 109.5 |
| C(7)-C(8)-C(9) | 101.8(14) |
| C(7)-C(8)-H(8) | 129.1 |
| C(9)-C(8)-H(8) | 129.1 |
| O(5)-C(22)-O(6) | 122.9(12) |
| O(5)-C(22)-C(21)#6 | 121.3(12) |
| O(6)-C(22)-C(21)#6 | 115.8(13) |
| N(3)-C(4)-C(5) | 107.1(16) |
| N(3)-C(4)-H(4) | 126.4 |
| C(5)-C(4)-H(4) | 126.4 |

Symmetry transformations used to generate equivalent atoms:

#1 $-y+1, x-y-1, z$ #2 $-y+2/3, x-y-2/3, z+1/3$
 #3 $-x+y+2, -x+1, z$ #4 $-x+y+4/3, -x+2/3, z-1/3$
 #5 $-x+y+5/3, -x+1/3, z+1/3$
 #6 $-y+1/3, x-y-4/3, z-1/3$
 Table 9. Bond lengths [Å] and angles [°] for **8b**.

| | |
|-----------------|------------|
| Cu(1)-N(2) | 1.945(2) |
| Cu(1)-N(3) | 1.946(2) |
| Cu(1)-O(2) | 1.9770(16) |
| Cu(1)-O(1) | 1.9989(16) |
| Cu(2)-N(1) | 1.923(2) |
| Cu(2)-N(5) | 1.934(2) |
| Cu(2)-O(5) | 1.9594(18) |
| Cu(2)-O(1) | 1.9774(17) |
| Cu(3)-N(4) | 1.946(2) |
| Cu(3)-N(6) | 1.961(2) |
| Cu(3)-O(1) | 1.9809(16) |
| Cu(3)-N(7) | 2.021(2) |
| Cu(3)-O(6) | 2.431(3) |
| O(2)-C(13) | 1.265(3) |
| N(6)-C(7) | 1.339(3) |
| N(6)-N(5) | 1.361(3) |
| N(2)-C(3) | 1.336(3) |
| N(2)-N(1) | 1.360(3) |
| N(7)-C(10) | 1.317(4) |
| N(7)-N(8) | 1.335(3) |
| O(4)-C(16) | 1.254(3) |
| C(14)-C(13) | 1.518(3) |
| C(14)-C(15) | 1.534(4) |
| N(4)-C(6) | 1.342(3) |
| N(4)-N(3) | 1.369(3) |
| N(8)-C(12) | 1.345(4) |
| C(16)-O(5)#1 | 1.269(3) |
| C(16)-C(15) | 1.540(3) |
| C(15)-C(18) | 1.526(4) |
| C(15)-C(17) | 1.540(4) |
| C(6)-C(5) | 1.380(4) |
| C(10)-C(11) | 1.387(5) |
| N(5)-C(9) | 1.337(3) |
| C(8)-C(7) | 1.381(4) |
| C(8)-C(9) | 1.383(4) |
| O(5)-C(16)#1 | 1.269(3) |
| C(13)-O(3) | 1.241(3) |
| C(11)-C(12) | 1.343(6) |
| N(1)-C(1) | 1.337(3) |
| N(3)-C(4) | 1.334(3) |
| C(1)-C(2) | 1.373(4) |
| C(3)-C(2) | 1.380(4) |
| C(4)-C(5) | 1.378(4) |
| N(2)-Cu(1)-N(3) | 168.40(10) |
| N(2)-Cu(1)-O(2) | 92.54(8) |
| N(3)-Cu(1)-O(2) | 93.19(8) |
| N(2)-Cu(1)-O(1) | 88.01(8) |
| N(3)-Cu(1)-O(1) | 88.22(8) |
| O(2)-Cu(1)-O(1) | 169.36(7) |
| N(1)-Cu(2)-N(5) | 165.66(9) |

| | |
|--------------------|------------|
| N(1)-Cu(2)-O(5) | 91.95(8) |
| N(5)-Cu(2)-O(5) | 93.67(8) |
| N(1)-Cu(2)-O(1) | 88.85(8) |
| N(5)-Cu(2)-O(1) | 88.57(8) |
| O(5)-Cu(2)-O(1) | 167.24(8) |
| N(4)-Cu(3)-N(6) | 174.69(10) |
| N(4)-Cu(3)-O(1) | 88.81(8) |
| N(6)-Cu(3)-O(1) | 87.80(8) |
| N(4)-Cu(3)-N(7) | 92.98(9) |
| N(6)-Cu(3)-N(7) | 90.04(9) |
| O(1)-Cu(3)-N(7) | 174.56(9) |
| N(4)-Cu(3)-O(6) | 94.68(10) |
| N(6)-Cu(3)-O(6) | 89.48(9) |
| O(1)-Cu(3)-O(6) | 91.37(9) |
| N(7)-Cu(3)-O(6) | 93.60(10) |
| C(13)-O(2)-Cu(1) | 113.71(15) |
| C(7)-N(6)-N(5) | 107.5(2) |
| C(7)-N(6)-Cu(3) | 134.8(2) |
| N(5)-N(6)-Cu(3) | 117.60(15) |
| C(3)-N(2)-N(1) | 107.5(2) |
| C(3)-N(2)-Cu(1) | 131.66(18) |
| N(1)-N(2)-Cu(1) | 120.61(15) |
| Cu(2)-O(1)-Cu(3) | 110.31(8) |
| Cu(2)-O(1)-Cu(1) | 115.36(8) |
| Cu(3)-O(1)-Cu(1) | 118.08(8) |
| C(10)-N(7)-N(8) | 106.3(2) |
| C(10)-N(7)-Cu(3) | 128.9(2) |
| N(8)-N(7)-Cu(3) | 124.00(19) |
| C(13)-C(14)-C(15) | 118.2(2) |
| C(6)-N(4)-N(3) | 107.3(2) |
| C(6)-N(4)-Cu(3) | 131.20(19) |
| N(3)-N(4)-Cu(3) | 121.54(16) |
| N(7)-N(8)-C(12) | 110.4(3) |
| O(4)-C(16)-O(5)#1 | 123.8(2) |
| O(4)-C(16)-C(15) | 119.0(2) |
| O(5)#1-C(16)-C(15) | 117.2(2) |
| C(18)-C(15)-C(14) | 111.1(2) |
| C(18)-C(15)-C(17) | 109.3(2) |
| C(14)-C(15)-C(17) | 107.9(2) |
| C(18)-C(15)-C(16) | 111.5(2) |
| C(14)-C(15)-C(16) | 110.0(2) |
| C(17)-C(15)-C(16) | 106.9(2) |
| N(4)-C(6)-C(5) | 110.6(3) |
| N(7)-C(10)-C(11) | 110.2(3) |
| C(9)-N(5)-N(6) | 108.3(2) |
| C(9)-N(5)-Cu(2) | 131.40(19) |
| N(6)-N(5)-Cu(2) | 120.19(16) |
| C(7)-C(8)-C(9) | 104.3(2) |
| C(16)#1-O(5)-Cu(2) | 115.32(16) |
| O(3)-C(13)-O(2) | 122.4(2) |
| O(3)-C(13)-C(14) | 119.6(2) |
| O(2)-C(13)-C(14) | 118.0(2) |
| C(12)-C(11)-C(10) | 105.5(3) |
| C(1)-N(1)-N(2) | 108.1(2) |
| C(1)-N(1)-Cu(2) | 130.23(18) |
| N(2)-N(1)-Cu(2) | 121.63(15) |
| C(4)-N(3)-N(4) | 107.5(2) |
| C(4)-N(3)-Cu(1) | 130.56(18) |
| N(4)-N(3)-Cu(1) | 121.71(17) |
| N(6)-C(7)-C(8) | 110.2(3) |

| | |
|------------------|----------|
| C(11)-C(12)-N(8) | 107.7(3) |
| N(1)-C(1)-C(2) | 109.7(2) |
| N(2)-C(3)-C(2) | 110.0(2) |
| N(5)-C(9)-C(8) | 109.7(3) |
| N(3)-C(4)-C(5) | 110.9(2) |
| C(4)-C(5)-C(6) | 103.7(2) |
| C(1)-C(2)-C(3) | 104.6(2) |

Symmetry transformations used to generate equivalent atoms:
#1 -x+1,-y+1,-z+2

Table 10. Bond lengths [\AA] and angles [$^\circ$] for **9a**.

| | |
|-----------------|----------|
| Cu(1)-N(1) | 1.95(3) |
| Cu(1)-O(2) | 1.96(2) |
| Cu(1)-O(1) | 1.99(2) |
| Cu(1)-N(6) | 2.00(3) |
| Cu(2)-N(2) | 1.91(3) |
| Cu(2)-N(3) | 1.96(3) |
| Cu(2)-O(1) | 1.99(2) |
| Cu(2)-O(4) | 2.00(2) |
| Cu(3)-N(5) | 1.89(3) |
| Cu(3)-N(4) | 1.93(3) |
| Cu(3)-O(1) | 1.98(2) |
| Cu(3)-O(5)#1 | 2.02(2) |
| C(2)-C(3) | 1.39(5) |
| C(2)-C(1) | 1.49(5) |
| C(11)-C(13) | 1.52(4) |
| C(11)-C(15) | 1.59(4) |
| C(11)-C(14) | 1.59(5) |
| C(11)-C(10) | 1.61(5) |
| C(10)-O(2) | 1.20(4) |
| C(10)-O(3) | 1.25(4) |
| O(5)-C(12) | 1.19(4) |
| O(5)-Cu(3)#2 | 2.02(2) |
| O(4)-C(12) | 1.31(4) |
| C(1)-N(2) | 1.35(4) |
| C(12)-C(13)#3 | 1.56(5) |
| N(2)-N(1) | 1.36(4) |
| N(3)-N(4) | 1.32(4) |
| N(3)-C(4) | 1.40(4) |
| C(9)-C(8) | 1.37(5) |
| C(9)-N(6) | 1.38(4) |
| N(1)-C(3) | 1.38(4) |
| N(5)-C(7) | 1.32(4) |
| N(5)-N(6) | 1.35(4) |
| N(4)-C(6) | 1.32(4) |
| C(4)-C(5) | 1.27(5) |
| C(7)-C(8) | 1.43(5) |
| C(13)-C(12)#4 | 1.56(5) |
| C(6)-C(5) | 1.39(6) |
| N(1)-Cu(1)-O(2) | 93.0(11) |
| N(1)-Cu(1)-O(1) | 88.5(11) |
| O(2)-Cu(1)-O(1) | 171.5(9) |

| | |
|--------------------|-----------|
| N(1)-Cu(1)-N(6) | 170.3(12) |
| O(2)-Cu(1)-N(6) | 90.3(11) |
| O(1)-Cu(1)-N(6) | 89.6(11) |
| N(2)-Cu(2)-N(3) | 169.2(12) |
| N(2)-Cu(2)-O(1) | 87.4(10) |
| N(3)-Cu(2)-O(1) | 85.3(11) |
| N(2)-Cu(2)-O(4) | 91.0(10) |
| N(3)-Cu(2)-O(4) | 94.1(11) |
| O(1)-Cu(2)-O(4) | 166.2(10) |
| N(5)-Cu(3)-N(4) | 174.8(12) |
| N(5)-Cu(3)-O(1) | 88.4(10) |
| N(4)-Cu(3)-O(1) | 88.6(12) |
| N(5)-Cu(3)-O(5)#1 | 91.9(10) |
| N(4)-Cu(3)-O(5)#1 | 91.2(12) |
| O(1)-Cu(3)-O(5)#1 | 179.0(9) |
| C(3)-C(2)-C(1) | 103(3) |
| C(13)-C(11)-C(15) | 109(3) |
| C(13)-C(11)-C(14) | 116(3) |
| C(15)-C(11)-C(14) | 112(3) |
| C(13)-C(11)-C(10) | 113(3) |
| C(15)-C(11)-C(10) | 105(3) |
| C(14)-C(11)-C(10) | 102(3) |
| O(2)-C(10)-O(3) | 123(3) |
| O(2)-C(10)-C(11) | 120(3) |
| O(3)-C(10)-C(11) | 116(3) |
| Cu(3)-O(1)-Cu(2) | 116.3(10) |
| Cu(3)-O(1)-Cu(1) | 112.8(10) |
| Cu(2)-O(1)-Cu(1) | 112.4(11) |
| C(12)-O(5)-Cu(3)#2 | 110(2) |
| C(12)-O(4)-Cu(2) | 145(3) |
| N(2)-C(1)-C(2) | 110(3) |
| O(5)-C(12)-O(4) | 124(4) |
| O(5)-C(12)-C(13)#3 | 125(3) |
| O(4)-C(12)-C(13)#3 | 111(4) |
| C(1)-N(2)-N(1) | 106(3) |
| C(1)-N(2)-Cu(2) | 131(3) |

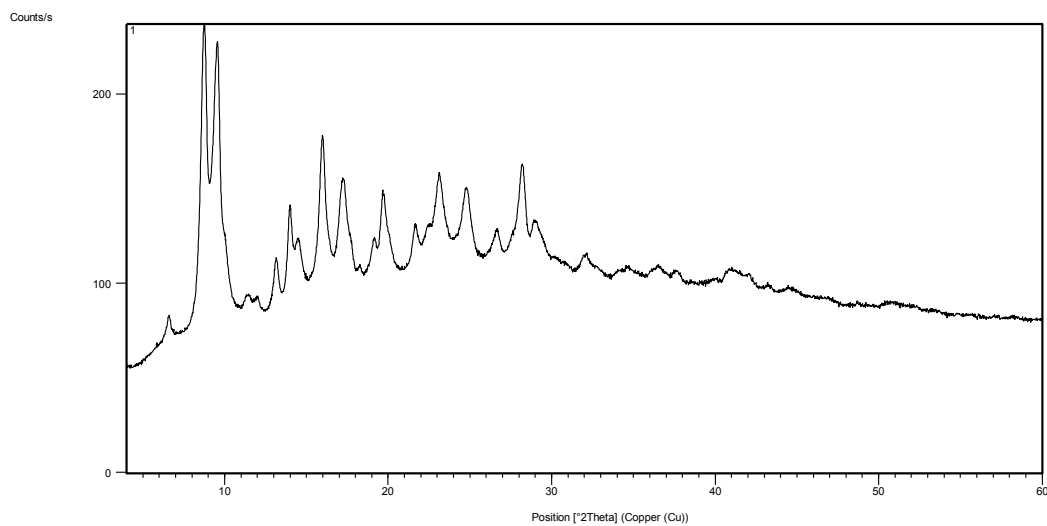
| | |
|---------------------|--------|
| N(1)-N(2)-Cu(2) | 123(2) |
| N(4)-N(3)-C(4) | 103(3) |
| N(4)-N(3)-Cu(2) | 124(3) |
| C(4)-N(3)-Cu(2) | 132(3) |
| C(8)-C(9)-N(6) | 107(4) |
| C(10)-O(2)-Cu(1) | 111(2) |
| N(2)-N(1)-C(3) | 112(3) |
| N(2)-N(1)-Cu(1) | 118(2) |
| C(3)-N(1)-Cu(1) | 130(3) |
| C(7)-N(5)-N(6) | 107(3) |
| C(7)-N(5)-Cu(3) | 129(3) |
| N(6)-N(5)-Cu(3) | 124(2) |
| N(5)-N(6)-C(9) | 111(3) |
| N(5)-N(6)-Cu(1) | 116(2) |
| C(9)-N(6)-Cu(1) | 132(3) |
| N(1)-C(3)-C(2) | 108(3) |
| N(3)-N(4)-C(6) | 112(3) |
| N(3)-N(4)-Cu(3) | 119(3) |
| C(6)-N(4)-Cu(3) | 127(2) |
| C(5)-C(4)-N(3) | 111(4) |
| N(5)-C(7)-C(8) | 111(4) |
| C(9)-C(8)-C(7) | 104(3) |
| C(11)-C(13)-C(12)#4 | 109(3) |
| N(4)-C(6)-C(5) | 106(3) |
| C(4)-C(5)-C(6) | 108(4) |

Symmetry transformations used to generate equivalent atoms:

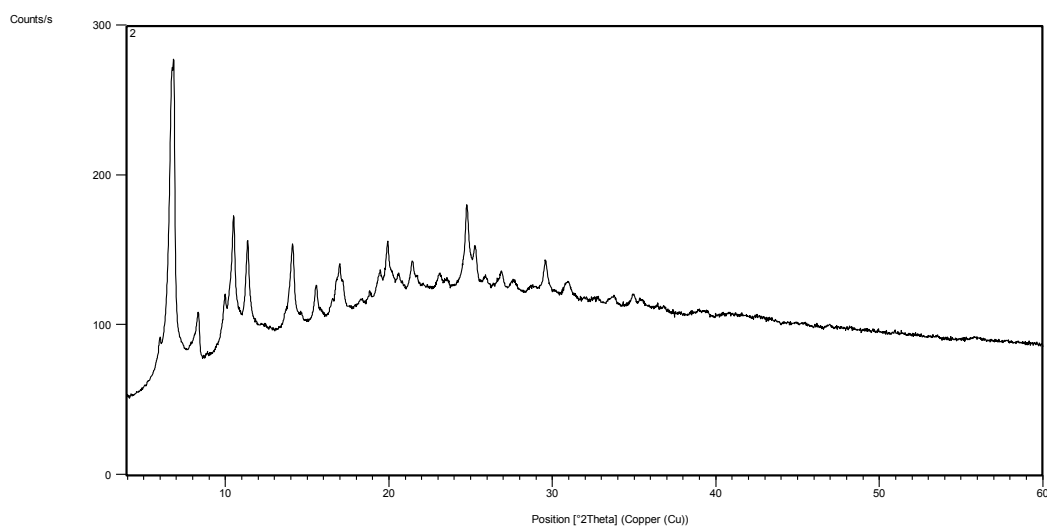
#1 $-y+1/3, x-y-1/3, z-1/3$ #2 $-x+y+2/3, -x+1/3, z+1/3$
 #3 $x+1/3, x-y-1/3, z+1/6$ #4 $x-1/3, x-y-2/3, z-1/6$

Appendix C XRPD Diffractograms

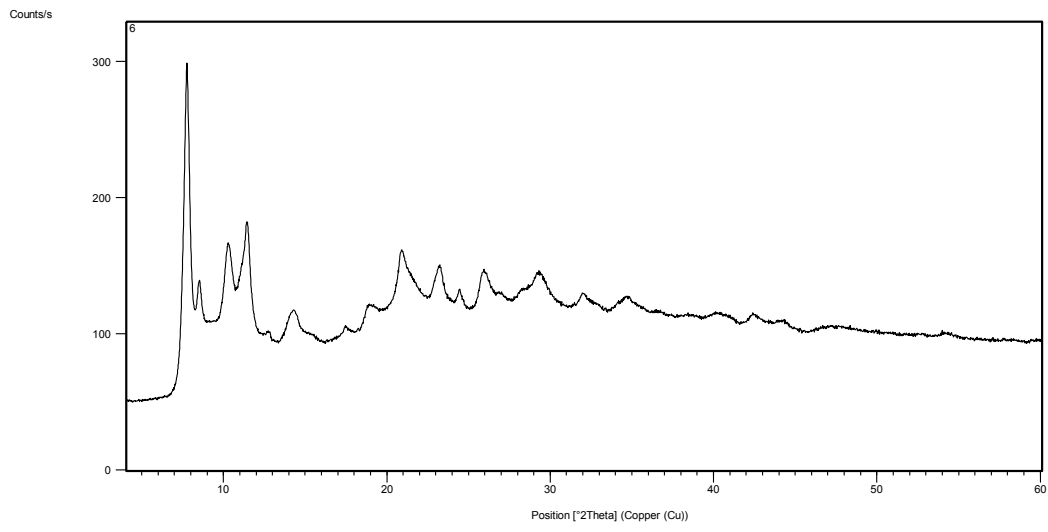
Diffractogram 2a



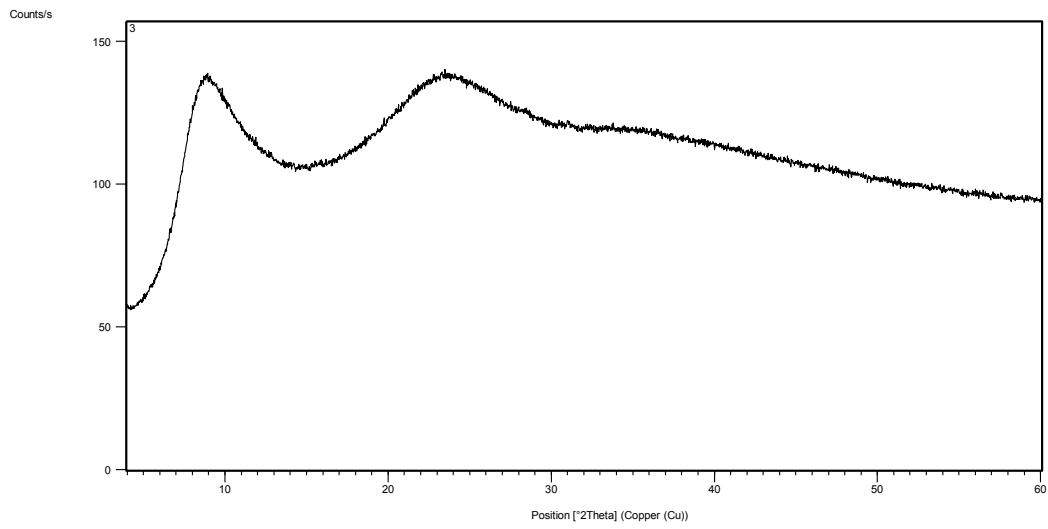
Diffractogram 3a



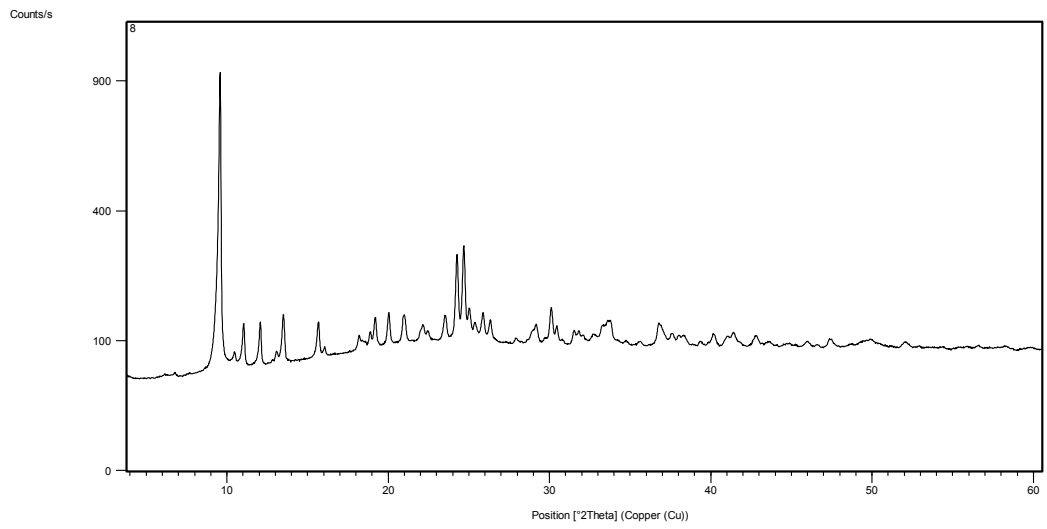
Diffractogram 4a



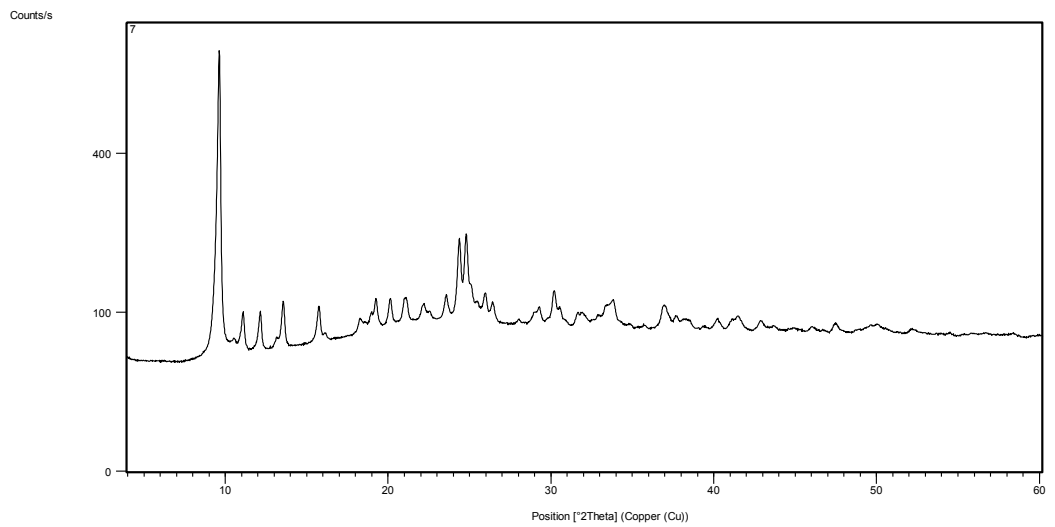
Diffractogram 5a



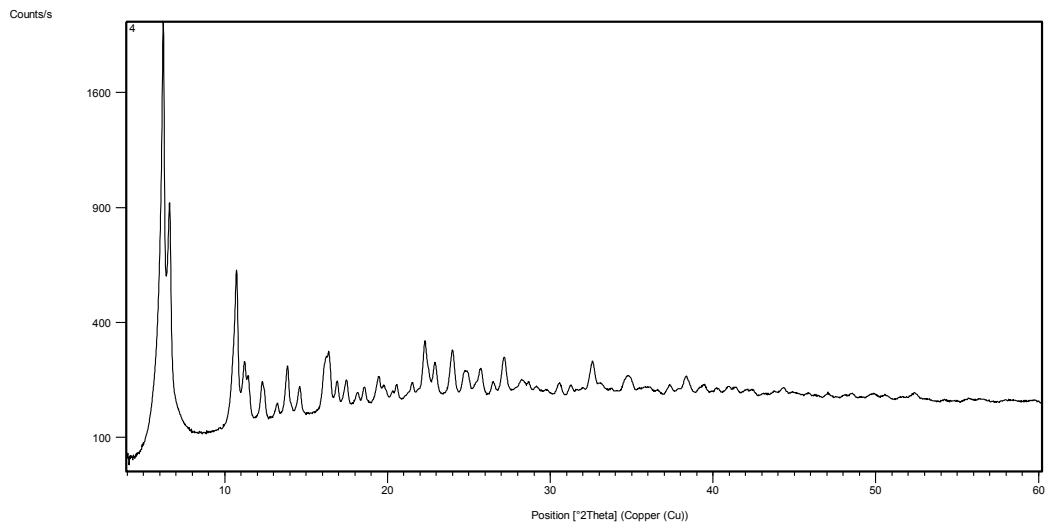
Diffractogram 6b



Diffractogram 7a



Diffractogram 9b



RINGRAZIAMENTI

A tutte le persone che in questo mio lungo percorso di studio hanno messo a disposizione le proprie competenze, la propria passione e il proprio sostegno.

Al Prof. Luciano Pandolfo per avermi appassionata e introdotta all'affascinante mondo dei Polimeri di Coordinazione e per aver messo a disposizione di questo progetto di tesi le sue competenze e risorse, oltre che, per la grande fiducia accordatami.

Al Prof. Fabrizio Nestola per la disponibilità, l'entusiasmo e la semplicità con cui ha saputo insegnarmi la complessa e potente tecnica di indagine strutturale SC-XRD.

Ad Arianna per la sua gentilezza, solarità e grande preparazione ma soprattutto, per l'esempio che ha saputo darmi mettendo tutte le sue competenze a mia disposizione, accompagnandomi in un percorso complesso.

Al Dott. Federico Zorzi per la disponibilità e competenza.

Ai miei genitori perché, comunque vada, ci sono sempre.

Ai miei nonni per il sostegno, la tenerezza e la fiducia.

A tutta la mia famiglia perché ognuno a proprio modo sa sostenermi ed essere partecipe nella mia vita, rappresentando un importante punto di riferimento e forza.

Ai miei amici tutti, a quelli che mi conoscono tanto e a quelli che mi conoscono meno, per la compagnia, le risate e per sopportarmi.

A Mirko per le lunghe e più svariate conversazioni nei quotidiani viaggi in treno.

Ad Annalisa per esserci sempre stata in questo duro percorso, per essere una fedele compagna di disavventure, per aver dato un importante contributo estetico a questa tesi, per aver sempre ascoltato tutte le mie paranoie ma soprattutto per la sua grande amicizia.

A Francesco perché è il mio più grande fan. Per aver saputo sopportare tutti i miei più disperati sfoghi, per la dolcezza, la fiducia, il sostegno e l'amore che mi ha sempre dedicato. Ma sopra ogni cosa per essere un ottimo motivo per arrivare alla fine di ogni giornata.

Ed infine, a tutti i gentili lettori.